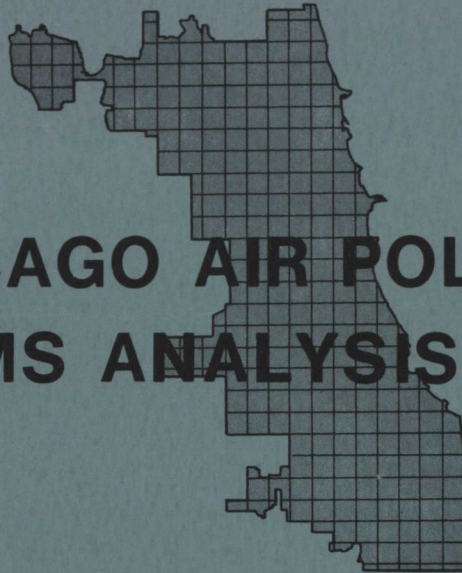


Government Publications  
Unit

DEC 13 1990

Washington University Libraries  
St. Louis, MO 63130

LEVEL 4



# CHICAGO AIR POLLUTION SYSTEMS ANALYSIS PROGRAM

A MULTIPLE-SOURCE URBAN ATMOSPHERIC DISPERSION MODEL

by

J. J. Roberts, E. J. Croke, A. S. Kennedy,  
J. E. Norco, and L. A. Conley

ARGONNE NATIONAL LABORATORY

CHICAGO DEPARTMENT OF ENVIRONMENTAL CONTROL

DEPARTMENT OF HEALTH, EDUCATION, AND WELFARE

NATIONAL AIR POLLUTION CONTROL ADMINISTRATION



U of C-AUA-USAEC

CENTER FOR ENVIRONMENTAL STUDIES

metadc101032

The facilities of Argonne National Laboratory are owned by the United States Government. Under the terms of a contract (W-31-109-Eng-38) between the U. S. Atomic Energy Commission, Argonne Universities Association and The University of Chicago, the University employs the staff and operates the Laboratory in accordance with policies and programs formulated, approved and reviewed by the Association.

#### MEMBERS OF ARGONNE UNIVERSITIES ASSOCIATION

The University of Arizona	Kansas State University	The Ohio State University
Carnegie-Mellon University	The University of Kansas	Ohio University
Case Western Reserve University	Loyola University	The Pennsylvania State University
The University of Chicago	Marquette University	Purdue University
University of Cincinnati	Michigan State University	Saint Louis University
Illinois Institute of Technology	The University of Michigan	Southern Illinois University
University of Illinois	University of Minnesota	The University of Texas at Austin
Indiana University	University of Missouri	Washington University
Iowa State University	Northwestern University	Wayne State University
The University of Iowa	University of Notre Dame	The University of Wisconsin

#### NOTICE

This report was prepared as an account of work sponsored by the United States Government. Neither the United States nor the United States Atomic Energy Commission, nor any of their employees, nor any of their contractors, subcontractors, or their employees, makes any warranty, express or implied, or assumes any legal liability or responsibility for the accuracy, completeness or usefulness of any information, apparatus, product or process disclosed, or represents that its use would not infringe privately-owned rights.

Printed in the United States of America  
Available from  
National Technical Information Service  
U.S. Department of Commerce  
5285 Port Royal Road  
Springfield, Virginia 22151  
Price: Printed Copy \$3.00; Microfiche \$0.95

ARGONNE NATIONAL LABORATORY  
9700 South Cass Avenue  
Argonne, Illinois 60439

CHICAGO AIR POLLUTION SYSTEMS ANALYSIS PROGRAM

ARGONNE NATIONAL LABORATORY  
CHICAGO DEPARTMENT OF ENVIRONMENTAL CONTROL  
DEPARTMENT OF HEALTH, EDUCATION, AND WELFARE  
National Air Pollution Control Administration

A Multiple-source Urban Atmospheric Dispersion Model

by

J. J. Roberts, E. J. Croke, A. S. Kennedy,\*  
J. E. Norco, and L. A. Conley

Center for Environmental Studies

May 1970

\*Applied Mathematics Division.

## FOREWORD

The City of Chicago Air Pollution Systems Analysis Study discussed in this report represents a joint effort conducted and funded by the Atomic Energy Commission, the U.S. Department of Health, Education, and Welfare, and the Chicago Department of Environmental Control.

Program direction, systems analysis, meteorology studies, computer model development, and computer programming are provided by the Argonne National Laboratory. The Chicago Department of Environmental Control supplies emission and air quality data for the atmospheric dispersion studies.

### Policy Review Committee

- |              |  |
|--------------|--|
| L. Link      | - Director, Center for Environmental Studies,<br>Argonne National Laboratory |
| R. Engelmann | - Division of Biology and Medicine,<br>U.S. Atomic Energy Commission         |
| R. McCormick | - National Air Pollution Control<br>Administration                           |

### Technical Review Committee

- |                |  |
|----------------|--|
| S. Booras      | - Environmental Pollution Control Systems                              |
| L. Niemeyer    | - National Air Pollution Control<br>Administration                     |
| J. Marchaterre | - Reactor Analysis and Safety Division,<br>Argonne National Laboratory |

TABLE OF CONTENTS

	<u>Page</u>
ABSTRACT . . . . .	11
PART I AN URBAN ATMOSPHERIC DISPERSION MODEL FOR STATIONARY SOURCES	
1. INTRODUCTION TO PART I . . . . .	13
1.1 Source-oriented Dispersion Models . . . . .	15
1.2 Transport of Airborne Pollutants . . . . .	17
1.2.1 Dispersion Kernel . . . . .	17
1.2.2 Generalized Wind Direction . . . . .	19
1.2.3 Variable Wind Speed and Direction . . . . .	19
1.2.4 Variable Atmospheric Stability . . . . .	21
1.2.5 Dispersion Coefficients . . . . .	23
1.2.6 Effective Stack Height . . . . .	28
1.2.7 Effective Wind Speed . . . . .	30
1.2.8 Finite Geometry for Dispersion . . . . .	31
1.2.9 Finite-source Geometry . . . . .	31
2. STRUCTURE OF THE COMPUTER CODE . . . . .	35
3. SUBROUTINE ISPDAV (ENTRY PUFF) . . . . .	37
3.1 Initialization of Data; Subroutine ADAT2 . . . . .	37
3.1.1 Area-source Grid . . . . .	38
3.1.2 The Receptor Grid . . . . .	38
3.1.3 A Standard Area-source Overlay Grid . . . . .	39
3.2 Storage of Hourly Data; Function JSUB . . . . .	40
3.2.1 Function JSUB . . . . .	41
3.3 Effective Stack Height; Subroutine PRISE . . . . .	42
3.4 Point-source Calculations . . . . .	42
3.5 Hourly Emissions from Area Sources . . . . .	43
3.5.1 Low-rise Residential/Commercial Hourly Emissions . . . . .	43
3.5.2 High-rise Residential/Commercial Hourly Emissions . . . . .	44
3.5.3 Industrial Area Sources . . . . .	44
3.6 Calculation of Concentrations due to Area Sources . . . . .	44
3.7 Output; Subroutine PROUT . . . . .	46

d. 5/8/74 RLB (C.O. ft)

## TABLE OF CONTENTS

	<u>Page</u>
4. FUNCTION ITRAN (ENTRY TRAN) . . . . .	49
4.1 The Effective Lid Height (HLID). . . . .	50
4.2 Puff Significance--Comparison with a Plume Model . . . .	51
4.3 Integrated-puff Calculation . . . . .	53
4.4 Higher-order Images . . . . .	54
4.5 The Option "NTRAN=1" . . . . .	55
4.6 Conclusion . . . . .	55
5. SUBROUTINE KERN (T,FT) . . . . .	56
PART II VALIDATION OF MODEL: ESTIMATION OF SO <sub>2</sub> LEVELS IN CHICAGO	
6. INTRODUCTION TO PART II . . . . .	57
7. DEVELOPMENT OF AN EMISSION INVENTORY . . . . .	59
7.1 Power Plants . . . . .	62
7.2 Industrial Sources . . . . .	71
7.2.1 Industrial-source Simulation Program . . . . .	72
7.2.2 PLANTSIM Computations . . . . .	78
7.3 Residential Space-heating Sources . . . . .	80
7.4 Commercial and Institutional Sources . . . . .	81
7.5 Additional Point Sources . . . . .	82
8. METEOROLOGICAL AND AIR QUALITY DATA . . . . .	84
8.1 Chicago's TAM Network . . . . .	84
8.2 Airport Data . . . . .	84
8.3 Argonne Meteorological Data . . . . .	84
8.4 Upper-air Data . . . . .	84
8.5 Atmospheric Stability . . . . .	85
8.6 Height of the Mixing Layer . . . . .	85

## TABLE OF CONTENTS

	<u>Page</u>
9. THE CHICAGO AIR QUALITY MONITORING SYSTEM . . . . .	88
9.1 TAM Station 1 . . . . .	88
9.2 TAM Station 2 . . . . .	89
9.3 TAM Station 3 . . . . .	89
9.4 TAM Station 4 . . . . .	89
9.5 TAM Station 5 . . . . .	90
9.6 TAM Station 6 . . . . .	90
9.7 TAM Station 7 . . . . .	90
9.8 TAM Station 8 . . . . .	91
10. STATISTICAL RESULTS . . . . .	92
APPENDIXES	
A. FORTRAN Listings for Integrated-puff Dispersion Model . .	101
B. Sample Problem . . . . .	130
REFERENCES . . . . .	147

## LIST OF FIGURES

<u>No.</u>	<u>Title</u>	<u>Page</u>
1.1.	Buildup of SO <sub>2</sub> as the Superposition of Consecutive 2-hr Releases . . . . .	18
1.2.	Coordinate System for This Discussion . . . . .	19
1.3.	Rotation of the Coordinate System . . . . .	19
1.4.	Propagation for Three Hours of an Instantaneous Release under Assumption $\sigma_x = \sigma_y$ . . . . .	20
1.5.	Three-step Variation in Stability Class; $\Delta = 5000$ sec; $\sigma$ Is Continuous . . . . .	21
1.6.	Three-step Variations in Stability Class; $\Delta = 5000$ sec; Approximate Method; T Is Continuous; $\sigma = \sigma_5 + \Delta\sigma_4 + \Delta\sigma_3$ . . .	22
1.7.	Transverse Dispersion Parameter . . . . .	25
1.8.	Vertical Dispersion Parameter . . . . .	25
1.9.	Horizontal Dispersion Coefficients for Hourly Averages as Function of Downwind Distance. . . . .	27
1.10.	Vertical Dispersion Coefficients for Hourly Averages as Function of Downwind Distance. . . . .	27
1.11.	Synthesis of an Area Source of Buildings of Height Z . . . . .	32
1.12.	Choice of $\sigma_{y0} = n/2.4$ Ensures that Concentrations Will Be Uniform along the Line A-A . . . . .	33
2.1.	Flow Diagram for Calculation of Pollution Levels . . . . .	36
3.1.	Superposition of Area Source and Receptor Grids for a Region . . . . .	39
3.2.	Standard Area-source Grid about Reference Receptor . . . . .	40
3.3.	Evaluation of Concentrations due to Area Sources . . . . .	45
3.4.	Sample Printout of Subroutine PROUT with Chicago Map Overlay. . . . .	47
4.1.	Trajectory of Leading Puff of 1-hr Release . . . . .	52
4.2.	Trajectory of Trailing Puff of 1-hr Release . . . . .	52
4.3.	Locus of Puff Centers at Time M due to Release between Hours M - 3 and M - 2 . . . . .	52
4.4.	Multiple Reflections between a Stable Layer and Ground Represented Mathematically by Two Sets of Image Sources . .	55



## LIST OF FIGURES

<u>No.</u>	<u>Title</u>	<u>Page</u>
7.1.	Chicago Map of Major Sources . . . . .	60
7.2.	Chicago Map of SO <sub>2</sub> Area Sources . . . . .	61
7.3.	Sulfur Dioxide Source Distribution . . . . .	62
7.4.	Typical Winter Weekday System Load Pattern. . . . .	65
7.5.	Typical Summer Weekday System Load Pattern . . . . .	65
7.6.	Daily Peak Loads vs Average Daily Temperature for Spring . . . . .	65
7.7.	Daily Peak Loads vs Average Daily Temperature for Summer . . . . .	66
7.8.	Daily Peak Loads vs Average Daily Temperature for Fall. . .	66
7.9.	Daily Peak Loads vs Average Daily Temperature for Winter . . . . .	66
7.10.	A Typical Relation between Total System Load and Individual Unit Loadings . . . . .	68
7.11.	Gross Thermal Input vs Load with Approximating Line. . . . .	68
7.12.	Power Plant Unit Source Description Card . . . . .	70
7.13.	Source Identification Card . . . . .	73
7.14.	Source Emission Card . . . . .	74
7.15.	Janitor Function for Low-rise Space Heaters . . . . .	81
7.16.	Pumping-station Pattern . . . . .	83
8.1.	Vertical Profile of Temperature, Hinsdale, Illinois, April 11, 1969, 10:20 a.m. . . . .	86
8.2.	Vertical Profile of SO <sub>2</sub> , Hinsdale, Illinois, April 11, 1969, 10:20 a.m. . . . .	86
10.1.	Individual TAM Stations Monthly Means, Winter 1967 . . . . .	96
10.2.	Twenty-four-hour Averages for TAM's 1-5, All Seasons . . .	97
10.3.	Six-hour Averages for TAM's 1-5, All Seasons . . . . .	97
10.4.	Six-hour Averages for TAM 1, All Seasons. . . . .	97
10.5.	Six-hour Averages for TAM 2, All Seasons. . . . .	97
10.6.	Six-hour Averages for TAM 3, All Seasons. . . . .	98
10.7.	Twenty-four-hour Averages for TAM 3, All Seasons . . . . .	98

## LIST OF FIGURES

<u>No.</u>	<u>Title</u>	<u>Page</u>
10.8.	Six-hour Averages for TAM 4, All Seasons. . . . .	98
10.9.	Six-hour Averages for TAM 5, All Seasons. . . . .	98
B.1.	Chicago Map Showing Origin of Cartesian-coordinate System. . . . .	131
B.2.	Sample Problem: Input to APICS System. . . . .	132
B.3.	Sample Problem: Input of Emissions from Area Sources . . .	133
B.4.	Sample Problem: Input to Subroutine ADAT2 . . . . .	136
B.5.	Tabular Printout of Meteorological and Air Quality Data. . . .	136
B.6.	Printout of Estimates of SO <sub>2</sub> on 2 x 2-mi Grid According to Subroutine PROUT with Chicago Map Overlay and TAM 4 Wind Speed and Direction . . . . .	138
B.7.	Time Series of SO <sub>2</sub> on 1/15/67. . . . .	146

## LIST OF TABLES

<u>No.</u>	<u>Title</u>	<u>Page</u>
1.1.	Method of Fig. 1.5 ("exact") vs Method of Fig. 1.6 (approx) . . . . .	22
1.2.	Restrictions on the Plume-rise Formula . . . . .	29
1.3.	Exponents for the Wind-profile Law . . . . .	31
1.4.	Parameters Used to Describe Area Sources in Chicago . . . . .	33
3.1.	Variables in ENTRY PUFF . . . . .	40
3.2.	Use of Function JSUB to Store Wind-speed Values in Array WSBAR . . . . .	41
7.1.	Source Identification Card . . . . .	75
7.2.	Source Emission Card . . . . .	75
7.3.	Computer Card Input to PLANTSIM for Major SO <sub>2</sub> Sources in Chicago, 1966-1967 . . . . .	76
7.4.	Additional Point Sources in Chicago, 1966-1967. . . . .	83
9.1.	Total Number of Recorded 1-hr SO <sub>2</sub> Dosages (1966-1967) . . . . .	88
10.1.	Compilation of Validation Statistics . . . . .	93
10.2.	Stations 1-5: 6-hr Incidents--Winter 1967 . . . . .	99
10.3.	Stations 1-5: 24-hr Incidents--Winter 1967 . . . . .	99



## A Multiple-Source Urban Atmospheric Dispersion Model

by

J. J. Roberts, E. J. Croke, A. S. Kennedy,  
J. E. Norco, and L. A. Conley  
Center for Environmental Studies  
Argonne National Laboratory

### ABSTRACT

This report is a comprehensive documentation of the dispersion-model development phase of the Chicago Air Pollution Systems Analysis Program. A multiple-source, urban atmospheric dispersion model has been developed which describes transients such as morning transitions in atmospheric stability and mixing layer height. The dispersion model has been validated by comparison with over 10,000 hourly averages of sulfur dioxide monitored by the Department of Environmental Control of the City of Chicago. For example, the model accounts for 50% of the variance in 6-hr averages of observed data and 70% of the variance in 24-hr averages. Of particular significance is the capability of the model to describe "area sources" as volumetric clouds of pollutant and thus to evaluate the effect of these sources on dose points within, as well as external to, the area.

The atmospheric transport kernel in the model describes the instantaneous release (delta function) of pollutant, advection according to piecewise constant hourly wind vectors, and Gaussian diffusion about the centroid. Continuous plumes are simulated by integration in time of this point-source Green's function.

This report details the transport theory and all other computerized algorithms that influence the dispersion problem and presents statistical results of extensive validation studies.



PART I  
AN URBAN ATMOSPHERIC DISPERSION MODEL  
FOR STATIONARY SOURCES

1. INTRODUCTION TO PART I

A multiple-source, computerized, atmospheric dispersion model has been formulated and programmed for the IBM-360-75 system at Argonne National Laboratory.

This "integrated-puff" model is based on a kernel which allows for time-dependent variations in meteorological and source variables. This model therefore provides a more realistic physical simulation of the processes of smoke-plume dispersion than has hitherto been used by models based on the steady-state Gaussian-plume equation. Of special importance is the demonstrated capability of the model to estimate pollutant concentrations during periods of low wind speed. Furthermore, the simulation of area sources is greatly facilitated by the three-dimensional nature of the puff algorithm.

A source-oriented model is essential for the development of optimal incident-control strategies and long-range abatement plans. For example, a preliminary version of the integrated-puff model was programmed and used to develop a prototype optimal control model for the urban power-plant network (Croke and Kennedy, 1969). The model will be used in combination with Chicago's emission-inventory data as the primary analytical tool in the performance of a series of air-pollution system-analysis studies. These include:

1. Cost-effectiveness studies of alternative control strategies for specific source aggregates, such as power plants, the food-processing industry, the steel industry, and asphalt batching.
2. Development of rapid-response, automated, optimal incident-control strategies for the urban power-plant network, optimal gas allocation to dual fuel sources, process-emission control, etc., using mathematical programming and other operations-research techniques.
3. Development of long-range air-pollution abatement plans, oriented around the computer simulation of the city combined with projections of its population, fuel use, production, and transportation-network growth patterns. Emission-control legislation, zoning ordinances, etc., can be tested in a simulation of the region of the future, and cost effectiveness can be studied to evaluate the economic impact of pollution-abatement measures.

The model described in this report has several important aspects in common with earlier efforts (e.g., Koogler, 1967; Turner, 1964; Clarke, 1964):

1. An emission inventory is developed; large emitters are considered as point sources, and smaller residential, commercial, and industrial emitters homogenized as area sources in a standard grid.
2. A mathematical algorithm (typically based on the representation of turbulent diffusion by a Gaussian distribution) is used to describe the advection and diffusion of plumes from each source or source area.
3. Contributions from individual plumes are summed and sometimes integrated over time to give pollution doses at arbitrary locations.
4. The model is validated by statistical comparison with field measurements taken by an array of monitors.
5. Although the results of the validation study may indicate a refinement of certain physical assumptions (such as the plume-rise formulation) or inclusion of additional sources (such as distant power plants), no further improvement by linear regression or similar curve-fitting techniques is permitted; that is, the model is not tuned to a particular receptor or city. This last point is particularly important if the model is to be used in the development of incident-control strategies and long-range urban planning.

The integrated-puff model has been discussed at various stages of its evolution in quarterly reports ANL/ES-CC-002, -003, and -004 and most recently in a paper presented at the Symposium on Multiple Source Urban Dispersion Models, Chapel Hill, N. C., October 27-30, 1969. The latter reference, which also appears as quarterly -005, presents a general discussion of the model as well as preliminary validation studies of SO<sub>2</sub> concentrations at five Chicago monitoring stations during January 1967.

The present report has five functions:

1. Consolidate earlier published material on the model.
2. Discuss the algorithms as programmed in the IBM-360/75 code, including recent developments, to facilitate the calculation of concentrations on a regular grid of dose points.
3. Describe input and output formats and a sample problem.
4. Present the results of a more extensive validation study.
5. Present FORTRAN listings.



## 1.1 Source-oriented Dispersion Models

The most significant classification of mathematical models for the estimation of pollutant concentrations is their division into:

1. Those models tuned to a particular receptor or set of receptors by methods such as the linear correlation of observed and calculated values, or by any number of other approaches, whereby one or more free parameters are judiciously chosen, typically according to a least-squares fit.

2. Those so-called "source-oriented" models, which rely solely on a detailed emission inventory and theories of atmospheric advection, turbulent diffusion, and possibly aerochemical reactions.

There has been a further attempt to classify the source-oriented models as "short" or "long" term, depending upon whether transients (e.g., hour-by-hour calculations) or percentile distributions are to be evaluated. Although models purporting to focus on annual statistics tend to be simpler in concept and thus more economical in terms of computer costs, it is unclear why a source-oriented model, which adequately predicts the statistical distribution of hourly averages, especially in the critical region above the 90th percentile, cannot be used to estimate hourly values in real time, given the appropriate emission and meteorological data. On the other hand, a successful transient model should be capable of developing a long-term statistical picture of air quality.

For example, the Martin-Tikvart (1969) model, before correlation with observed values, appears to overpredict seasonal averages by a factor of three, even at high pollutant levels. The fault may be with emission inventories, or with the handling of the statistics of variations in mixing layer height, or with any combination of these and other assumptions. However, if the model could perform its statistical function satisfactorily, there is every reason to expect that, with minor modifications, it would be adequate to describe temporal variations in air quality. The more sophisticated Fortak (1969) model is also of this genre; monthly averages are usually estimated accurately; however, large deviations often occur above the 90th percentile.

Models designed to synthesize temporal as well as spatial variations in sources, meteorology, and thus air quality tend to emphasize the details of atmospheric dispersion with rigor governed mainly by an imperfect knowledge of the physical and chemical processes and by computer capabilities. The major ground rule for the development of the integrated-puff model at Argonne was to formulate the most sophisticated source-oriented estimation technique consistent with the two limitations mentioned above. If this model could adequately estimate variations in pollutant levels using

input variables normally available in an air-quality-control region, it could then serve as an effective tool in the development of strategies for episodal control. Furthermore, the model could be run with extensive historical data or run in steady state for a number of cases (as with Martin-Tikvart and Fortak) to acquire air-quality statistics.

It was also assumed that, once a successful model had been designed, simplifications to reduce computer requirements could then be proposed and evaluated.

Although atmospheric dispersion calculations based on the partial differential equation of diffusion and advection (K-theory) have been proposed, the multisource, transient models described in the open literature have been based on the assumption of a Gaussian distribution of effluent. Existing source-oriented, time-dependent models fall into two categories:

1. Those based on an adoption of the steady-state plume equation,

$$\chi(x,y,z) = \frac{Q}{2\pi u \sigma_y \sigma_z} \exp \left[ - \left( \frac{y^2}{2\sigma_y^2} + \frac{z^2}{2\sigma_z^2} \right) \right], \quad (1.1)$$

where advection in the  $x$  direction is usually depicted by a wave front moving at the mean wind speed,  $u$ . Models in this category then differ in the manner in which they treat subsequent variations in wind direction and speed (Koogler, 1967; Turner, 1964, 1968; Johnson et al., 1969).

2. Those based on a Gaussian-puff kernel (point-source Green's function),

$$G(x, y, z, t - t') = \frac{\exp \left( - \left\{ \frac{[x - u(t - t')]^2}{2\sigma_x^2} + \frac{y^2}{2\sigma_y^2} + \frac{z^2}{2\sigma_z^2} \right\} \right)}{(2\pi)^{3/2} \sigma_x \sigma_y \sigma_z} \quad (1.2)$$

with concentrations from continuous emissions calculated by a convolution integral,

$$\chi(x, y, z, t) = \int_0^t dt' Q(t') G(x, y, z, t - t') \quad (1.3)$$

(Start and Markee, 1967; Roberts et al., 1969; Shieh, 1969).

The transient nature of models in the second category recommends their use in analyses of the concentration field due to short-term releases

from single sources (for example, theoretical nuclear-reactor accident studies of Start and Markee, 1967, or in studies of urban air quality during periods of marked diurnal variations in meteorological variables).

The only source-oriented models evaluated by extensive validation studies are Turner's St. Louis model (Turner, 1968),\* which epitomizes the plume formulation, and the integrated-puff model (Roberts et al., 1969), which is the subject of this report and has been tested on SO<sub>2</sub> data in Chicago. Comparison of these two studies indicates that the latter yields superior estimates of pollution levels. For example, 3341 twenty-four-hour averages with a mean of approximately 0.04 ppm observed in the St. Louis study are estimated with a skill score (based on chance) of approximately 0.20 (Croke et al., 1968a; Turner, 1968). A corresponding analysis of 1800 six-hour averages with a mean of 0.11 ppm in this Chicago study yields a skill score of 0.55 with an R<sup>2</sup> value of 0.43 (see Section 10). However, the reason for this significant difference in performance may lie in the relative quality of emission or meteorological data, and a fair comparison of the two models should be made using identical input variables.

## 1.2 Transport of Airborne Pollutants

Pollution concentrations from a given source are evaluated in the integrated-puff model by forming a convolution sum of two time series: (1) piecewise (hourly) constant stack emissions and (2) a discrete transfer function, based on the mathematical representation of an integrated puff. The latter is found by integration of a Gaussian kernel representing advection according to a time series of piecewise constant wind vectors, and three-dimensional dispersion according to a time series of piecewise constant classes of atmospheric stability. For example, results indicate that one of the more important types of short-term pollution incidents, the morning fumigation, which is characterized by low winds (up to 6 mph) and by a sharp transition from stable stratification to strong vertical mixing, is simulated successfully. Details of the development of the kernel and limitations on its range of applicability are discussed in the remainder of this section.

### 1.2.1 Dispersion Kernel

For a steady mean wind  $U$  in the downwind ( $x$ ) direction, with  $y$  and  $z$  representing unbounded\*\* crosswind and vertical dimensions, a normal distribution yields the following Green's Function:

---

\*Reported in Croke et al., 1968b, pp. 34-43.

\*\*Modifications to account for the finite geometry associated with the ground and inversions aloft are considered in Sections 1.2.8 and 4.1.

$$\frac{X(t, t')}{Q(t')} = \frac{\exp\left(-\left\{\frac{[x - U(t - t')]^2}{2\sigma_x^2} + \frac{y^2}{2\sigma_y^2} + \frac{z^2}{2\sigma_z^2}\right\}\right)}{(2\pi)^{3/2}\sigma_x(t-t')\sigma_y(t-t')\sigma_z(t-t')} e^{-0.693(t-t')/T_{1/2}}, \quad (1.4)$$

where  $X(t, t')$  is the concentration at time  $t$  due to an instantaneous release  $Q$  at time  $t'$  and position  $(0, 0, 0)$  (Pasquill, 1962; Slade, 1966). The origin of the Cartesian system is arbitrary. The dispersion coefficients  $\sigma_x$ ,  $\sigma_y$ , and  $\sigma_z$  are assumed to be functions only of the delay time  $T = t - t'$  and the atmospheric stability class as defined by Turner (Turner, 1964).  $T_{1/2}$  is the half-life of radioactive decay or of any other removal mechanism that can be characterized by an exponential decay.

Assume  $Q(t)$  piecewise constant over a fundamental time interval  $\Delta$  (the computer program is written for  $\Delta = 1$  hr); then, for the special case of a steady wind in the  $x$ -direction, the concentration  $X(x, y, z, M)$  at time  $t - M\Delta$  can be found by a convolution of the piecewise constant emissions with a series of integrals (the discrete transfer function) evaluated over periods of duration  $\Delta$ :

$$\begin{aligned} X(x, y, z, M) &= \sum_{N=1}^M Q_{M-N+1} \int_{(N-1)\Delta}^{N\Delta} dT \frac{\exp\left\{-\left[\frac{(x-UT)^2}{2\sigma_x^2} + \frac{y^2}{2\sigma_y^2} + \frac{z^2}{2\sigma_z^2}\right]\right\} \exp(-0.639T/T_{1/2})}{(2\pi)^{3/2}\sigma_x(T)\sigma_y(T)\sigma_z(T)} \\ &= \sum_{N=1}^M Q_{M-N+1} G_N. \end{aligned} \quad (1.5)$$

This is represented schematically in Fig. 1.1 by the buildup of  $\text{SO}_2$  due to three ( $M = 3$ ) consecutive 2-hr ( $\Delta = 2$ ) piecewise constant emissions.

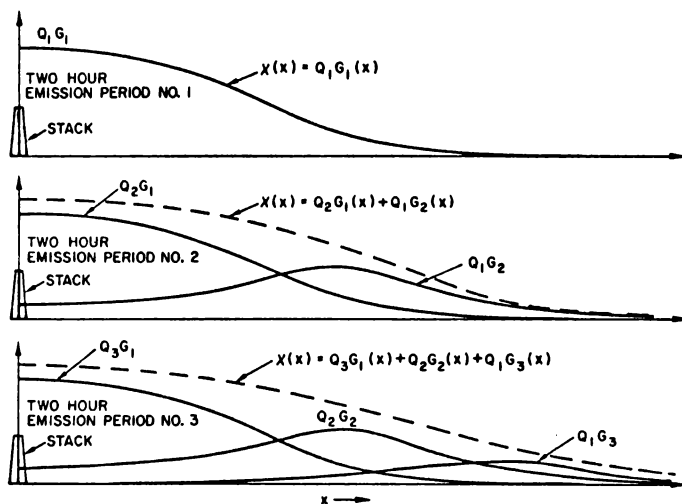


Fig. 1.1

Buildup of  $\text{SO}_2$  as the Superposition of Consecutive 2-hr Releases. ANL Neg. No. 112-9734.

Equation 1.5, the contribution from an individual source to the concentration at time  $M\Delta$ , must then be summed over all sources.

The following development is a generalization of this equation to account for variations (piecewise constant) in wind direction, wind speed,

and atmospheric stability. The coordinate system used will take  $z$  in the vertical direction perpendicular to the plume axis (assumed horizontal), and the  $x$  and  $y$  directions (also velocity components,  $u, v$ ) in the horizontal plane, as shown in Fig. 1.2. If  $\theta$  is the conventional wind direction, then  $u = U \sin \theta$  and  $v = U \cos \theta$ .

### 1.2.2 Generalized Wind Direction

Let the dose point  $x, y$  in the coordinate system of Fig. 1.2 be associated with the angle  $\psi = \tan^{-1}(x/y)$ . Consider a coordinate system rotated from the standard system of Fig. 1.2 through an angle  $\theta$ , so that the dose point  $(x, y)$  is now represented by its cross wind and downwind distances  $\bar{x}$  and  $\bar{y}$  (see Fig. 1.3).

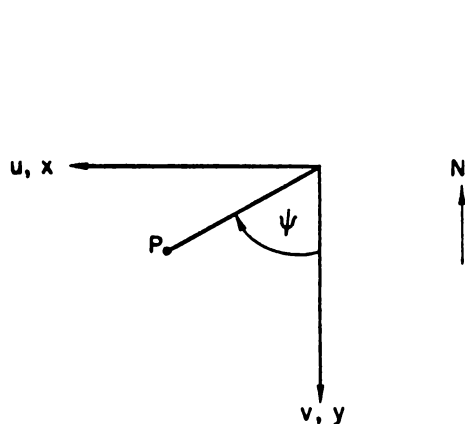


Fig. 1.2. Coordinate System for This Discussion.  
ANL Neg. No. 113-1106.

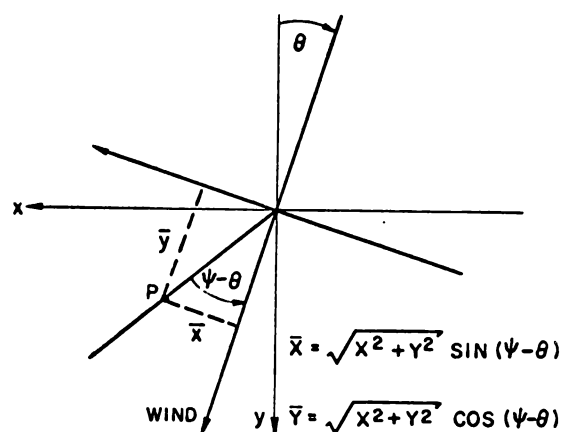


Fig. 1.3. Rotation of the Coordinate System.  
ANL Neg. No. 113-1107.

The equations for  $\bar{x}$  and  $\bar{y}$  (in Fig. 1.3) can be substituted directly into Eq. 1.5, and, since  $\sin \psi = x/\sqrt{x^2 + y^2}$ ,  $\cos \theta = v/U$ ,  $\cos \psi = y/\sqrt{x^2 + y^2}$ , and  $\sin \theta = u/U$ , the integrals in Eq. 1.5, expressed in terms of the standard coordinate system of Fig. 1.2, become

$$\int_{(N-1)\Delta}^{N\Delta} dT \frac{\exp\left\{-\left[\frac{(x-uT)^2 + (y-vT)^2}{2\sigma_h^2} + \frac{z^2}{2\sigma_z^2}\right]\right\}}{(2\pi)^{3/2}\sigma_h^2(T)\sigma_z(T)} e^{-0.693T/T_{1/2}}. \quad (1.6)$$

Note that this simplification is contingent upon the assumption of  $\sigma_x = \sigma_y = \sigma_h$ , a horizontal dispersion coefficient. There are valid arguments (to be reviewed in Section 1.2.4) why this assumption is questionable, except perhaps for very low wind speeds. From a computational standpoint, the puff appears circular if  $\sigma_x = \sigma_y$ , and, consequently, since its  $x$ - $y$  shape is independent of wind direction, the generalization of the kernel to accommodate variations in wind direction is greatly simplified.

### 1.2.3 Variable Wind Speed and Direction

Consider at time  $M\Delta$  the circular puff ( $\sigma_x = \sigma_y = \sigma_h$ ) corresponding to an emission during the time period  $(M-N)\Delta$  to  $(M-N+1)\Delta$ . (Note that

the index  $N$  "looks backwards" in time.) The leading edge of the puff (emitted  $T = N\Delta$  hours ago) undergoes  $x$ -advection according to

$$[u_{M-N+1} + u_{M-N+2} + \dots + u_M] \Delta, \quad (1.7)$$

and the trailing edge of the puff (emitted 1 hr later at  $T = (N-1)\Delta$ ) undergoes  $x$ -advection according to

$$(u_{M-N+2} + \dots + u_M) \Delta. \quad (1.8)$$

Thus, the integrals over  $T$  represented by Eq. 1.6, which describe a continuous constant emission (from leading to trailing edge) during a period  $\Delta$ , become

$$G_{M,N} = \int_{(N-1)\Delta}^{N\Delta} dT \frac{\exp \left[ - \left( \left\{ x - \Delta \sum_{j=M-N+2}^M u_j - u_{M-N+1} [T - \Delta(N-1)] \right\}^2 / 2\sigma_h^2(T) \right) + \left\{ y - \Delta \sum_{j=M-N+2}^M v_j - v_{M-N+1} [T - \Delta(N-1)] \right\}^2 / 2\sigma_h^2(T) \right] + z^2 / 2\sigma_z^2(T)}{(2\pi)^{3/2} \sigma_h^2(T) \sigma_z(T)} e^{-0.693T/T_{1/2}}, \quad (1.9)$$

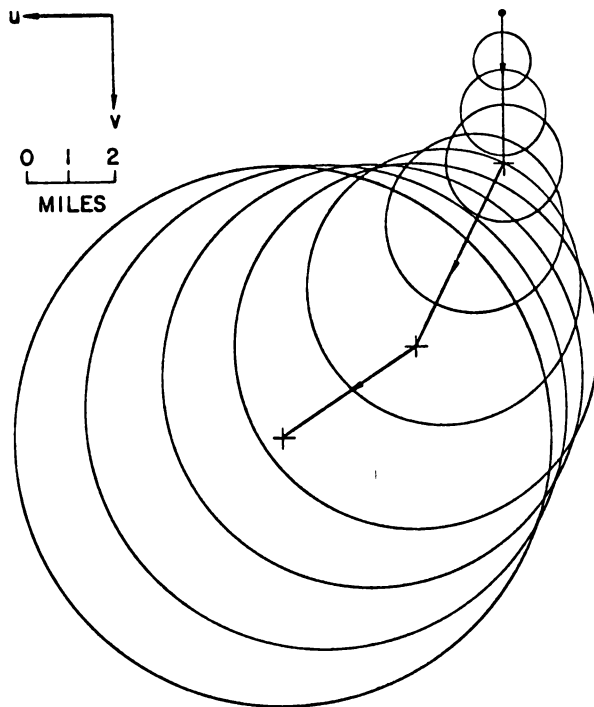


Fig. 1.4. Propagation for Three Hours of an Instantaneous Release under Assumption  $\sigma_x = \sigma_y$ . ANL Neg. No. 113-1108.

where variations in wind velocity are represented by the piecewise constant series  $[u_j]_1^M$ , and  $[v_j]_1^M$ . The propagation of a circular puff for varying wind speed and direction is easily visualized by the schematic diagram of Fig. 1.4. In Fig. 1.4 the center of the instantaneous release at time = 0 ( $t' = 0$  in Eq. 1.4) is advected according to the three consecutive, hourly-average, space-independent velocity vectors.

The simulation of lake breezes and unusual urban circulations requires continuity in the wind field and conservation of the mass of pollutant and thus the introduction of a vertical velocity component. This component, as well as the horizontal quantities  $u$  and  $v$ , will be highly dependent upon space and time. Equation 1.9 considers only time dependence of the

wind, although one can use different sequences  $[u_j]_1^M$  and  $[v_j]_1^M$ , depending upon the location of the dose point. Using the lake breeze, and in particular

a dose point near the confluence, as an example, we must allow for two converging streams and a vertical motion that is highly space-dependent. The algorithms presented in this report are not yet expressed in a sufficiently general manner to handle this space dependence. However, it is relatively straightforward to approximate a three-dimensional velocity field by the three components  $u(x, y, t)$ ,  $v(x, y, t)$ , and  $w(x, y, t)$  and restate the basic algorithm.

#### 1.2.4 Variable Atmospheric Stability

In a manner completely analogous to the x-advection equations (Eqs. 1.7 and 1.8) for the series  $[u_j]_1^M$ , variations in atmospheric stability can be approximated by the series  $[i_j]_1^M$ , where  $i$  is the stability class (1, 2, ..., 7), and the dispersion coefficients in Eq. 1.9 are modified to account for different rates of horizontal and vertical growth throughout the lifetime of the puff.

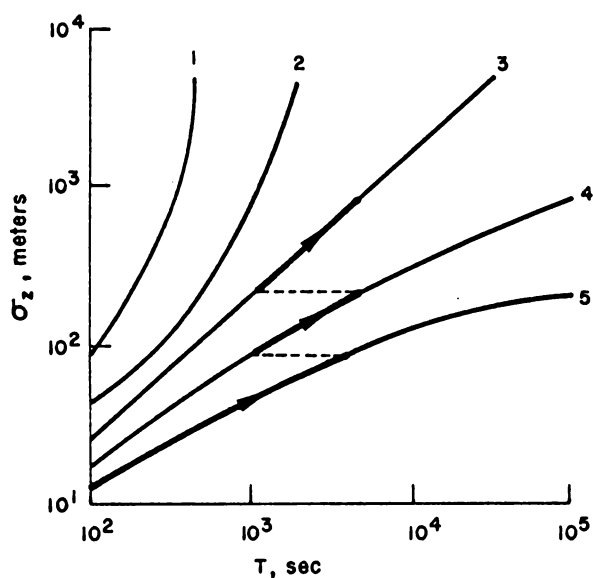


Fig. 1.5. Three-step Variations in Stability Class;  $\Delta = 5000$  sec;  $\sigma$  Is Continuous. ANL Neg. No. 113-1110.

This procedure requires calculation of a pseudotime for travel within each new stability class. Although the stability class does not change every hour, a computer program based on hourly steps must provide a general algorithm for handling this situation. Unfortunately, the process in Fig. 1.5 appears devoid of any simple algorithm suitable for economic programming on the computer. The problem is that the dispersion coefficient  $\sigma$  should be kept continuous in spite of the fact that we are forced to use a set of discrete functions.

An approximation to the "continuous  $\sigma$ " scheme of Fig. 1.5 is proposed in Fig. 1.6 for which the time-of-flight is continuous and the value of

Postulating variations in  $\sigma$  with  $T$  according to Turner's Nashville study, and requiring continuity of  $\sigma$  at each time step, we might describe a three-step process by the paths shown in Fig. 1.5. At the conclusion of the first 5000 sec period in Fig. 1.5,  $\sigma_z = 90$  meters according to stability class 5. A change in stability to class 4 during the second period requires operation along a different  $\sigma_z$  curve. Continuity of cloud dimensions at this juncture implies  $\sigma_z = 90$  corresponding to a new, pseudo time-of-flight  $T = 1000$  sec.

Associated with each puff are functions of time,  $\sigma_h(t)$  and  $\sigma_z(t)$ , which could in principle be calculated according to the procedure of Fig. 1.5.

$\sigma$  is determined by adding changes in  $\sigma$ . The two procedures are compared in Table 1.1, where it is shown that a tolerable error is incurred by the approximate method of Fig. 1.6 as opposed to the "exact" method of Fig. 1.5. In this comparison, a single change in stability occurs at the beginning of period 2.

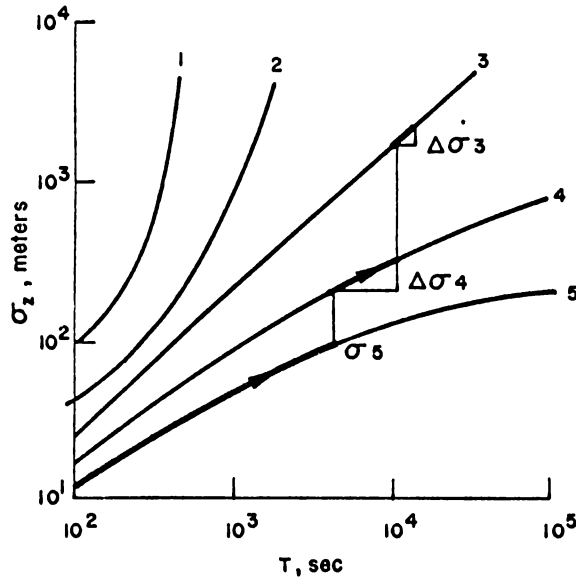


Fig. 1.6

Three-step Variations in Stability Class;  
 $\Delta = 5000$  sec; Approximate Method; T  
 Is Continuous;  $\sigma = \sigma_5 + \Delta\sigma_4 + \Delta\sigma_3$ .  
 ANL Neg. No. 113-1109.

TABLE 1.1. Method of Fig. 1.5 ("exact") vs Method of Fig. 1.6 (approx)  
 $\Delta = 5000$  sec;  $\sigma$  at 10,000 sec

Stability Class		$\sigma_y, m$		$\sigma_z, m$	
Period 1	Period 2	Exact	Approx	Exact	Approx
4	5	2000	1900	200	230
5	4	1900	1700	200	220
3	5	2400	2500	1000	1100
5	3	2500	2100	1100	1120

A comparatively simple algorithm can be written to implement the procedure of Fig. 1.6. We require  $\sigma(M, N, T)$  in the integrals of Eq. 1.9. Given  $S(i, T)$ , a set of functions of the time-of-flight  $T$  describing a family of stability curves parameterized by class  $i$ , and given a sequence of stability classes  $[i_j]_1^M$  corresponding to real time values of the class for each time period  $j = 1, M$  of duration  $\Delta$ , then one can construct the function  $\sigma(M, N, T)$  based on Fig. 1.6.

Let  $M = 3$  (end of hour 3);  $N$  is time looking back,  $T$  is travel time of puff. For  $N = 1$ , we have  $\int_0^\Delta$  for which



$$\sigma(M, N, T) = \sigma(3, 1, T) = S(i_3, [0]\Delta + T - [N - 1] \Delta) = S(i_3, T). \quad (1.10)$$

For  $N = 2$ , we have  $\int_{\Delta}^{2\Delta}$  for which

$$\begin{aligned} \sigma(3, 2, T) = & S(i_2, [0]\Delta + T - [N - 1] \Delta) + \{S(i_3, [1]\Delta + T - [N - 1] \Delta) \\ & - S(i_3, [0]\Delta + T - [N - 1] \Delta)\}. \end{aligned} \quad (1.11)$$

By defining  $S(i, t) = 0$  for  $t \leq 0$ , we can generalize Eq. 1.11 to

$$\begin{aligned} \sigma(M, N, T) = & \sum_{j=M-N+1}^M \{S(i_j, [j - (M - N + 1)] \Delta + T - [N - 1] \Delta) \\ & - S(i_j, [j - (M - N + 1) - 1] \Delta + T - [N - 1] \Delta)\}, \end{aligned} \quad (1.12)$$

which reduces to

$$\sigma(M, N, T) = \sum_{j=M-N+1}^M \{S(i_j, \Delta[j - M] + T) - S(i_j, \Delta[j - M - 1] + T)\}. \quad (1.13)$$

In the computer code, this calculation is performed in subroutine KERN with the actual dispersion coefficients (see Section 1.2.5) defined by the functions SIGX, SIGY, and SIGZ.

### 1.2.5 Dispersion Coefficients

The integrated-puff model is similar to earlier dispersion models in that a Gaussian distribution with appropriate dispersion parameters is the fundamental assumption. Although the puff model is closer to physical reality, it is still dependent upon and sensitive to these dispersion coefficients.

There are a number of sets of functions for  $\sigma_y$  and  $\sigma_z$  with either downwind distance or time-of-flight as the independent variable, and for the most part these curves are in mutual agreement. Some modifications (for example, by Turner, 1968, in the St. Louis study) have been made to account for greater instability over a city, since the various sets of curves are based on experiments over level, rural terrain. Field experiments in St. Louis by McElroy and Pooler (1968) support these modifications, although their estimates of the coefficient of vertical diffusion may be excessive if applied to smoke plumes, because their data were obtained by tracer releases at ground level.

A serious consideration is the choice of the function  $\sigma_y(j, t)$  required for the integrated-puff model. The results of field experiments on instantaneous and steady released (Cramer, 1964; McElroy and Pooler, 1968) have been processed to yield dispersion coefficients which fit the plume model:

$$X = \frac{Q \exp \left[ - \left( \frac{y^2}{2\sigma_y^2} + \frac{z^2}{2\sigma_z^2} \right) \right]}{\pi \sigma_y \sigma_z U} . \quad (1.14)$$

Extensive horizontal measurements were used to determine  $\sigma_y$  statistically;  $\sigma_z$  was inferred from these. Clearly, the introduction of an additional dispersion coefficient  $\sigma_x$  with a corresponding change in the basic equation will alter the analysis of the experiments and thus the conclusions as to the magnitude of dispersion coefficients.

Another concern is the assumption  $\sigma_x = \sigma_y$ , which results in the advecting/diffusing circular puff described by Fig. 1.4. Although not strictly correct, it is convenient to consider  $\sigma_x$  as the superposition of two components: (1) horizontal turbulence due to eddies of a scale smaller than the puff size, and (2) upwind/downwind elongation due to vertical shear. Thus, although the assumption  $\sigma_x = \sigma_y$  may be reasonable for unstable and neutral conditions of atmospheric stability, it may be inappropriate when the effect of wind shear is magnified by the existence of a stable atmosphere which inhibits vertical mixing (Bowden, 1965; Cramer, 1968).

The basic integral (Eq. 1.5) is of the form

$$X \propto \int_A^B \frac{\exp \left\{ - \left[ \frac{(x - UT)^2}{2\sigma_x^2} + \frac{y^2}{2\sigma_y^2} + \frac{z^2}{2\sigma_z^2} + 0.693T/T_{1/2} \right] \right\}}{\sigma_x \sigma_y \sigma_z} dT, \quad (1.15)$$

where  $\sigma_x$ ,  $\sigma_y$ , and  $\sigma_z$  are functions of travel time  $T$ . The original version of the integrated-puff model (ANL/ES-CC-005) used the set (designated in this section by  $\sigma_{TSL}$ ) of time-dependent dispersion curves used by Turner (1968) in his St. Louis model. These are shown in Figs. 1.7 and 1.8 for seven classes of atmospheric stability.

For the limiting case  $U \rightarrow 0$ , the integrated-puff model represented by Eqs. 1.5 and 1.15 yields steady state results which are significantly different from standard plume formulas.

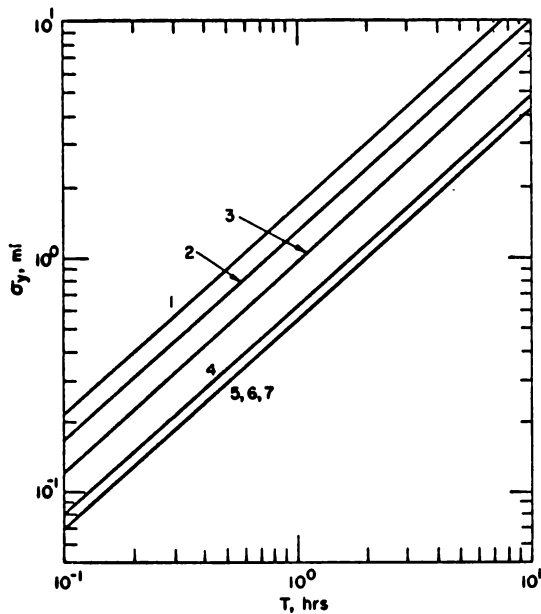


Fig. 1.7. Transverse Dispersion Parameter (Turner, 1967). ANL Neg. No. 113-2876.

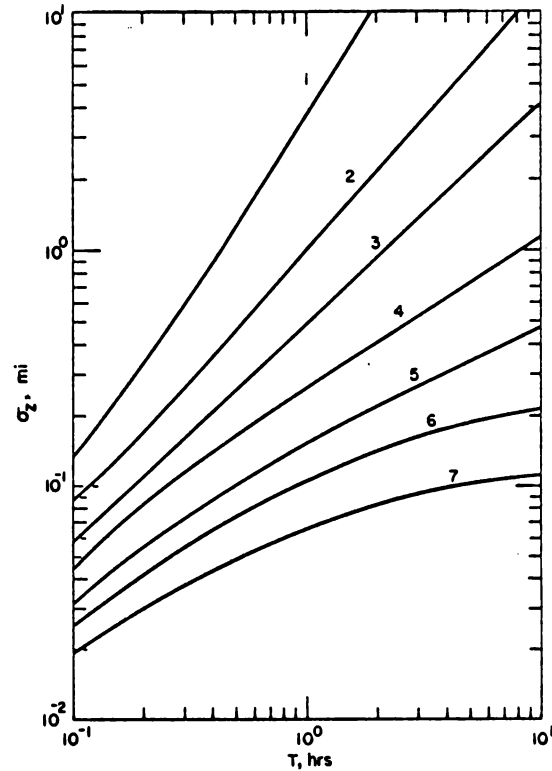


Fig. 1.8. Vertical Dispersion Parameter (Turner, 1967). ANL Neg. No. 113-2869.

Substitution of the following into Eq. 1.15:

$z = 0$	(ground level source)
$y = 0$	(centerline calculation)
$\sigma_y(T) = \sigma_x(T) = \sigma_{x_{TSL}}(T) = \alpha_x T$	(linear approximation)
$\sigma_z(T) = \sigma_{z_{TSL}}(T) = \alpha_z T$	(linear approximation)
$A = 0, B = \infty$	(steady state calculation)
$T_{1/2} = \infty$	(no decay)

permits integration in closed form to yield, in the limit  $U \rightarrow 0$ ,

$$X_{U \rightarrow 0} \propto 1/x^2.$$

Steady state plume equations for ground level source and centerline dose points are of the form

$$X \propto \frac{1}{U\sigma_y\sigma_z}.$$

Substitution of  $\sigma_y = \sigma_y(T)$  and  $\sigma_z = \sigma_z(T)$  where  $T = x/U$  as in Turner's St. Louis model yields:

$$X_{U \rightarrow 0} = 0 \quad \text{for } x > 0$$

since, as  $U \rightarrow 0$ ,  $T = x/U \rightarrow \infty$  for  $x > 0$  as do

$$\sigma_y(T) \text{ and } \sigma_z(T).$$

Substitution of  $\sigma_y = \sigma_y(x)$  and  $\sigma_z = \sigma_z(x)$  as in Turner's Workbook on Atmospheric Dispersion Estimates yields:

$$X_{U \rightarrow 0} = \infty$$

since  $\sigma_y(x)$  and  $\sigma_z(x)$  remain finite and independent of  $U$ .

At high wind speeds ( $>10$  mph), both plume and integrated-puff models that use  $\sigma(T)$  describe the effluent from a point source as a very narrow, highly concentrated beam. In the simulation of ground-level concentrations due to large power plants, the severe directional dependence associated with the above situation causes fluctuations of up to 1 ppm for changes in the mean hourly wind direction of less than  $3^\circ$ . Hourly-average, direction-sensitive peaks of this magnitude are not observed in the Chicago data (2 years of hourly  $\text{SO}_2$  readings at eight monitoring stations). A first attempt to remedy this anomaly, which seriously affects estimates of peak hourly but not daily average dose rates, is to introduce an alternate set of dispersion coefficients.

In almost all Gaussian plume models of atmospheric diffusion (for example, Pasquill, 1962 and Turner, 1967), dispersion coefficients are expressed in terms of the downwind distance  $x$  rather than the time-of-flight  $T$ . Thus, the rate of spread is not expressed as an explicit function of wind speed. Typically, first approximations to  $\sigma_y$  and  $\sigma_z$  are obtained by fitting power laws

$$\sigma_y = A_y X^{B_y}, \quad \sigma_z = A_z X^{B_z}$$

to field data. Figures 1.9 and 1.10 show the horizontal and vertical dispersion coefficients suggested by Turner (1967), modified for hour-long rather than 10-min averages. (In this discussion, this set will be designated  $\sigma_{\text{TWB}}$ .)

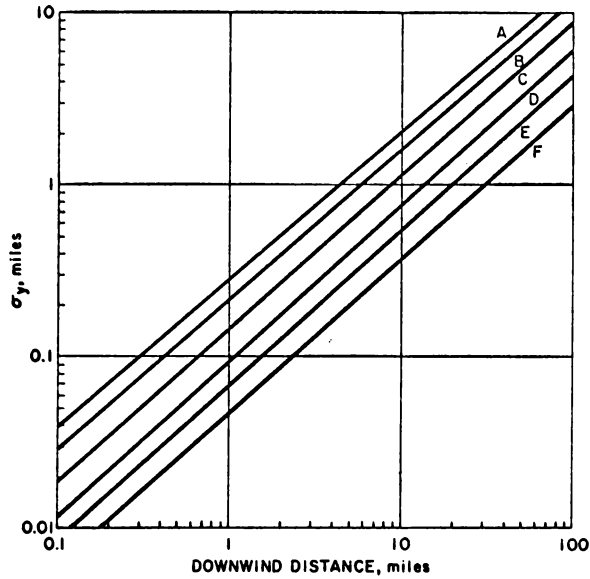


Fig. 1.9. Horizontal Dispersion Coefficients for Hourly Averages as Function of Downwind Distance [Fig. 3.2 of Tumer, 1967, multiplied by  $(60/10)^{0.2}$  to correct for difference in averaging times]

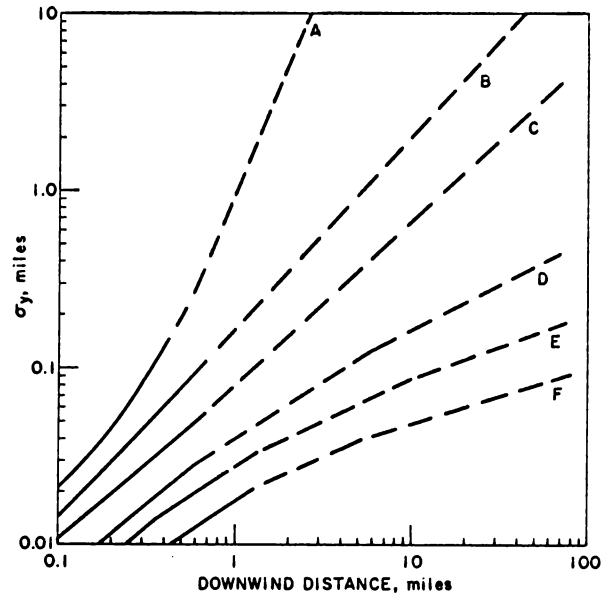


Fig. 1.10. Vertical Dispersion Coefficients for Hourly Averages as Function of Downwind Distance [Fig. 3.3 of Tumer, 1967, multiplied by  $(60/10)^{0.2}$  to correct for difference in averaging times]

The apparently unrealistic directional sensitivity at high wind speeds of the model with  $\sigma_{TSL}(T)$  was therefore partially corrected by the following assumption:

$$\sigma(i, t) = \max \left\{ \sigma_{TSL}(t), \sigma_{TWB}(Ut) \right\}, \quad (1.16)$$

where the downwind distance,  $x$ , of the puff center is expressed by  $x = Ut$ . The result is a transition from  $\sigma_{TSL}(t)$  to  $\sigma_{TWB}(x = Ut)$  for wind speeds greater than 7 mph. The exact value of the wind speed for which  $\sigma_{TSL}$  equals  $\sigma_{TWB}$  in Eq. 1.16 depends upon the time  $T$ , the atmospheric stability class, and whether the vertical or horizontal dispersion coefficient is being evaluated. For example, with a wind speed of 20 mph and a receptor 10 miles downwind of a power plant,  $\sigma_{y,TSL}(0.5 \text{ hr}) = 0.33 \text{ mile}$  (a  $\pm\sigma$  cone of  $4^\circ$ ) and  $\sigma_{y,TWB}(10 \text{ mi}) = 0.75 \text{ mi}$  (a  $\pm\sigma$  cone of  $9^\circ$ ). The use of Eq. 1.16 is therefore responsible for about a 60% reduction in the plume peak and a corresponding increase in width. Equation 1.16 rarely influences the estimation of vertical dispersion since usually  $\sigma_{z,TSL}(t) \approx \sigma_{z,TWB}(Ut)$ . Nevertheless, even with the assumption of Eq. 1.16, both plume and puff models will, in general, reflect this directional sensitivity for major point sources. Looking at the problem from another angle, one can conclude that, since the trajectory of the centerline of a plume can rarely be specified to better than  $\pm 10^\circ$ , the short-term estimated and observed concentrations can easily differ by a factor of 2, regardless of the model employed. Thus, whether one is

estimating pollutant contributions and verifying by comparison with observations, or if one is using a regression approach to correlate observed data with point-source emissions, the uncertainty caused by an inability to specify plume trajectories implies a fundamental uncertainty in the ability to verify the model. These observations are in contrast to Hilst (1969) who, considering a statewide model of relatively homogeneous area sources, concluded that his results were insensitive to  $\sigma_y$ .

The dispersion coefficients  $\sigma_y(i, t)$  and  $\sigma_z(i, t)$  defined by Eq. 1.16 and Figs. 1.7-1.10 are calculated by the functions SIGX, SIGY, and SIGZ in the computer program.

### 1.2.6 Effective Stack Height

The effective stack height  $H$  is the height above ground that best defines the centerline of the plume. The plume is assumed to originate as a point source at an altitude  $H$  feet above ground at the location of the stack. If aerodynamic downwash causes the plume to break up and mix rapidly downward in the vicinity of the stack,  $H$  may be set equal to the actual physical height,  $H_s$ . Observations of a local utility indicate that this phenomenon occurs frequently for wind speeds greater than 15 mph. Otherwise, a plume rise  $\Delta H$  is added to the physical stack height  $H_s$ , so that

$$H = H_s + \Delta H, \quad (1.17)$$

where  $\Delta H$  is estimated as described below.

Smoke plume-rise calculations in this model are based on a plume-rise formula derived from observations at TVA stations and other power plants (Carson and Moses, 1967). (The momentum term in their original formulation is omitted in the following equation since its contribution is generally negligible compared to thermal buoyancy.)

$$\Delta H \text{ (ft)} = KQ_s^{1/2}/U, \quad (1.18)$$

where

$\Delta H$  = plume rise (ft),

$Q_s$  = heat-emission rate from stack (Btu/hr),

$U$  = wind speed (mph) at height of stack,

and

$K = 0.870$  (unstable; class 3),  $0.354$  (neutral; class 4),  
 $0.222$  (stable; class 5).

Three restrictions placed on the use of Eq. 1.18 are listed in Table 1.2.

TABLE 1.2. Restrictions on the Plume-rise Formula (Eq. 1.18)

---

1. Low Wind Speeds (U)

If U is estimated to be less than 4 mph, the value 4 mph is used in Eq. 1.18.

2. Stability Class and the Coefficient K

If the physical stack height ( $H_s$ ) is equal to or greater than 200 ft,  $K = 0.354$  (neutral) is used, even though the stability index indicates unstable conditions.

3. Mixing-layer or Lid Height ( $H_m$ )

- a. If the physical stack height  $H_s$  is greater than  $H_m$ , an infinite value for  $H_m$  is assumed with plume rise and dispersion according to stable atmospheric conditions.
  - b. A minimum plume rise  $\Delta H_{\min}$  (DHMIN in subroutine ISPDV) is calculated, based on the coefficients for stably stratified air. If this minimum effective stack height,  $H = H_s + \Delta H_{\min}$ , is greater than the lid height  $H_m$ , it is used; the plume is then analyzed as described in restriction 3a.
  - c. If  $(H_s + \Delta H_{\min}) < H_m$  and if the plume rise  $\Delta H$  based on the actual stability class yields an effective stack height greater than  $H_m$ , i.e., if  $(H_s + \Delta H_{\min} < H_m)$  and  $(H_s + \Delta H \geq H_m)$ , the effective stack height is restricted to the lid height  $H_m$ .
- 

Restriction 1 in Table 1.2 limits the minimum wind speed to be used in Eq. 1.18. This reflects the fact that the equation is an empirical one in which the parameters  $n$  and  $m$  in an equation of the form  $\Delta H = KQ_s^n U^m$  were found by multiple linear regression. A comparison of Eq. 1.18 with TVA data (Carpenter *et al.*, 1967) indicates good agreement down to wind speeds of about 6 mph. Below this, the  $1/U$  factor in the equation causes an overestimation of the plume rise. An arbitrary restriction on a minimum value of  $U$  in Eq. 1.18 has therefore been made.

Restriction 2 occurs because for plume-rise calculations the vertical variation of temperature at heights greater than 200 ft is best characterized by a neutral lapse rate, even though unstable conditions may exist the first few hundred feet above ground.

Restriction 3 is a variation on the standard assumption of an impenetrable lid. Rather than obey a law of perfect reflection, effluent emitted beneath an inversion is assumed to penetrate the stable layer at least as far as would be anticipated if the effluent were emitted in stably stratified air. This characterization is particularly important in estimating ground-level concentrations due to power plants. For example, a 300-MWe plant (single stack) will have a plume rise of approximately 400 ft in stable air and 600 ft under neutral conditions (note restriction 2 in Table 1.2) when the wind speed at the physical stack height,  $H_s$ , is 10 mph.

For a representative physical stack height of 400 ft, restriction 3 implies the following:

1. If  $H_m = 3000$  ft, the effective stack height is 1000 ft and the peak ground-level concentration of 0.1 ppm occurs approximately 7 miles downwind.

2. If  $H_m = 900$  ft, the effective stack height is limited to 900 ft and the 0.2-ppm isopleth can be approximated by a narrow footprint with an area of  $4 \text{ mi}^2$  with a peak concentration of 0.3 ppm occurring 6 miles downwind.

3. If  $H_m = 500$  ft, the effective stack height is assumed to be 800 ft and the maximum ground-level concentration, 0.05 ppm 10 miles from the source, is calculated assuming dispersion in stable air with an infinite lid height. This estimate would presently be used for this particular stack for all lids  $< 900$  ft and certainly is suspect for  $H_m$  between 800 and 899 ft. A transition in stability class from stable to neutral (or unstable) when  $(H - \sigma_z) = H_m$  might be more realistic. If the ground-level concentration for  $H_m = 500$  ft were calculated based on the assumption of an impenetrable lid at 500 ft, the concentration 2 miles downwind would be greater than 1.0 ppm and the 0.5-ppm ground-level isopleth would extend 8 miles downwind. Short-term peaks of this magnitude are not observed at the Chicago TAM stations, whereas peaks of 0.1 to 0.3 ppm are often found when major point sources are upwind.

A single value of plume rise is ascribed to each of the three classes of area sources whenever the wind is less than a critical wind speed. This is discussed in Section 1.2.9.

In the computer code, function PRISE performs the plume-rise calculation according to the methods outlined in this section.

### 1.2.7 Effective Wind Speed

The mean wind speed at the physical stack height  $H_s$  should be used in the plume-rise equation (Eq. 1.18). In the evaluation of the dispersion kernel (Eq. 1.9), wind at the effective stack height  $H$ , corresponding to the plume centerline, is used. In each case, the desired value for the wind speed will usually be greater than that measured at a local airport (typically at 30 to 100 ft above the ground). The following equation provides a correction term for altitudes up to 1000 ft:

$$U \text{ (at height } Z_2) = U \text{ (at height } Z_1) (Z_2/Z_1)^P, \quad (1.19)$$

where the exponent  $P$  is dependent on the stability class, as shown in Table 1.3.



TABLE 1.3. Exponents for  
the Wind-profile Law  
(DeMarrais, 1959)

Stability Class	P
Stable ( $\geq 5$ )	0.5
Neutral (4)	0.2
Unstable ( $\leq 3$ )	0.2

The experimental data from DeMarrais (1959) indicated a slightly more uniform vertical-wind-speed profile for unstable than for neutral conditions, but the model is not sensitive to this distinction.

### 1.2.8 Finite Geometry for Dispersion

The fundamental puff kernel has been defined for  $z$  from  $-\infty$  to  $+\infty$  with  $z = 0$  on the plume axis. If we assume perfect reflection at the ground, the concentration  $C$  at time  $M$  at a receptor position  $(x, y, z)$  due to a single source at position  $(x', y', z')$  is

$$C = X(x - x', y - y', z - z', M) + X(x - x', y - y', z + z', M) \quad (1.20)$$

where the coordinates have been stated relative to the ground and Eq. 1.9 determines  $X$ .

When the effective stack height is less than or equal to the height of the mixing layer, an impenetrable barrier for vertical dispersion is assumed to exist. In earlier work (e.g., Turner, 1967), the distribution under the lid is calculated by a single plume until vertical diffusion implies the pollutant had reached the lid; a transition to the equation for uniform vertical mixing is then made. An alternate approach used in this model represents multiple reflections between ground and the inversion by pairs of image sources. Depending upon the lid height and the time of travel, up to five pairs of images may be required to adequately represent a condition of uniform vertical mixing in an urban area.

Since the lid height may vary during the lifetime of each 1-hr puff, algorithms have been formulated to allow for specification of a different effective lid height for each hour  $M$ , look-back time  $N$  (see Eq. 1.5), and source  $J$ .

The algorithms employed in selecting the most representative lid height for a given puff are discussed in detail in Section 4.1, along with other calculations performed by the function ITRAN.

### 1.2.9 Finite-source Geometry

The realistic modeling of residential, commercial, and industrial zones characterized by multiple sources too numerous to represent by individual plumes is critical to the success of a source-oriented atmospheric-dispersion model. A similar need for synthesizing emissions from these area sources arises in the design of regional implementation plans based on land-use, a method whereby one seeks to assign emission-density limits ( $\text{lb/hr-mi}^2$ ) to land in each of several zoning classes

(Roberts and Croke, 1970). Often major point sources can be modeled more realistically by assigning initial dimensions to the plume in order to approximate, for example, multiple stacks or aerodynamic downwash.

The integrated-puff model is ideally suited to the task of synthesizing these source configurations. In contrast to the plume equation, limited to crosswind and vertical coordinates and thereby representing a two-dimensional front, the puff incorporates the downwind coordinate and thus represents a three-dimensional cloud of pollutant.

Be it an area source or a point source with initial dimensions, the source of finite initial volume is approximated by a pseudo upwind point source. This is similar to algorithms employed in plume models, but as mentioned above, the more sophisticated puff kernel results in a volumetric source rather than a two-dimensional wave front. Therefore, in addition to a more realistic description of downwind dispersion, the puff model can directly evaluate the effect of the area source upon the area itself.

The volumetric source is synthesized by specifying three initial dispersion coefficients:  $\sigma_{x0}$ ,  $\sigma_{y0}$ , and  $\sigma_{z0}$ . These are then associated with times  $t_x$ ,  $t_y$ , and  $t_z$ , which are the solutions to

$$\sigma_{x0} = \sigma_x(i, t_x), \sigma_{y0} = \sigma_y(i, t_x), \sigma_{z0} = \sigma_z(i, t_z), \quad (1.21)$$

where  $\sigma(i, t)$  is the family of functions describing the dispersion coefficients at time  $t$  for stability class  $i$ . Equation 1.21 is solved in the subroutine PSEUDO. A virtual source is thus defined at upwind distances  $\delta x = ut_x$ ,  $\delta y = vt_y$ , from the center of the volumetric source. Since the model is presently constrained by the assumption of circular ( $\sigma_x = \sigma_y$ ) puffs, it follows that  $t_x = t_y$ . (See Fig. 1.11.) The transport equation (Eq. 1.9) is then modified with  $(x - \delta x)$  replacing  $x$ ,  $(y - \delta y)$  replacing  $y$ , and  $T + t_x$ ,  $T + t_y$ , and  $T + t_z$  replacing  $T$  in the appropriate locations.

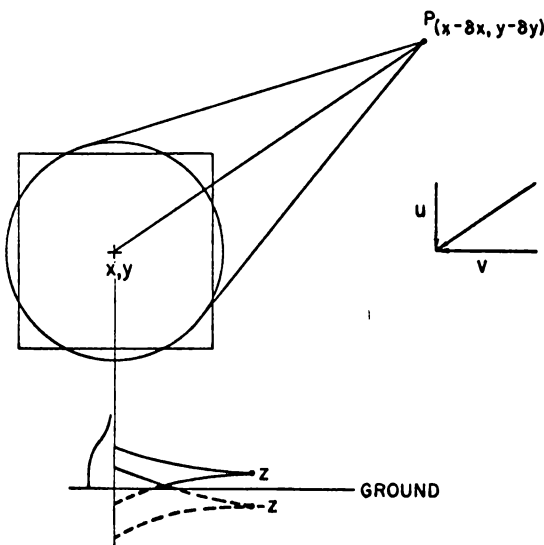


Fig. 1.11. Synthesis of an Area Source of Buildings of Height  $Z$ . ANL Neg. No. 113-1111.

For a square area source of side length  $n$ , the initial value of the horizontal dispersion coefficients  $\sigma_{y0}$  and  $\sigma_{x0}$  ( $\sigma_{y0} = \sigma_{x0}$ ) is defined by

$$\sigma_{y0} = n/2.4. \quad (1.22)$$

Figure 1.12 depicts a row of square area sources of uniform strength. Pollutant concentrations along the line A-A are determined by summation of concentrations due to each individual

area source. The concentration profile for each square is governed by  $\sigma_{y0}$ . Uniformity of emissions above A-A implies that, when the concentration fields for all squares are superimposed, the dose at point a in Fig. 1.12 should equal that at point b. Equation 1.22 ensures this. The choices of  $\sigma_{z0}$  and the effective source height  $z$  (Fig. 1.11) for area sources depend upon the representative building height for each square mile and the mode of initial transport; i.e., emissions are characterized either by plume rise or by downwash. The quantity  $\sigma_{z0}$  also approximates the actual variation in stack heights within a given class, as well as the vertical spread due to transport within the area source.

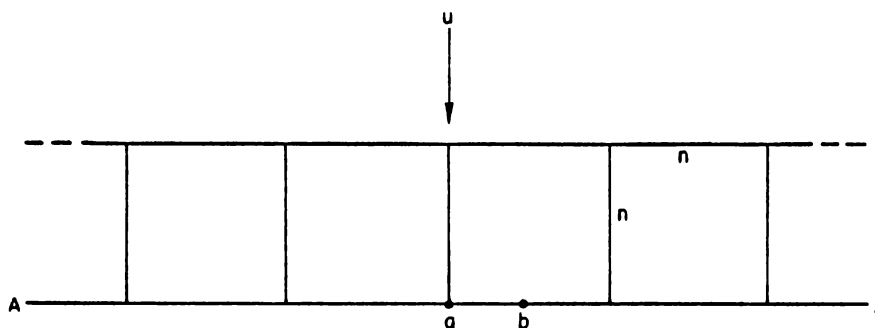


Fig. 1.12. Choice of  $\sigma_{y0} = n/2.4$  Ensures that Concentrations Will Be Uniform along the Line A-A. ANL Neg. No. 113-2867 Rev. 1.

Table 1.4 shows values of building height, critical wind speeds, plume rise, and  $\sigma_{z0}$  for each of the three classifications of area sources in Chicago. For example, if the wind speed is 10 mph, low-rise residential buildings are represented by a source at  $z = 50$  ft with  $\sigma_{z0} = 50$  ft, and industrial-area sources by  $z = 300$  ft and  $\sigma_{z0} = 150$  ft.

TABLE 1.4. Parameters Used to Describe Area Sources in Chicago

Source Class	Physical Stack Height, ft	Critical Wind Speed, $WS_c$ , mph	$WS \leq WS_c$		$WS > WS_c$	
			Plume Rise, ft	$\sigma_{z0}$ , ft	Plume Rise, ft	$\sigma_{z0}$ , ft
Low-rise Residential/Commercial	50	6	50	50	0	50
High-rise Residential/Commercial	200	6	100	200	0	200
Industrial	150	15	150	150	0	150

Major point sources are also characterized by initial dimensions  $\sigma_{x0}$  ( $= \sigma_{y0}$ ) and  $\sigma_{z0}$ , which, for properly designed stacks, depend upon whether a critical wind speed (here 15 mph at 75 ft) is exceeded. Downwash conditions are assumed to occur always for sources with poor aerodynamic characteristics such as vents or stubby stacks. Under normal

plume-rise conditions, the parameters  $\sigma_{x0}$ ,  $\sigma_{y0}$ , and  $\sigma_{z0}$  are each set at 100 ft to describe the initial source volume. Under downwash conditions,  $\sigma_{x0}$  and  $\sigma_{y0}$  are set at 750 ft and  $\sigma_{z0}$  at 150 ft. As with area sources, these choices are somewhat intuitive and, since the downwash effect is a primarily local one, really should be tailored to each source or source type. For example, one may assume that large commercial and residential establishments are dominated by buildings with improperly designed stacks and that a good assumption for initial source dimensions to simulate downwash would then be the size of a representative building (Shieh, 1969). In Chicago, major point sources in this category are typified by Union Station, approximately one city block wide and 100-150 ft high. This observation influenced our selection of initial source dimensions under downwash conditions. It is also worth noting that all sources homogenized and treated as area sources are effectively given a  $\sigma_{x0} = \sigma_{y0} = 0.4$  mile.

## 2. STRUCTURE OF THE COMPUTER CODE

The transport of airborne pollutants in the integrated-puff model is characterized by the algorithms presented in Section 1.2. Regardless of sophistication, the accuracy of any estimation of pollutant concentration is dependent upon knowledge of the temporal variations of source and meteorological inputs. Thus the "model" must be considered as the composite of all calculational methods involved in achieving an estimate.

In spite of this argument, a distinction is made in the organization of this report between the routines (here separate computer codes) used to generate the input data (emissions and meteorological information) and the subprograms which, linked together, calculate the pollutant concentration according to Section 1.2.

Since the nature of the input data depends upon the geographical region and particular pollutant under study, aspects of the modeling effort concerned with organizing meteorological and source data are described in Part II on validation of the model by estimation of SO<sub>2</sub> levels in Chicago.

Figure 2.1 is a flow diagram indicating critical calculations and major subroutines in the model. It is not a traditional computer flow chart, in that some of the calculations (for example, the simulation of hourly emissions from major sources) are performed by separate codes. The dispersion code begins with PROGRAM APDATA, a routine written in PL1 which reads and organizes hourly source and meteorological data stored on magnetic tape. This routine reflects the special features of the Argonne Master Air Pollution Information and Computation (APICS) system, and, for the purposes of this report, its main feature is the transmittal of the input data, one hour at a time, to the FORTRAN subroutine ISPDAV via the entry PUFF. The calculation of pollution levels over the receptor grid is then managed by PUFF according to Fig. 2.1. The three major subprograms (PUFF, TRAN, and KERN) are described in the following sections. Listings for all routines appear in Appendix A. The code is designed to be coupled with the APICS system and is in a developmental stage. The logic can easily be made more efficient, and the multiplicity of DATA statements (for example, those describing additional point sources not already in the PLANTSIM file) should be handled as card input. Such an effort is currently under way so that the complete flow diagram of Fig. 2.1 can be incorporated in a single FORTRAN code, independent of the APICS system.

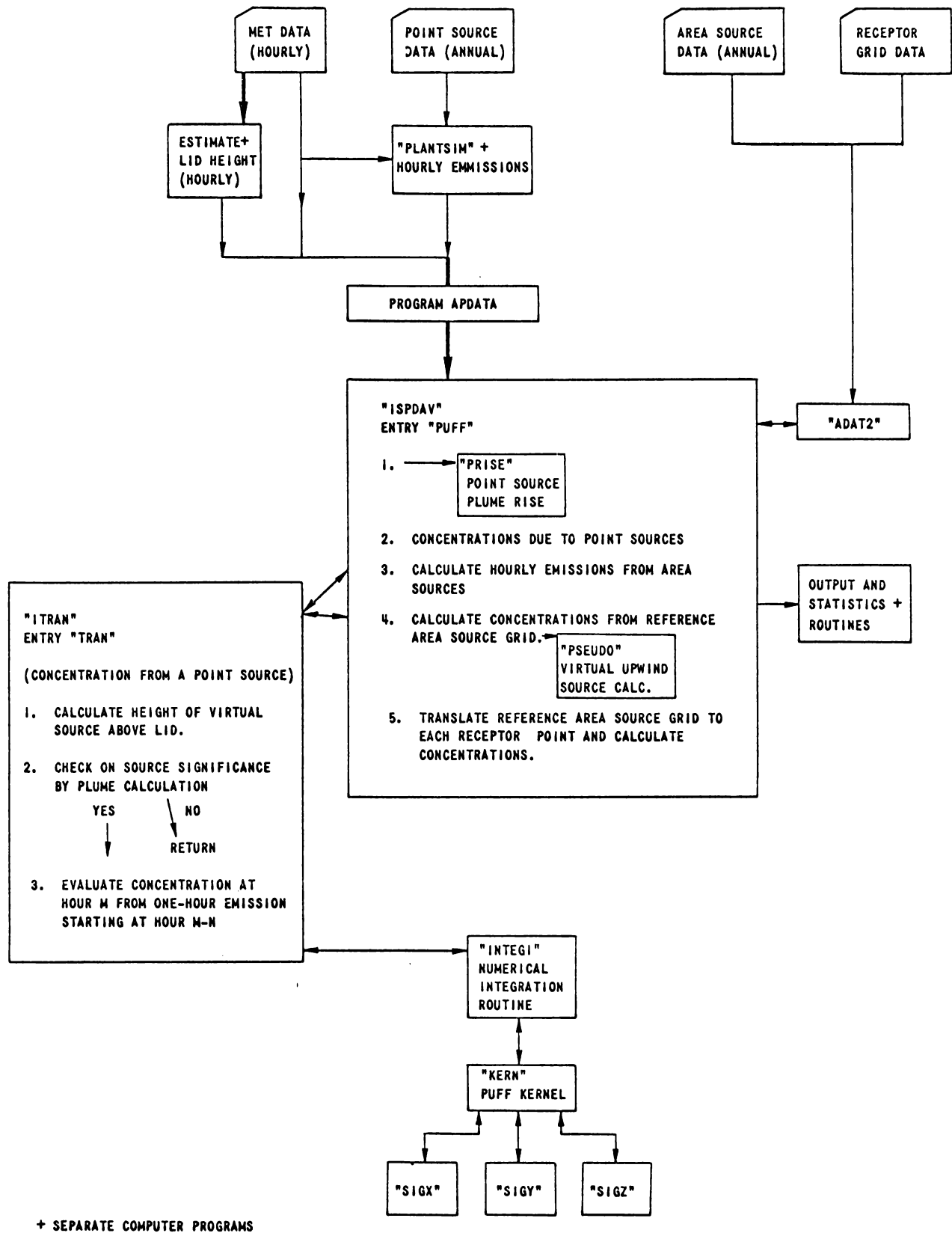


Fig. 2.1. Flow Diagram for Calculation of Pollution Levels. ANL Neg. No. 113-1161.

### 3. SUBROUTINE ISPDAV (ENTRY PUFF)

Subroutine ISPDAV, which is normally entered from APDATA via the entry PUFF (see Fig. 2.1 and listing in Appendix A), is the principal subroutine of the dispersion code. It performs or controls eight major functions via other subroutines. These are denoted in the ISPDAV listing by numbered comment cards:

1. Initialize all arrays, including specifications of receptor grid and area-source data read in via subroutine ADAT2.
2. Store all meteorological data for hour M.
3. Calculate effective stack height for each major point source specified by PLANTSIM.
4. Calculate concentration at each receptor point from point sources specified by PLANTSIM and from additional point sources.
5. Calculate hourly emissions from area sources.
6. Evaluate coupling coefficients between each square in a standard area-source grid and a reference receptor point.
7. Apply the coupling coefficients to calculate concentrations due to actual area sources by applying the standard area-source grid to each receptor point.
8. Print out concentrations at each receptor point, and, if desired, punch cards to serve as input to statistical codes.

These eight functions are described in the remainder of this section. Wherever appropriate, variables in the listing (Appendix A) are referenced so that this writeup serves as a guide to the FORTRAN listings and provides a detailed description of the computations.

#### 3.1 Initialization of Data; Subroutine ADAT2

Subroutine ISPDAV is called only once from program APDATA in order to initialize dimensions of the arrays EMIS and HEFF, which eventually contain point-source hourly emissions and effective stack heights. Among the variables initialized by DATA statements in this section of the code are parameters characterizing emissions from major point sources which are not in the PLANTSIM file. For example, in the listing, 27 additional point sources (not in the original City of Chicago inventory) are defined by their coordinates (XPT, YPT, ZPT), number of stacks (NS), percent sulfur in fuel (SPCT), annual SO<sub>2</sub> emission (QPTOT, M-lb/yr), and a pattern classification.\* These could, of course, be incorporated in the PLANTSIM file by rerunning that code.

---

\*See Section 7.5.

Subroutine ADAT2 is called from ISPDVAV in order to read card input specifying the geometry of the region. Three grids are defined at this point:

1. The area-source grid for the region.
2. The receptor grid.
3. A standard area-source overlay grid to facilitate calculations of concentrations from actual area sources.

### 3.1.1 Area-source Grid

All points in the region are represented by a right-hand Cartesian coordinate system with +X to the west and +Y to the south (Fig. 1.2). Data recorded in any other system can easily be read into the program and converted by one or more additional statements. The region is overlaid by a uniform grid on which square area sources are defined. This area-source grid is specified by five parameters: its origin in the Cartesian coordinate system (XSORIG, YSORIG); the number of grid squares in the X and Y directions (NSXMAX, NSYMAX); the length of the side (miles) of each source grid square (DGRID). The origin of the area-source grid system is the Northeast corner (see Fig. 3.1). Each grid square is assigned a pollutant emission rate (QTOT, LB/YEAR) for each of the three source types: low-rise space heaters, high-rise space heaters, and industry. Corresponding to these are three representative stack heights assumed to apply to the entire region.

An array EMAX(5,3) is also specified which estimates the maximum hourly emission (lb/hr) for each class (NCL=1,2,3) from any single grid square in the region, EMAX(1,NCL); from any square area source in the region composed of four grid squares (2 x 2), EMAX(2,NCL); from any one composed of 16 (4 x 4), EMAX(3,NCL); from any one composed of 64 (8 x 8), EMAX(4,NCL); etc. The EMAX array is employed with the standard area source overlay (Section 3.1.3) and reflects the fact that the maximum hourly emission from any N x N square area is usually significantly less than  $N^2$  x (maximum emission from any single square in the region). EMAX is discussed further in Section 3.1.3 and in the sample Chicago problem (see Appendix B).

### 3.1.2 The Receptor Grid

An array of points at which concentrations are to be estimated must lie within and must coincide with vertices of the area source grid.\* For example, the area-source grid (Section 3.1.1) might be 10 squares by 12 squares, 2 miles on a side; receptors could then be defined by a 2 x 3 array of squares 6 miles on a side with its origin coinciding with the corner

---

\*In validation studies using data from eight receptors in Chicago, minor modifications were required in subroutine ITRAN to compensate for stations located at intervening points.



of an area-source square. Figure 3.1 presents this example. The receptor grid is defined by five parameters: an origin in the Cartesian system (XRORIG, YRORIG); the grid spacing (DRGRID, must be a multiple of DGRID); and the number of squares in the X and Y directions (NWEST, NSTH). The total number of receptor points is thus: (NWEST+1) x (NSTH+1).

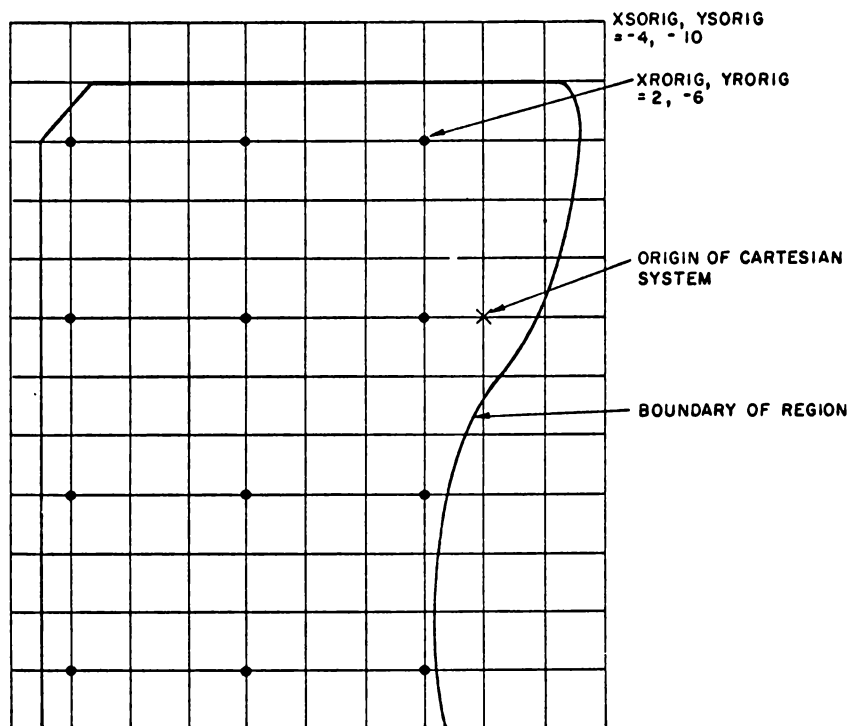


Fig. 3.1. Superposition of Area Source and Receptor Grids for a Region  
 (XSORIG,YSORIG) = (-4,-10), (NSXMAX,NSYMAX) = (10,12),  
 DGRID = 2; (XRORIG,YRORIG) = (2,-6), (NWEST,NSTH) =  
 (2,3), DRGRID = 6. ANL Neg. No. 113-1162.

### 3.1.3 A Standard Area-source Overlay Grid

A standard area-source overlay grid is defined by input to subroutine ADAT2. Figure 3.2 shows the one used in the present code (see sample input deck, Appendix B). At the center of the array is a reference receptor with coordinates (0,0). Area-source squares of increasing size surround this central point and are numbered 1-16 (1 mile x 1 mile), 17-48 (2 miles x 2 miles), and 49-88 (4 miles x 4 miles). The arrays (XSGRID(I), YSGRID(I), I=1,88) that designate the coordinates of the lower left corner of each square relative to the central receptor are read by ADAT2.

The first step in calculating the area-source concentrations at points on the actual receptor grid is to evaluate coupling coefficients (COUP) between each square of the standard area-source grid and the reference receptor. For example, COUP(43,1,4) is the concentration (ppm) at hour M at the center of Fig. 3.2 due to a 1-hr-long emission EMAX(1,2)

49	50	51	52	53	54	55			
56	57	58	59	60	61	62			
63	64	17	18	19	20	21	22	65	66
		23	24	25	26	27	28		
67	68	29	30	5	6	7	8	31	32
		33	34	9	1	2	10		
71	72	37	38	11	3	4	12	73	74
		43	44	13	14	15	16		
75	76	77	78	79	80	81			
82	83	84	85	86	87	88			

Fig. 3.2. Standard Area-source Grid about Reference Receptor. ANL Neg. No. 113-1163.

(1 stands for low-rise space heaters; 2 stands for the second largest square size, 2 miles x 2 miles, which is the size of square number 43) between the hours M - 4 and M - 3. This standard area-source grid and associated array of coupling coefficients for 88 areas, three source classifications, and up to 6 hours of historical emission and meteorological data is then translated about the receptor grid (Section 3.1.2), and concentrations are found by multiplying each element of the COUP array by the ratio of the actual emission to the value of the EMAX array used to calculate the COUP value. These algorithms are explained in greater detail in Section 3.7..

### 3.2 Storage of Hourly Data; Function JSUB

The evaluation of the sequence of algorithms necessary to calculate pollutant concentrations at hour M begins with the statement in APDATA which calls:

ENTRY PUFF (NR, TEMP, WSA, WDA, STAB, HLID, NSRC, XS, YS, ZS, PERCENT, QSO2, QHEAT, SO2VAL, MM, KTAM, SOBS).

These variables are defined in Table 3.1.

TABLE 3.1. Variables in ENTRY PUFF

Name	Dimensions (if an array)	Description	Units
NR	- 1	Hour of day	hr
TEMP	-	Temperature	°F
WSA	1	Wind speed	mph
WDA	1	Wind direction	deg
STAB	-	Stability class (Turner, 1967)	-
NSRC	-	Number of point sources in PLANTSIM file	-
XS	(NSRC)	X-coordinate of source	mi
YS	(NSRC)	Y-coordinate of source	mi
ZS	(6, NSRC)	Physical heights of up to six stacks at each source	ft
PERCENT	(6, NSRC)	Fraction of total plant emissions from each stack	-
QSO2	(NSRC)	SO <sub>2</sub> emission rate	lb/hr
QHEAT	(NSRC)	Thermal emission rate	therms/hr
SO2VAL	(1)	Returns calculated value of SO <sub>2</sub> at the receptor point (NRTAM) for tabular printout. Also can be punched on cards with SOBS.	ppm
MM	-	Number of consecutive hours of problem solution.	hr
KTAM	(8)	(Array not presently used)	-
SOBS	(1)	Observed value of SO <sub>2</sub> ; available for punched-card output for use in statistics codes.	ppm

### 3.2.1 Function JSUB

All the input parameters at hour MM or key variables derived from these (such as effective stack height) must be stored, since the basic equation (Eq. 1.9) has a summation of the form

$$X = \sum_{N=1}^M Q_{M-N+1} G_{M,N} \quad (3.1)$$

However, the upper limit in the summation, which represents the maximum number of hours for which a puff is significant, can be set at some value NMAX (or M, whichever is smaller). For the Chicago region, NMAX = 6. Thus only the six most recent hours of source and meteorological data need be stored to perform the truncated summations of the form

$$X = \sum_{N=1}^{\min(NMAX, M)} Q_{M-N+1} G_{M,N} \quad (3.2)$$

This summation is performed using the function

$$JSUB(J) = \text{modulo}_6(J - 1) + 1, \quad (3.3)$$

where  $\text{mod}_K(0) = 0$ ,  $\text{mod}_K(1) = 1$ ,  $\text{mod}_K(K - 1) = K - 1$ ,  $\text{mod}_K(K) = 0$ , and, in general,  $\text{mod}_K(J) = [J - (I \times K)]$ , where I is the largest nonnegative integer for which  $\text{mod}_K(J)$  is nonnegative. Table 3.2 shows how this function is used to store a sequence of hourly wind-speed values in the array WSBAR. For each hour MM of the problem, entry PUFF is called and a single value of

TABLE 3.2. Use of Function JSUB to Store Wind-speed Values in Array WSBAR

MM, hr of Problem	JSUB(MM)	WSA at hr MM, mph	WSBAR(1)	WSBAR(2)	WSBAR(3)	WSBAR(4)	WSBAR(5)	WSBAR(6)
1	1	2.0	2.0	-	-	-	-	-
2	2	2.5	2.0	2.5	-	-	-	-
3	3	3.0	2.0	2.5	3.0	-	-	-
4	4	3.5	2.0	2.5	3.0	3.5	-	-
5	5	3.0	2.0	2.5	3.0	3.5	3.0	-
6	6	4.0	2.0	2.5	3.0	3.5	3.0	4.0
7	1	4.5	4.5	2.5	3.0	3.5	3.0	4.0
8	2	3.5	4.5	3.5	3.0	3.5	3.0	4.0
9	3	5.0	4.5	3.5	5.0	3.5	3.0	4.0
10	4	6.0	4.5	3.5	5.0	6.0	3.0	4.0
11	5	5.5	4.5	3.5	5.0	6.0	5.5	4.0
12	6	6.0	4.5	3.5	5.0	6.0	5.5	6.0
13	1	7.0	7.0	3.5	5.0	6.0	5.5	6.0

wind speed WSA(1) is transmitted in the calling sequence. This value is then stored in the wind-speed array by the statement

$$\text{WSBAR}(\text{JSUB}(\text{MM})) = \text{WSA}(1).$$

As shown in Table 3.2, this automatically keeps the six most recent values of wind speed in storage. Similarly, the value  $Q_{M-N+1}$  in Eq. 3.2 is then located by the expression  $Q(\text{JSUB}(M-N+1))$ .

### 3.3 Effective Stack Height; Subroutine PRISE

The effective stack height is calculated in subroutine PRISE according to the prescription in Section 1.2.6. Downwash is assumed to occur at aerovane wind speeds (not corrected for stack height) greater than 15 mph. Choice of this threshold is supported by observations at a local utility with multiple, well-designed stacks. Sources in PLANTSIM with stacks that violate basic aerodynamic guidelines (such as  $H_s \ll 2.5 \times$  building height) are singled out for permanent downwash by the array NOSTK. In the ISPDV listing (Appendix A), there are nine such sources in Chicago specified by a DATA statement.

When downwash is associated with a given stack at hour M, the appropriate entry in the array NDW is set equal to 1 and the effective stack height is set equal to the physical stack height. Larger initial plume dimensions are used (See Sections 1.2.9 and 3.4).

### 3.4 Point-source Calculations

There are two categories of point sources, those in the PLANTSIM file and those additional sources described in ISPDV by data statements (Section 3.1). Other than the requirement for algorithms to prorate annual emissions from the additional point sources, the calculations of concentrations on the receptor grid due to major point sources are identical for both categories.

Receptors are taken one at a time. The subprograms NXF, NYF, and RGRID convert a sequential receptor number (1, ..., NRCP) to Cartesian coordinates XRG, YRG. A single receptor height, ZREC, is used for all receptors in the grid. Sources are then considered one at a time. An initial plume volume  $\sigma_{x_0} = \sigma_{y_0} = \sigma_{z_0} = 100$  ft is assumed, except under downwash conditions when the initial values of the three dispersion coefficients are  $\sigma_{x_0} = \sigma_{y_0} = 750$  ft,  $\sigma_{z_0} = 150$  ft. Subroutine PSEUDO is used to locate the virtual source (Section 1.2.9). The wind-speed array is modified by a power law to estimate the increase with altitude (Section 1.2.7).

Sulfur dioxide decay, normally neglected, is set at 4 hr if the temperature is greater than 60°F. This is clearly an inadequate characterization of

the phenomena associated with removal of airborne SO<sub>2</sub>. However, as long as the sulfur remains in the gaseous state, it may be best for incident control or long-range planning to neglect decay under all conditions (except perhaps for scavenging by rain); the model would then estimate "total sulfur" rather than SO<sub>2</sub>.

Having defined the location of the virtual point source and values for all other pertinent factors, the code then evaluates the concentration (ppm) at the receptor by a statement of the form

$$\text{CHI} = \text{EMIS}(\text{JSUB}(\text{M}-\text{N}+1)) * \text{TRAN}(\text{N}, \text{M}, \text{K}, \text{J}, \text{NTRAN}) * 0.38\text{E}-4 \quad (3.4)$$

where CHI is the concentration at hour M due to an emission EMIS between the hours M - N and M - N + 1 from stack K at plant J. The parameter NTRAN is a flag which shortens the calculations in function ITRAN (entry TRAN) when there is more than one stack at a given plant. The algorithms describing the transport of an hour-long release of pollutant from a point source are executed in TRAN. These are described in Section 4.

The total concentration at time M at each receptor due to all-point sources is thus the summation of CHI values according to Eq. 3.5:

$$X_{\text{point sources}} = \sum_{\text{J}=1}^{\text{NSRC}} \sum_{\text{N}=1}^{\text{min}(\text{M}, \text{NMAX})} \sum_{\text{K}=1}^6 \text{CHI}(\text{M}, \text{N}, \text{K}, \text{J}). \quad (3.5)$$

### 3.5 Hourly Emissions from Area Sources

Subroutine ADAT2 reads in annual emissions for each of three classes of sources--low-rise residential/commercial, high-rise residential/commercial, and industry--for up to 1000 square area sources of side length DGRID miles (Section 3.1.1). These are prorated to estimate hourly emission rates according to the following prescriptions:

#### 3.5.1 Low-rise Residential/Commercial Hourly Emissions

Low-rise residential/commercial hourly emissions are assumed proportional to the number of heating degree-days with a fixed fraction, PCTHW, of the annual fuel use prorated uniformly for hot water use. The heating cycle occurs between the hours TON (usually 6 a.m.) and TOFF (usually 10 p.m.) with a "hold fire" equivalent to the hot-water heat rate at all other times. Thus in this section of subroutine ISPDAV

$$Q_{\text{heating}} = \frac{Q_{\text{annual}} \times (1 - \text{PCTHW}) \times (65 - \text{TEMP}) \times \text{TE}}{\text{DDAVG} \times \text{TONOFF}}, \quad (3.6)$$

$$\text{TEMP} \leq 65^{\circ}\text{F} \text{ and}$$

$$\text{TON} \leq \text{time of day} \leq \text{TOFF},$$

$$Q_{\text{hot water}} = Q_{\text{annual}} \times \text{PCTHW}/8760, \quad (3.7)$$

and

$$Q_{\text{total}} = Q_{\text{heating}} + Q_{\text{hot water}} \text{ (lb/hr)}, \quad (3.8)$$

where

DDAVG = average number of degree days per year,

PCTHW = fraction of annual fuel use used for hot water,

TEMP = average temperature (°F) for that hour,

TONOFF = TOFF - TON + 1

$$\text{TE} = \begin{cases} 1.5, & \text{TON} \leq \text{time of day} \leq \text{TON} + 1 \\ 1.0, & \text{TON} + 1 < \text{time of day} \leq \text{TOFF} \end{cases}$$

The variable TE synthesizes a "janitor function" whereby sources operate at a higher than usual fuel rate during the first two hours of the heating day.

The value of PCTHW depends upon geographical location and can usually be estimated adequately by fuel dealers. Equations 3.5 and 3.6 assume that coal-fired space heaters also supply the building hot-water requirements. Some buildings, generally the larger ones, may rely on natural-gas or oil-fired hot-water heaters, especially during summer months.

### 3.5.2 High-rise Residential/Commercial Hourly Emissions

High-rise residential/commercial hourly emissions are estimated from annual values according to Eqs. 3.6-3.8 with TON = 1 and TOFF = 24. These sources, which are often high-pressure steam systems, are therefore assumed to respond to the outside temperature at all times.

### 3.5.3 Industrial Area Sources

Hourly emissions are based on the formula for uniform proration:

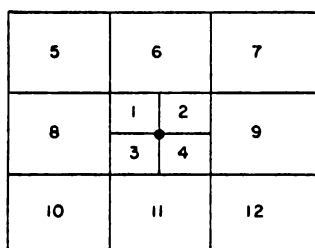
$$Q_{\text{hourly}} = Q_{\text{annual}}/8760. \quad (3.9)$$

## 3.6 Calculation of Concentrations due to Area Sources

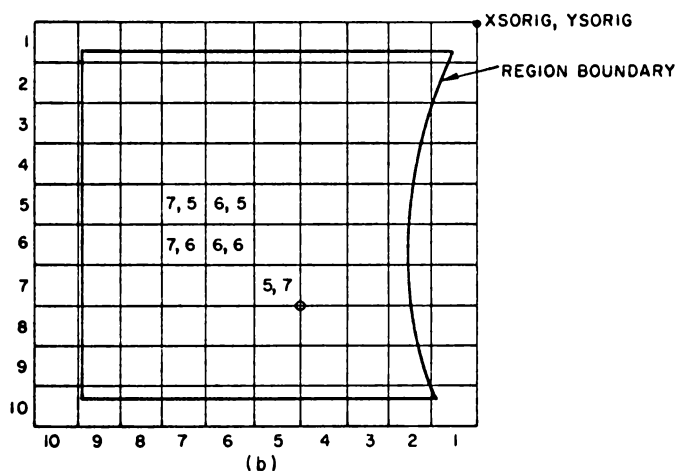
Earlier sections of this report have described some of the features of these calculations. The representation of an area source by a virtual upwind point source is discussed in Section 1.2.9, where Table 1.4 lists representative stack heights and initial plume dimensions for Chicago. According to the meteorological variables associated with each hour, and for each source class and size (length of side) of area, a relative position of the virtual

source is found from subroutine PSEUDO and information stored for each hour in the time arrays TXX and TZZ and the distance arrays DXX and DYY.

Instead of calculations to estimate separately the contribution at each point on the receptor grid due to emissions from each area in the regional source array, a preliminary evaluation of coupling coefficients between area sources on a reference grid (see Fig 3.2) and a central reference receptor is made. This coupling-coefficient (COUP) array is then used to evaluate actual concentrations by translating the central reference receptor about the desired receptor grid and using actual emissions from the regional source grid rather than the reference emissions (EMAX array) used to calculate the coupling coefficients. This approach offers a tremendous saving in computer run time whenever concentrations are to be evaluated for a dense regional grid. However, it is based on the assumption of a space-independent wind field for the region (or at least for the part of the region that influences the receptor grid). (Clearly, the next level of sophistication for this dispersion model, and a realistic one, is to eliminate this uniform wind assumption and ensure reasonable computer run times by precalculating the integrals of Eq. 1.9.)



(a)



(b)

Fig. 3.3. Evaluation of Concentrations due to Area Sources. (a) Standard area source overlay and (b) Regional source grid with a single receptor point. ANL Neg. No. 113-1164.

The use of the COUP array is best elucidated by a simplified example. Figure 3.3a shows a standard overlay consisting of 12 area sources with a central reference receptor. Consider only one class of source (e.g., industry). A preliminary survey of the spatial distribution of actual emissions indicates that the maximum hourly emission from a  $1 \times 1$  square is  $EMAX(1)$  lb/hr, and that for a  $2 \times 2$  square is  $EMAX(2)$  lb/hr (usually significantly less than  $4 \times EMAX(1)$ ). The concentration at time  $M$ ,  $COUP(JSUB(M-N+1), NSG)$  ppm,\* due to an emission  $EMAX( )$  lb/hr from square number  $NSG$  during hour  $M - N + 1$  is calculated assuming a virtual upwind point source and transport according to the integrated-puff theory (Eq. 1.9). The value of  $EMAX$  depends upon whether square number  $NSG$  is  $1 \times 1$  or  $2 \times 2$ . Up to 6 hr ( $N \leq 6$ ) of historical

\*The indices in this example are simplified versions of those used in the code.

meteorological data is used in the evaluation of pollutant concentrations, and function JSUB, described in Section 3.2, determines the location of the COUP value at time M associated with each value N. Hourly emissions EMIT(JSUB(M-N+1)) are defined on the regional source grid, Fig. 3.3b, where I is the horizontal and J the vertical index of a particular 1 x 1 grid square.\* The concentration at time M at the receptor point in Fig. 3.3b, due to emissions from square 5,7, is found by

$$X(1) = \sum_{N=1}^{NMAX} \text{COUP}(\text{JSUB}(M-N+1),1) \times \text{EMIT}(\text{JSUB}(M-N+1),5,7)/\text{EMAX}(1). \quad (3.10)$$

Similarly, the concentration at the receptor due to the combined emissions from squares (7,5), (6,5), (7,6), and (6,6) is found by

$$X(5) = \sum_{N=1}^{NMAX} \text{COUP}(\text{JSUB}(M-N+1),5) \times [\text{EMIT}(\text{JSUB}(M-N+1),7,5) + \dots + \text{EMIT}(\text{JSUB}(M-N+1),6,6)]/\text{EMAX}(2). \quad (3.11)$$

The concentration due to all area sources is then the sum

$$X_{\text{area}} = \sum_{NSG=1}^{12} X(NSG), \quad (3.12)$$

and the total concentration at the receptor is the sum of the concentration due to area sources and major point sources (Section 3.3).

### 3.7 Output; Subroutine PROUT

Calculated values are printed out in two formats. Concentrations at each grid point for receptor arrays of up to 12 points in the East-West dimension ( $NRWEST \leq 11$ ) are displayed by subroutine PROUT. The receptor data array, RECDAT, contains a breakdown of the total concentration into contributions from utilities, industry, and residential/commercial sources, as well as the sum of these. Subroutine PROUT prints these four numbers for each receptor point. The variable NPRINT determines how often the RECDAT array is displayed. A sample printout is shown in Fig. 3.4.

If one of the receptor points (numbered NRTAM by a DATA statement) corresponds to a particular monitoring site, the hourly values computed for this point can be transmitted back to program APDATA via the array SO2VAL. The two sets of concentrations, observed and calculated, will then

---

\*In the code, a single running index, NAREA, is used instead of I,J.



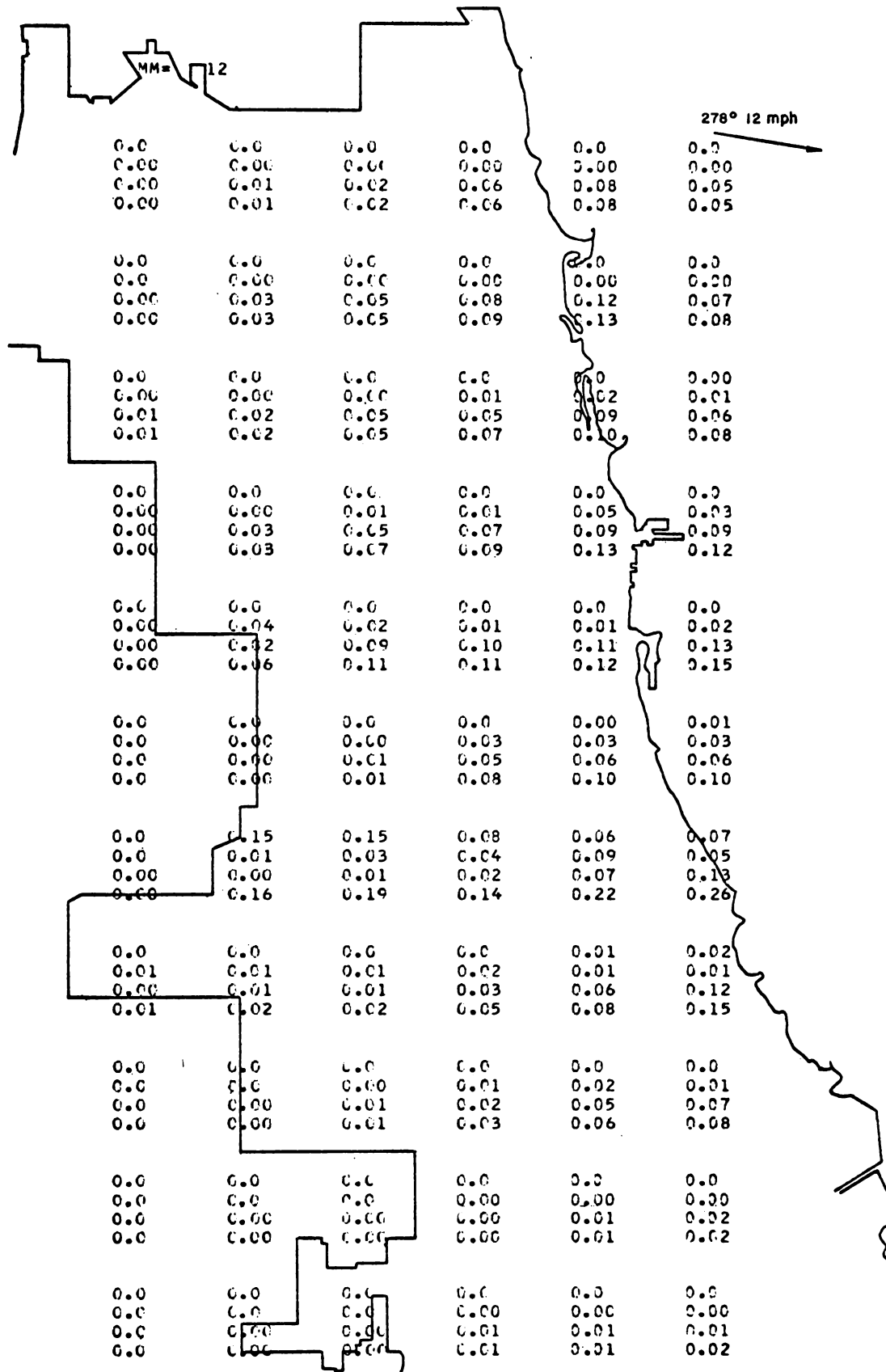


Fig. 3.4. Sample Printout of Subroutine PROUT with Chicago Map Overlay. 12 Noon 1/15/67; Wind WNW at 10 mph.

be printed along with any other meteorological or emission parameters selected by the OUTSTATION cards in the input data deck. To exercise this option, the variable VALOP, presently defined by a DATA statement, must be set equal to 1.0.

Punched-card output is also available when one of the receptors corresponds to a particular monitoring site. In addition to the printout comparing observed and estimated pollution concentrations, the two arrays can be transferred to punched cards for subsequent statistical analysis and graphical display. The variable PNCHOP defined by a DATA statement in ISPDV should be set equal to 1.0 to exercise this option.

#### 4. FUNCTION ITRAN (ENTRY TRAN)

A statement in entry PUFF of the form

$$\text{CHI} = \text{EMIS}(\text{JSUB}(\text{M}-\text{N}+1), \text{K}, \text{J}) * \text{TRAN}(\text{N}, \text{M}, \text{K}, \text{J}, \text{NTRAN}) * 0.381 \text{ E-4}$$

calculates the concentration CHI (ppm) at hour M due to a steady emission EMIS (lb/hr) between the hours (M - N) and (M - N + 1) from stack K at plant J. (The element NTRAN in the calling sequence is discussed in Section 4.5.) Entry TRAN of function ITRAN thus calculates the normalized (X/Q) concentration at a single receptor due to a given point source. TRAN is linked to PUFF by common statements which transmit the source and receptor coordinates and all pertinent meteorological variables. If the source is actually a virtual source located upwind of a physical stack or area source, the quantities TX, TY, and TZ (hr) are also specified so that

$$\sigma_{x_0} = \sigma_x(\text{TX}), \quad \sigma_{y_0} = \sigma_y(\text{TY}), \quad \text{and} \quad \sigma_{z_0} = \sigma_z(\text{TZ}).$$

The time increments associated with pseudo upwind point sources representing area sources have been previously calculated in subroutine PSEUDO.

Function TRAN performs the following five major calculations:

1. Compares the effective stack height and the time dependence of the lid height during the puff lifetime to determine an effective lid height for positioning the virtual sources simulating multiple reflections between ground and lid.

2. Represents the puff by a steady plume and calculates concentration at receptor; if this concentration is less than EPS (usually 0.001 ppm SO<sub>2</sub>), the source is neglected for that hour and TRAN = 0. Otherwise,

3. Calculates the concentration at the dose point using the integrated-puff transport model; this requires integration via subroutine INTEG1 of the puff kernel, KERN. This calculation is performed at most for only the actual source, the first below-ground reflection, and the first above-lid reflection.

4. Calculates concentrations from higher-order multiple images by standard Gaussian exponential factors; i.e., given X<sub>3</sub> = [concentration at receptor from a source image located Z<sub>3</sub> miles above the receptor], then the concentration X<sub>4</sub> due to the image located Z<sub>4</sub> miles above the receptor is approximated by

$$X_4 = X_3 \exp \left\{ \frac{Z_3^2 - Z_4^2}{2\sigma_z^2} \right\}. \quad (4.1)$$

5. Sums concentrations due to real source and all images to get the quantity TRAN.

These five basic calculations in TRAN are designated by appropriate comment cards in the FORTRAN listing and are discussed in detail in the remainder of this section.

#### 4.1 The Effective Lid Height (HLID)

The existence (or assumption) of physical limits to vertical dispersion requires special treatment when plume or integrated-puff formulas are the basic transport models, since the fundamental equations are written for an infinite medium. A reasonable approach for steady-state solutions (Turner, 1967) uses the point-source plume equation over the travel distance  $X_C$  defined by  $\sigma_z(X_C) = 0.74 H_m$ ; for travel distance greater than  $2X_C$ , uniform vertical mixing is assumed; for intermediate distances, a linear interpolation is used. Since, mathematically, the solution for uniform mixing is equivalent to the superposition of an infinite number of multiple reflections (four pairs usually suffice), this method has been employed in TRAN. It has an advantage over the first method in that the proximity of the actual plume (center line +  $2\sigma_z$ ) to the lid is considered rather than  $\sigma_z$  alone, an advantage that is particularly important when time-dependent variations of lid height are considered.

To calculate the concentration at time M due to an emission between hours (M - N) and (M - N + 1), a single lid height must be selected that is most representative of the N hours since the emission began. The following rules are used in TRAN to determine the value of HLID:

1. If  $N = 1$ , then  $HLID = HMIX(JSUB(M-N+1)) = HMIX(JSUB(M));*$  i.e., for releases at most 1 hr old, TRAN uses the mixing layer height that occurred during the period of the emission. (All meteorological data and emission data are stored as constant values for each hour.)

2. If the puff has existed for more than 1 hr, i.e.,  $N > 1$ , beneath a mixing layer which is steadily rising such as often occurs after sunrise, then the final (maximum) mixing height is used; i.e., if  $N > 1$  and  $HMIX(JSUB(M-N+I)) \leq HMIX(JSUB(M-N+I+1))$  for  $I = 1$  to  $(N - 1)$ , then the effective lid height HLID is set equal to  $HMIX(JSUB(M))$ . This assumption for a steadily rising lid is based on the consideration that, if the proximity of the lid to a given plume results in a notable limitation of the vertical dispersion, then a rising lid implies a steadily increasing dilution volume, and thus the lid height during the most recent hour is most representative.

3. The problem of approximating plume behavior during a period of steadily falling lid height is more complicated. When the lid is higher

---

\*See Section 3.2.1 for discussion of function JSUB.

than [effective stack height +  $2\sigma_z$ ], the interaction between plume and lid is insignificant. As the steadily falling lid moves downward through the plume, it is assumed that pollutant now above the lid is not reflected by the lid. (Clearly, the lid does not act in the manner of a piston compressing the plume into a smaller volume.) Thus, the situation of a steadily falling lid during the lifetime of a puff is approximated in TRAN by setting HLID equal to the first value of the lid height that is less than [effective stack height +  $2\sigma_z$ ]. This phenomenon is important in regions such as Los Angeles, where the diurnal rising and falling of the lid with reasonably brisk winds aloft will remove a significant amount of otherwise trapped pollutant.

4. The effect of a lid height that rises and falls during the lifetime of a puff has not been studied sufficiently, and, based on the arguments for the previous two cases, the HLID is set at the maximum value occurring during the lifetime of the puff.

5. If at the time of the emission, the effective stack height is greater than the mixing-layer height ( $KSTAB \geq 1$ ), and if the lid does not rise above the puff centerline, the stability class used to calculate puff dispersion is set equal to 5 (stable) and no lid effects are considered. This assumption is more satisfactory than a complete neglect of emissions above the lid, but certainly does not attempt to approximate the details of diffusion from the stable layer downward into the more unstable layer beneath the lid. (See Section 1.2.6.)

6. The fumigation phenomenon, which depicts a plume emitted into stable air above a rising lid and then subjected to strong vertical diffusion as the mixing layer rises above the plume centerline, is modeled by setting the effective lid height, HLID, equal to the maximum mixing-layer height during the puff lifetime, and then adjusting the hourly stability indices so that  $JSTAB = 5$  (stable) when  $HMIX < [\text{effective stack height}]$  and  $JSTAB = 4$  or 3 (depending on insolation) when  $HMIX \geq [\text{effective stack height}]$ .

#### 4.2 Puff Significance--Comparison with a Plume Model

A version of the continuous Gaussian-plume formulation is employed to test whether a given 1-hr release between hours (M - N) and (M - N + 1) is significant at time M for a given receptor. This test precedes and, if negative, will cause TRAN to skip the actual calculation of the concentration according to integrated puff formulation. The plume test is best described by the following example.

Figure 4.1 describes the history of the leading puff of a 1-hr release beginning at time M - 3. The trailing puff or end of the hour-long release describes the path in Fig. 4.2. Figure 4.3 shows the superposition of these two trajectories and the locus (dotted line) of the whole hour-long release. The actual concentration field is represented by horizontal and vertical

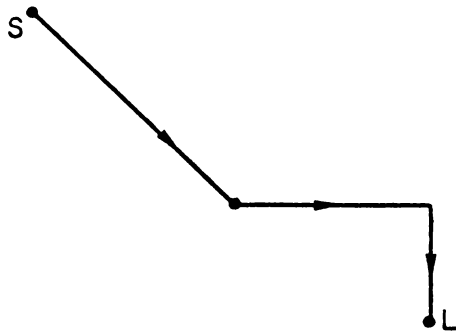


Fig. 4.1

Trajectory of Leading Puff of 1-hr Release. ANL Neg. No. 113-1166.

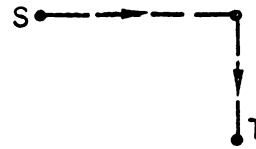


Fig. 4.2

Trajectory of Trailing Puff of 1-hr Release. ANL Neg. No. 113-1167.

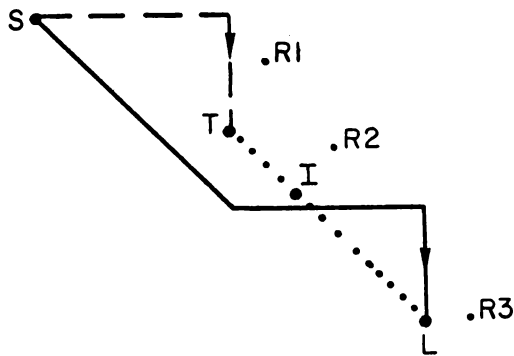


Fig. 4.3

Locus (· · ·) of Puff Centers at Time M due to Release between Hours M - 3 and M - 2. ANL Neg. No. 113-1168.

diffusion about the line segment TL. Figure 4.3 also shows three representative dose points (R1, R2, and R3) for which the concentration is to be estimated via the standard Gaussian-plume formula,

$$X_{\text{Test}} = \frac{Q}{2\pi U \sigma_y \sigma_z} \left\{ \exp \left[ \frac{-Y^2}{2\sigma_y^2} \right] \right\} \left\{ \exp \left[ \frac{-Z^2}{2\sigma_z^2} \right] + \exp \left[ \frac{-Z_2^2}{2\sigma_z^2} \right] + \exp \left[ \frac{-Z_3^2}{2\sigma_z^2} \right] \right\} \quad (4.2)$$

and

$$\sigma_y = \sigma_y(T + T_y), \quad \sigma_z = \sigma_z(T + T_z),$$

where

$Y$  = minimum distance from the receptor point to the centerline segment TL; in Fig. 4.3,  $Y = R1 - T$ ,  $R2 - I$ , and  $R3 - L$  for the three receptor points, R1, R2, and R3;

$T$  = time of flight to the point on the centerline segment used to determine the distance  $Y$ ;  $T$  is used to calculate the dispersion coefficients  $\sigma_y$  and  $\sigma_z$ ; for sources with initial dimensions, e.g., area sources, represented by  $\sigma_{y_0}$  and  $\sigma_{z_0}$ , the quantities  $T_y$  and  $T_z$  satisfy  $\sigma_{y_0} = \sigma_y(T_y)$ ,  $\sigma_{z_0} = \sigma_z(T_z)$ ;

$U$  = mean wind speed during time  $T$ ;

$Z_1$  = vertical distance from plume centerline to receptor;

$Z_2$  = vertical distance from the first below-ground image to the receptor;

and

$Z_3$  = vertical distance from the first above-lid image to the receptor;

and

$Q$  = source emission rate during hour  $(M - N)$  to  $(M - N + 1)$ .

A receptor  $R$  upwind of the source  $S$  may be influenced by upwind diffusion during the first hour of the release, i.e., when  $N = 1$ . In this case, according to the notation of Fig. 4.3,  $Y = R - T = R - S$ ,  $T = 0$ , and Eq. 4.2 may be invalid, since  $\exp[-Y^2/2\sigma(0)] = 0$  if  $T_y = 0$ . In this situation, we check whether the advection rate  $U$  is sufficiently greater than the horizontal diffusion rate  $\sigma_y(T)$  by evaluating the concentration  $X_{\text{test}}$  at  $R$  based on the distance  $Y = R - L = U$  and dispersion coefficient  $\sigma_y$  (1 hr).

The concentration at a given receptor due to each 1-hr release from each source is thus approximated by a modified version of the standard plume equation. If  $X_{\text{test}} < \text{EPS}$ , the release is considered to have a negligible effect. The tolerance  $\text{EPS}$  is most conveniently set at from 1 to 10% of the lowest detectable pollutant concentration. The accuracy of validation runs for TAM's 1-5 in January 1967 was not affected by raising the tolerance from 0.0001 to 0.001 ppm  $\text{SO}_2$ .

#### 4.3 Integrated-puff Calculation

If the test of puff significance (Section 4.2) indicates that  $X_{\text{test}} \geq \text{EPS}$ , the concentration (normalized) at the receptor due to the release between hours  $(M - N)$  and  $(M - N + 1)$  is calculated according to the theory of the integrated-puff model (see Section 1.2.1). Thus Eq. 1.9 must be evaluated by integration

$$G_{M,N} = \int_{N-1}^N dT \frac{\exp \left[ - \left( \frac{\left\{ x - \sum_{j=M-N+2}^M u_j - u_{M-N+1}[T - (N-1)] \right\}^2 / 2\sigma_h^2}{+ z^2 / 2\sigma_z^2} + \frac{\left\{ y - \sum_{j=M-N+2}^M v_j - v_{M-N+1}[T - (N-1)] \right\}^2 / 2\sigma_h^2}{(2\pi)^{3/2} \sigma_h^2 \sigma_z} \right) \right]}{(2\pi)^{3/2} \sigma_h^2 \sigma_z} \exp \left( - \frac{0.693T}{T_{1/2}} \right). \quad (4.3)$$

This is performed separately for the source ( $Z = Z_1$ ), the first below-ground image ( $Z = Z_2$ ), and the first above-lid image ( $Z = Z_3$ ) with the following two exceptions:

1. From the plume test (Section 4.2), we have calculated the quantities  $E1 = \exp(-Z_1^2/2\sigma_z^2)$ ,  $E2 = \exp(-Z_2^2/2\sigma_z^2)$ , and  $E3 = \exp(-Z_3^2/2\sigma_z^2)$ . If  $E2/E1 \geq 0.7$ , then the coupling coefficient  $G_{M,N}(Z_2)$  based on  $Z_2$  is set equal to  $(E2/E1) G_{M,N}(Z_1)$ ; i.e., only one integration is performed and a simple exponential correction is used to estimate the other integral. This approximation yields  $G_{M,N}(Z_2)$  within 1% of the value resulting from actual integration of Eq. 4.3 with  $Z = Z_2$ . If possible, a similar simplification is used for  $G_{M,N}(Z_3)$ .

2. If  $E2/E1 < 0.05$ , the image at  $Z_2$  is neglected. A similar test is used for the image at  $Z_3$ .

In TRAN, the integration is performed by the statement

```
CALL INTEG1(KERN,N-1,N,XINT,AMAG,EPSIL,ADD1),
```

where INTEG1 is a standard numerical-integration subroutine, KERN is a function subprogram (Section 5) that calculates the integrand in Eq. 4.3, and ADD1 is the value  $G_{M,N}(Z_1)$  returned INTEG1.

#### 4.4 Higher-order Images

The synthesis by an infinite-medium point-source kernel of plume transport between two impenetrable boundaries (ground and lid) requires up to five pairs of images depending on the lid height, wind speed, stability class, and relative positions of source and receptor.

For example, in Fig. 4.4, the first image source above the lid is the reflection about  $H_m$  of the actual source. Its vertical displacement for use in Eq. 4.3 is  $(2H_m - S - R)$ , where  $S$  is the source height and  $R$  the receptor height. The second image source above the lid is the reflection about  $H_m$  of the first below-ground image. Its vertical displacement above the receptor is  $(2H_m + S - R)$ .

According to Section 4.3, the coupling coefficient  $G_{M,N}(Z_3)$  is evaluated by numerical integration of Eq. 4.3 or by one of the approximations described above. For the higher-order images, the coupling coefficients are estimated by the relationship

$$G_{M,N}(Z_i) = G_{M,N}(Z_3) \exp\left(+\frac{Z_3^2}{2\sigma_z^2(T + T_z)}\right) \exp\left(-\frac{Z_i^2}{2\sigma_z^2(T + T_z)}\right), \quad (4.4)$$



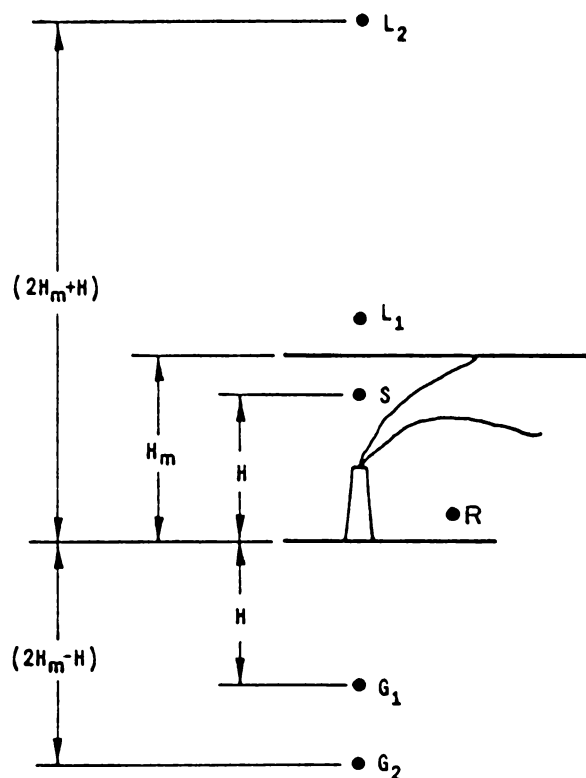


Fig. 4.4 Multiple Reflections between a Stable Layer and Ground Represented Mathematically by Two Sets of Image Sources. The image  $G_1$  is reflected above the lid at  $L_2$ . The image  $L_1$  is reflected below ground at  $G_2$ . ANL Neg. No. 113-2859.

which is simply an exponential correction according to a Gaussian-plume theory. Under conditions of low mixing layer and travel distances on the order of 10-20 miles, the multiple-image formulation with the exponential approximation of Eq. 4.4 and five image pairs is within 10% of an integrated-puff solution using a kernel representing uniform vertical mixing. There is presently no special advantage in revising the computer code by introducing a transition from a point-source kernel to one representing uniform vertical mixing (as in Turner, 1967), since these exponential approximations require negligible computer time compared to the numerical integration required to obtain the real source-coupling coefficient  $G_{M,N}(Z_1)$ .

#### 4.5 The Option "NTRAN=1"

The computer program, in particular subroutine PUFF, considers each stack as a separate source. For two or more stacks at the same plant,

it is possible to calculate the concentration at a given receptor due to the first stack and then estimate the contribution from additional stacks by exponential corrections according to Eq. 4.4. For the original stack calculation, NTRAN=0 in the calling sequence of TRAN. For subsequent calculations, NTRAN=1. To ensure that, if the first stack has a negligible influence ( $X_{test} < EPS$  in Eq. 4.2) due to low emission rather than to geometric considerations, the contribution from a second stack with a significant output is calculated in detail rather than by the exponential approximation of Eq. 4.4. The exponential approximation is also forbidden when a plant has one stack below the lid and a second one above the lid.

#### 4.6 Conclusion

This completes the description of the algorithms associated with TRAN. Subroutine INTEG1 is called from TRAN to integrate the kernel (KERN) in Eq. 4.3. The dispersion-coefficient functions SIGX, SIGY, and SIGZ are also used in TRAN.

## 5. SUBROUTINE KERN (T, FT)

Subroutine KERN evaluates the integrand in the fundamental integrated-puff equation (see Sections 1.2.1 and 4.3)

$$G_{M,N} = \int_{N-1}^N dT \frac{\exp \left[ - \left( \left\{ x - \sum_{j=M-N+2}^M u_j - u_{M-N+1}[T - (N-1)] \right\}^2 / 2\sigma_h^2 \right) + \left\{ y - \sum_{j=M-N+2}^M v_j - v_{M-N+1}[T - (N-1)] \right\}^2 / 2\sigma_h^2 \right]}{(2\pi)^{3/2} \sigma_h^2 \sigma_z} \exp \left( - \frac{0.693T}{T_{1/2}} \right). \quad (5.1)$$

where the dispersion coefficients are functions of the time of flight T and the classes of atmospheric stability occurring during this time. Subroutine KERN is linked to TRAN and PUFF by common statements which include the requisite meteorological and geometrical parameters. The evaluation of Eq. 5.1 is initiated in TRAN by statements of the form

CALL INTEG1(KERN,N-1,N,XINT,AMAG,EPSIL,ADD1),

where INTEG1 is a standard numerical-integration routine and ADD1, the value of  $G_{M,N}$  returned by INTEG1.

The basic method of numerical integration used in subroutine INTEG1 is a variable interval Simpson's Rule modified in such a way as to yield results two orders higher in accuracy than Simpson's Rule.

Evaluation of the integrand in Eq. 5.1 is straightforward, except for the calculation of the dispersion coefficients when the atmospheric stability class varies during the lifetime of the puff. As discussed in Section 1.2.4 and Fig. 1.6, the dispersion coefficient associated with a puff of lifetime T is estimated by the general equation

$$\sigma(M,N,T) = \sum_{j=M-N+1}^M \{S(i_j, T+j-M) - S(i_j, T+j-M-1)\}, \quad N-1 \leq T \leq N \quad (5.2)$$

where  $S(i, T)$  is the dispersion coefficient as a function of lifetime T or distance  $X = UT$  for constant stability class i, and  $S(i, t) = 0$  for  $t \leq 0$ .

In KERN, Eq. 5.2 is programmed according to the logic of

$$\left. \begin{aligned} \sigma(M,N,T) &= S(i_M, T) \quad \text{for } N = 1 \\ \text{and} \\ \sigma(M,N,T) &= \sum_{j=M-N+2}^M [S(i_j, T+j-M) - S(i_j, T+j-M-1)] + S(i_{M-N+1}, T+1-N) \quad \text{for } N > 1. \end{aligned} \right\} (5.3)$$

PART II  
VALIDATION OF MODEL:  
ESTIMATION OF SO<sub>2</sub> LEVELS IN CHICAGO

6. INTRODUCTION TO PART II

The multiple-source urban atmospheric dispersion model described in Part I of this report is essentially a scheme for describing the advection and diffusion of airborne material emitted from a source of finite initial dimensions. To estimate the spatial and temporal variations in pollution levels, the model must be supplied with a time series of emission inventory and meteorological data as well as measured pollutant concentrations for comparison with predictions. These data-management requirements have been met by the development of a master Air Pollution Information and Computation System (APICS; Kennedy and Anderson, 1969; Chamot *et al.*, 1970) designed to automate the entire process of data storage, retrieval, manipulation, analysis, and display associated with the dispersion-model studies.

The APICS system consists of an IBM PL-1 data storage and retrieval code and a series of operational subroutines and computational codes tailored to the analysis of air-pollution data. With this system, the data stored in the master file can be partitioned in any way desired. Any combination, array, or subset of emission, meteorology, and/or air quality data can be formed and retrieved. The selected data array can be accessed through a FORTRAN subroutine which allows the user to manipulate the array in any desired way. For example, the analyst may form a new data array, which consists of products of components of the original array raised to some power, etc. Standard subroutines for computing atmospheric stability, smoke plume rise, etc., are included as options in this system.

The array of data in the master file may be analyzed in a multivariate linear-regression analysis code or a discriminant analysis code which is part of the system, and the results may be displayed as tables, histograms, or CALCOMP plots.

The air-pollution data-management system described above provides a uniquely powerful tool for developing and testing dispersion models. The transport algorithms introduced in Sections 1-5 (FORTRAN listings appear in Appendix A), the emission-simulation model described in Section 7, and the meteorological and air-quality data described in Section 8 have been incorporated into the APICS system, so that the testing and validation process, conducted with a 2-yr computerized inventory of hourly average meteorology and sulfur dioxide air-quality data, is totally automated. Meteorology and emission data from the master data file are input to the dispersion model, and sulfur dioxide concentrations are calculated; these results are

compared with the corresponding measured air-quality data and displayed in a single operation within the Argonne IBM 360-75 computer. The sensitivity of the model to variations of critical meteorological parameters and the effects of modifications in the structure of the model itself can be tested.

Part II of this report describes the acquisition and manipulation of emission and meteorological data for the City of Chicago from January 1966 to October 1967.\* Tables and maps showing all emission inventory data are included along with a sample problem (given in Appendix B). Results of winter and summer validation studies involving approximately 10,000 station-hours of data are presented in Section 10.

---

\*Much of the descriptive material appeared in ANL/ES-CC-005 and is repeated here for completeness.

## 7. DEVELOPMENT OF AN EMISSION INVENTORY

A major task element of the Chicago Air Pollutions Systems Analysis program was the development in cooperation with the Chicago DAPC\* of an inventory of hourly average emissions for the power plants and industrial, residential, commercial, and institutional SO<sub>2</sub> sources which are the primary contributors to Chicago's sulfur dioxide air-pollution problem.

Figure 7.1 shows the location and distribution of the largest individual coal- and oil-burning sources of sulfur oxides. Figure 7.2 shows the source density of residential, commercial, and industrial emitters which were too numerous to inventory individually. Figure 7.3 depicts the distribution and magnitude, by source category, of Chicago's SO<sub>2</sub> emitters.

Power plants (Section 7.1); major industrial, municipal, commercial, and residential point sources (Section 7.2); and homogenized industrial, commercial, and residential area sources (Section 7.3) have been studied and data acquired in a somewhat piecewise fashion. Hourly SO<sub>2</sub> output for power plants has been derived from actual megawatt logs for the 1966-1967 period; other major sources are analyzed by prorating annual fuel-use data according to seasonal and diurnal patterns established by plant-by-plant interviews; industrial-area source data are derived from a 1963 Chicago DAPC survey of annual fuel use; commercial SO<sub>2</sub> emissions are based on a 1961 survey by the Markets and Rates Department of the Peoples Gas, Light and Coke (PGLC) Company; and residential-area source data are from a 1968 survey by the same company.

This melange of informational sources is to be expected (Ozolins and Smith, 1966), and, with the exception of hourly power-plant output, all data and computational requirements are compatible with routine procedures for obtaining a regional emission inventory by rapid-survey and direct-mailing techniques.

The routine accumulation of hourly power-plant data is clearly impractical. Computerized algorithms have recently been developed at Argonne which simulate seasonal and diurnal patterns of electric generation and hence emission from power plants. Although the input for these calculations is somewhat more complex than for industrial sources, the data requirements are consistent with plant statistics normally compiled by utilities. Since a limited number of plants of this type usually represent a significant portion of total particulate and SO<sub>2</sub> emissions from stationary sources, effort expended in this area by a regional air-pollution authority is worthwhile. Statistical comparisons of estimated and actual power-plant output for the Commonwealth Edison system will be the subject of a future report.

Studies at Argonne on diurnal and seasonal variations of emissions of particulates and SO<sub>2</sub> from stationary sources have therefore resulted in

---

\*Department of Air Pollution Control; presently called the Department of Environmental Control.

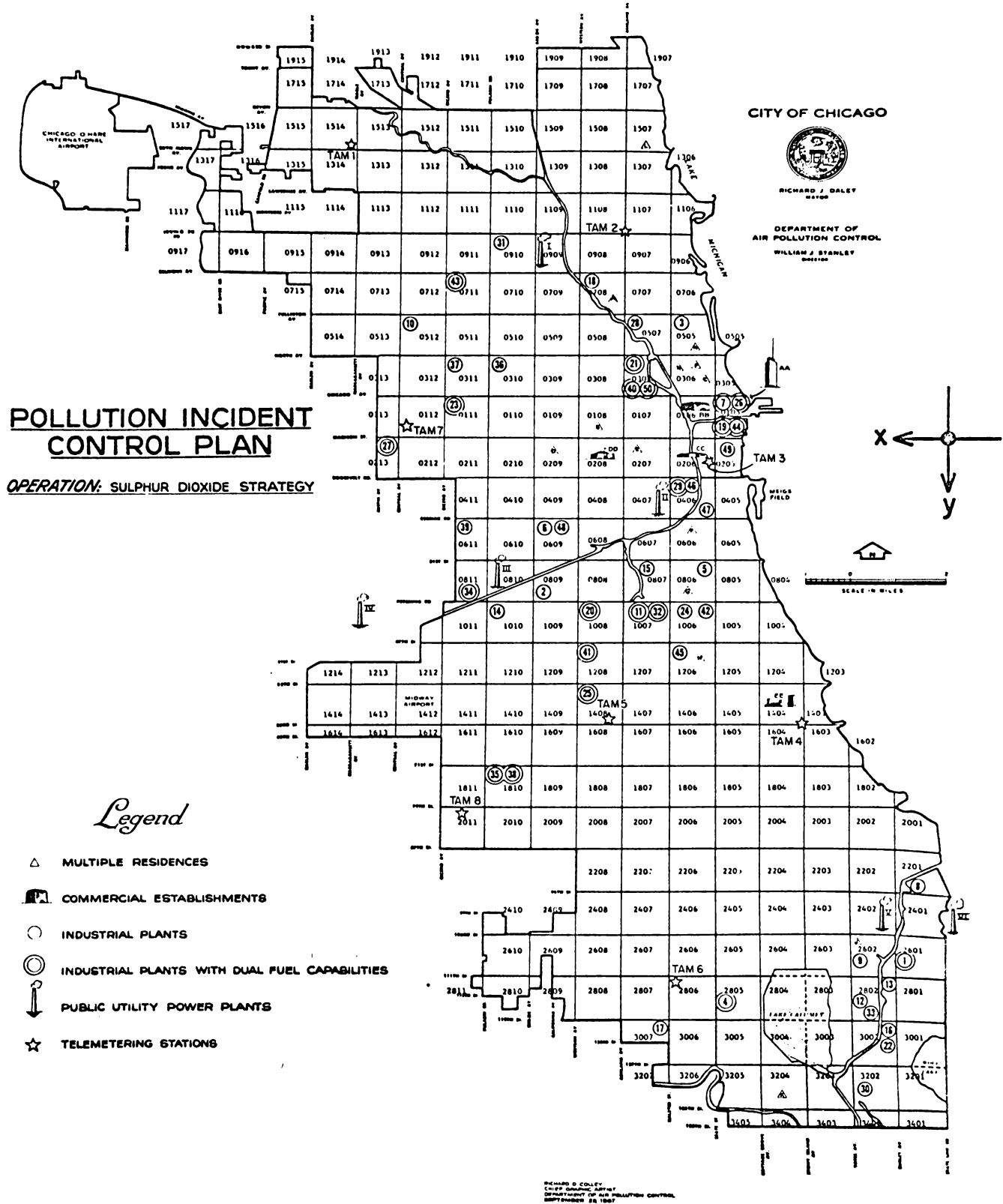


Fig. 7.1. Chicago Map of Major Sources. ANL Neg. No. 112-8979 Rev. 3.

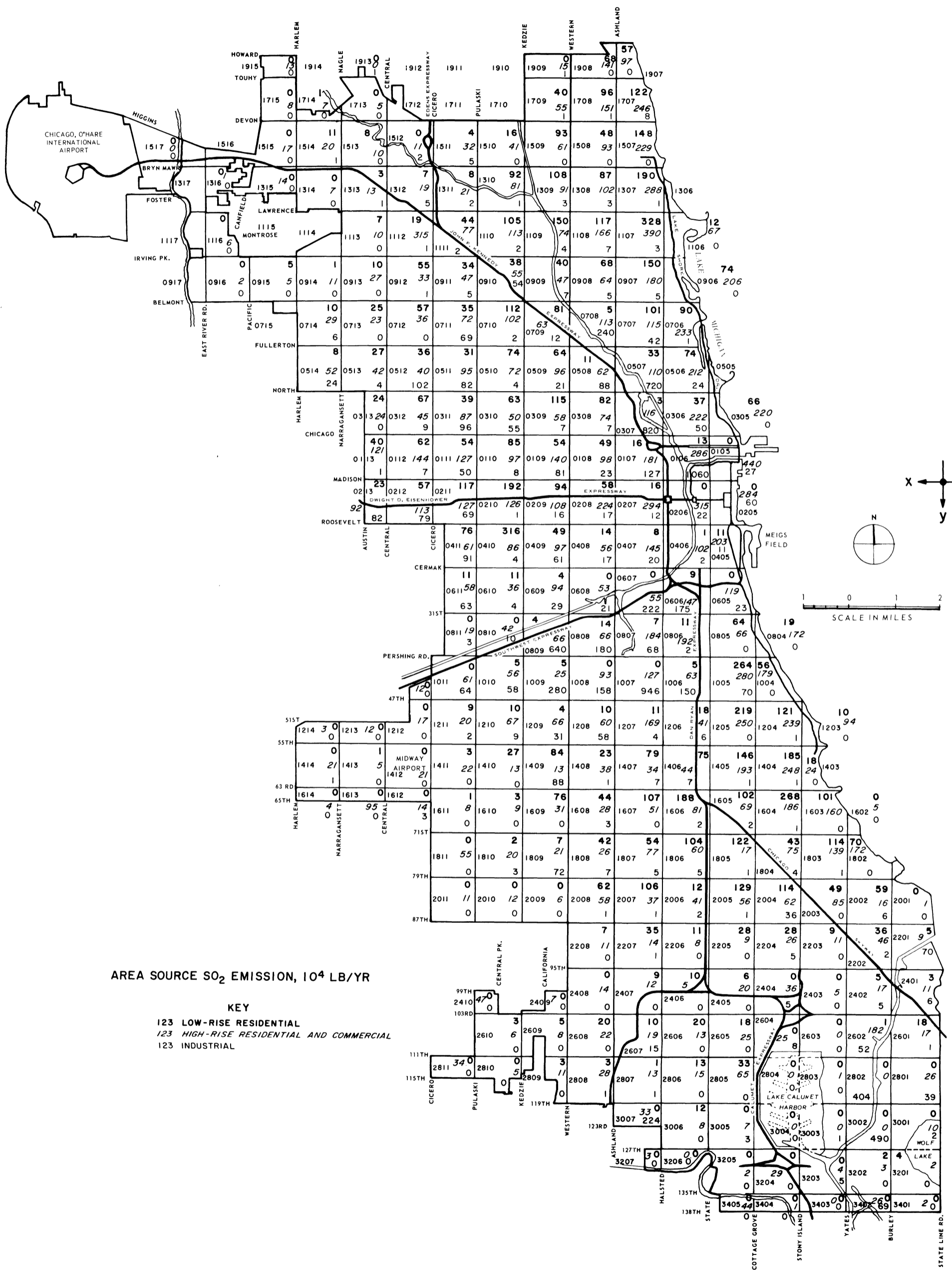


Fig. 7.2. Chicago Map of SO<sub>2</sub> Area Sources.  
ANL Neg. No. 113-1169.

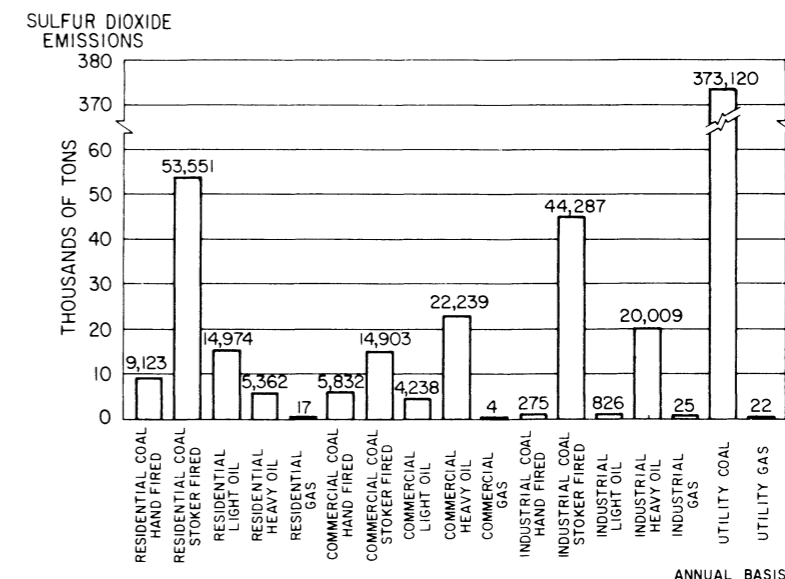


Fig. 7.3. Sulfur Dioxide Source Distribution Prepared by Chicago DAPC, 1967. ANL Neg. No. 112-7209.

a single, realistic simulation program, whose input is compatible with readily obtainable fuel use and industrial-process data. The following sections present formats for acquisition of emission data, tables, and maps listing the complete inventory used in the validation studies, and the algorithms that prorate these long-term emissions.

### 7.1 Power Plants

Electric power for the Northern Illinois region is provided by a network of 15 power-generating stations. Of these, six are located in the Chicago metropolitan area. These six coal-fired plants, shown in Fig. 7.1, account for approximately 65% of the sulfur oxides released into the Chicago atmosphere. The following table indicates the relative contribution of each plant in terms of its annual fuel consumption (1967 data, Chicago DAPC).

Plant Designation	SO <sub>2</sub> , tons per year	SO <sub>2</sub> , percent of city total
Crawford	107,954	18.97
Ridgeland	100,540	17.67
Fisk	73,438	12.90
State Line	70,606	12.42
Northwest	10,566	1.86
Calumet	10,016	1.76
Total	373,120	65.58

Of these installations, four--the Fisk, Crawford, Ridgeland, and State Line plants--are capable of partial or total conversion from coal to natural gas during periods when the latter fuel is available at "dump or interruptible" rates.



Because of the extremely large emission rates associated with the urban power plants and because of their complex, but relatively consistent, diurnal emission cycle, the acquisition of the most accurate body of emission data that could be obtained was a priority task element of the emission inventory. Fortunately, the Chicago utility maintains excellent records of plant operation. These were provided for January 1966 through December 1967. The data array required was:

1. Hourly power generation, in megawatts (MW), for each generator unit of each power plant, including an indication of whether the power was generated with coal or gas.
2. Monthly coal and natural-gas consumption rates for each boiler-generator combination.
3. Monthly average coal-sulfur content analyses for each plant.
4. A set of boiler-turbine-generator efficiency curves for each generator unit. These presented efficiency versus power output for each unit.
5. A set of stack temperature versus output curves for each plant.
6. A physical description of each plant layout, including the relationship between boilers, turbines, generators, and stacks, stack heights, etc.

The above information was combined in a computer algorithm which yielded a calculation of the hourly fuel consumption, and SO<sub>2</sub> emission rates for each stack of each plant of the system. Details of the computational procedure are provided in the program progress reports (Croke et al., 1968a,b,c).

The resultant body of power-plant emission data was stored in the master data file of the Air Pollution Information and Computation System (APICS) from which it could be retrieved and automatically input to the dispersion model.

As a general rule, the acquisition of hourly megawatt output is clearly impractical except perhaps for special, real-time computer runs made during episodal situations. Dispersion models (e.g., Clark, 1964; Turner, 1964) have usually assumed a uniform proration of annual fuel use, thus disregarding marked seasonal and diurnal variations in both total system load and in the division of this load among the units within the system. In contrast, Argonne\* has recently developed algorithms which, using statistics normally compiled by utilities, realistically simulates these variations. Although the results of these calculations were not input

---

\* Work performed by J. E. Norco with data and advice from the Commonwealth Edison Company.

to the dispersion model for the validation study (actual hourly megawatt data was used), these algorithms are presented in the remainder of this section since they will appear in the production version of the code.

The ability to simulate the electric generation, and hence the emissions from power plants, is enhanced by the reproducibility of the demand for electricity. Within a given season, daily load patterns have essentially the same shape, but are shifted up or down depending on meteorological variables such as temperature, brightness, and wind speed.

The description of the expected emissions is accomplished in three steps:

1. Estimate the peak power demand of the entire generating system for the day in question.
2. "Fit" an hourly load pattern to this peak, and produce hourly system-load variations.
3. Determine individual unit loadings, and convert these to emission rates.

A detailed description of these procedures follows:

1. Analysis of one year of daily system load charts indicates that seasonal similarities can be isolated by dividing the year into the four seasons:

Winter--December, January, February

Spring--March, April, May

Summer--June, July, August

Fall--September, October, November

The daily charts are simply a plot of the system load versus the hour of the day. (See Figs. 7.4 and 7.5.) Within each season, graphs are made of the peak daily load versus the average daily temperature. (See Figs. 7.6, 7.7, 7.8, and 7.9.) From these graphs, the peak load, as a linear function of temperature, is estimated for each season. Although the variation could be reduced by incorporating additional variables, the accuracy of this simulation does not warrant it. In fact, with the exception of the summer season, the peak might very well be considered a constant. These linear functions are built into the program, but revisions or changes can easily be made by changing the coefficients.

2. Several load patterns for days within a given season are superimposed to develop a typical pattern. It is found that the patterns for all weekdays are similar, as are the patterns for all weekend days. Since little weekend data are usually available, a typical load pattern for weekend days is used for all the seasons.

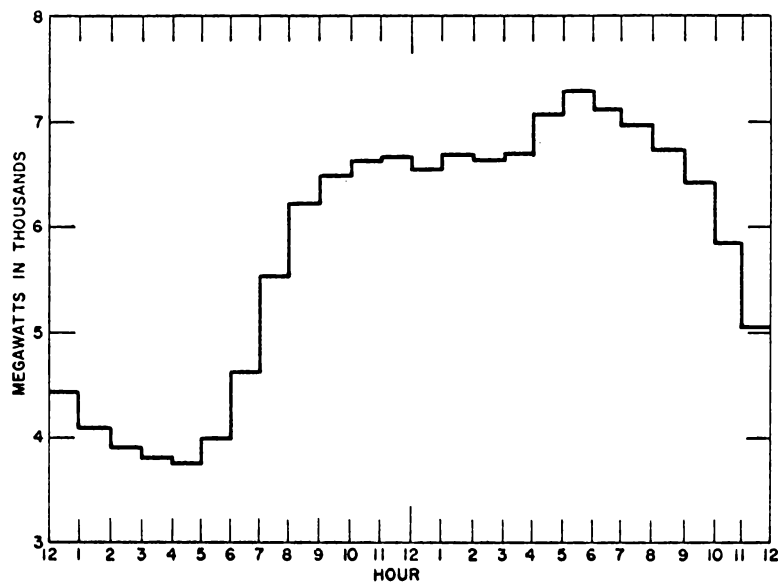


Fig. 7.4  
 Typical Winter Weekday System Load  
 Pattern. ANL Neg. No. 113-1170.

Fig. 7.5  
 Typical Summer Weekday  
 System Load Pattern. ANL  
 Neg. No. 113-1171.

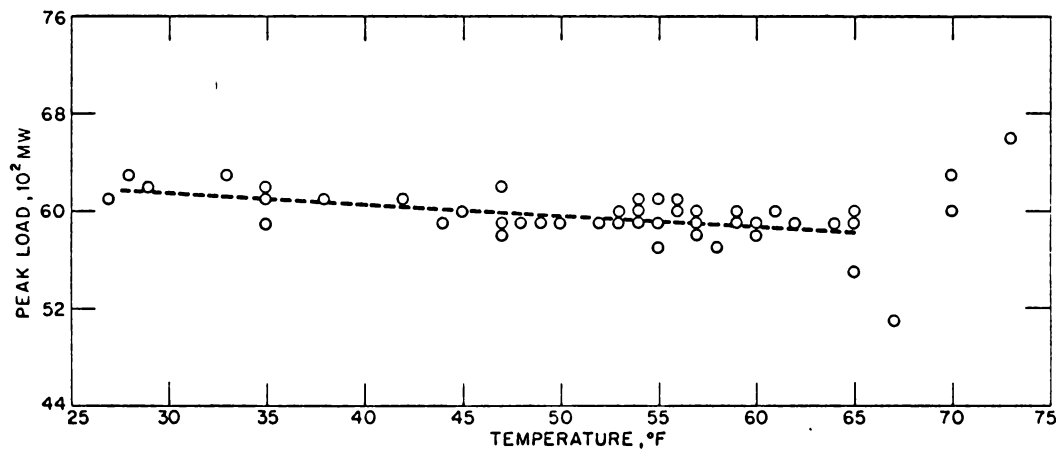
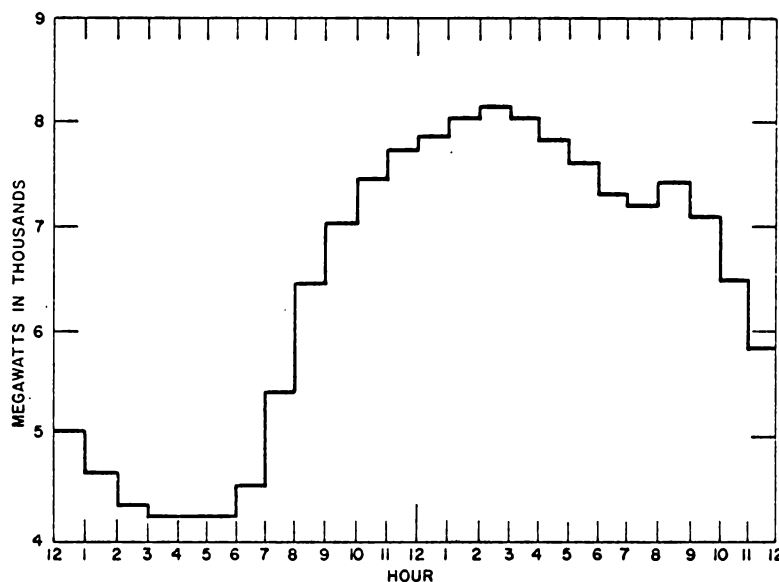


Fig. 7.6. Daily Peak Loads vs Average Daily Temperature for Spring. ANL Neg. No. 113-1172.

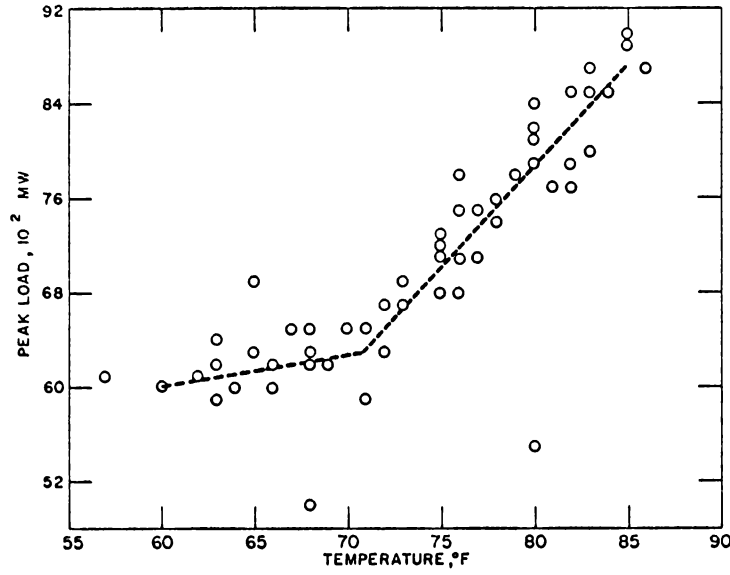


Fig. 7.7  
Daily Peak Loads vs Average Daily  
Temperature for Summer. ANL  
Neg. No. 113-1173.

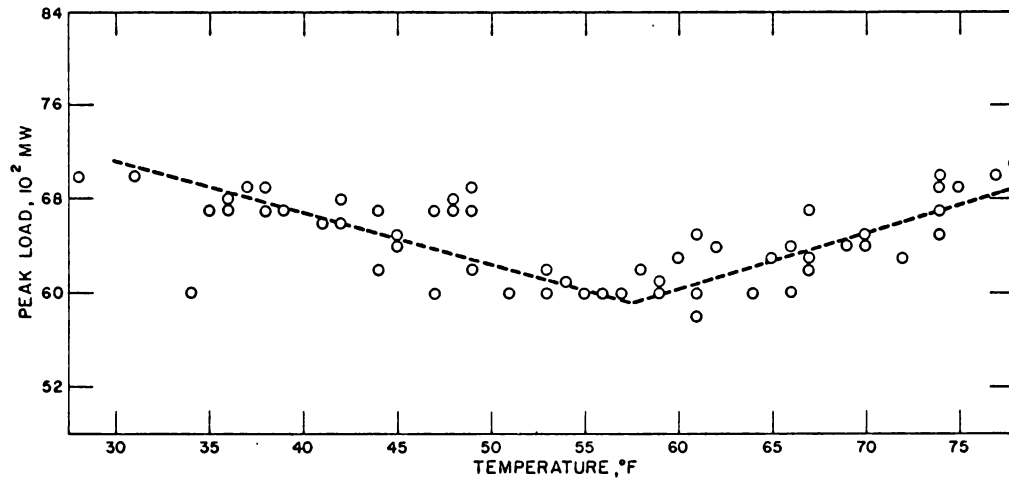


Fig. 7.8. Daily Peak Loads vs Average Daily Temperature for Fall. ANL Neg. No. 113-1174.

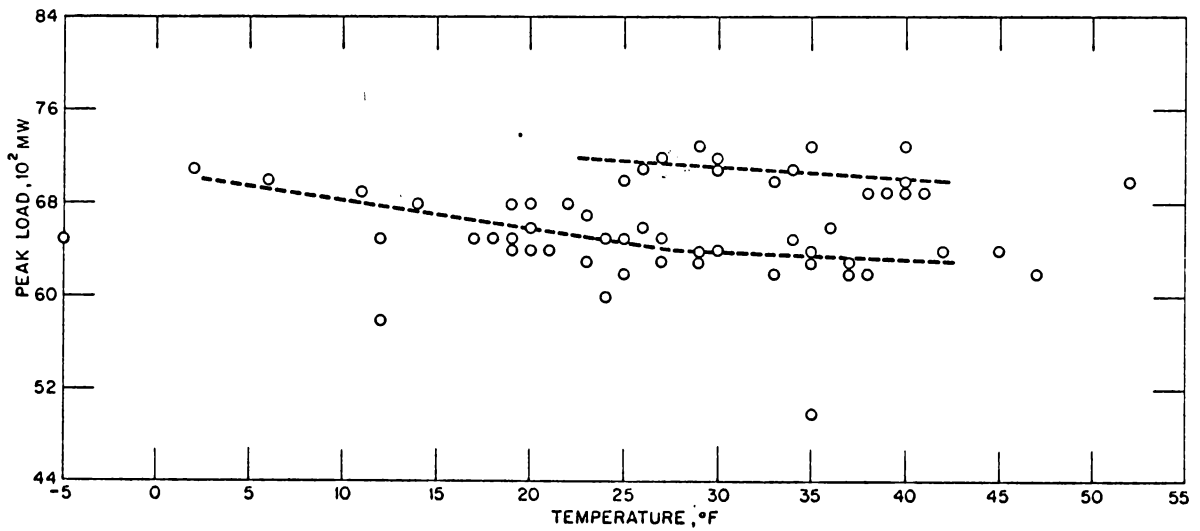


Fig. 7.9. Daily Peak Loads vs Average Daily Temperature for Winter. ANL Neg. No. 113-1175.

In the spring and fall, the average daily temperature affects the shape significantly enough to warrant the use of two weekday patterns for these two seasons: one for temperatures below and one for temperatures above 50°F.

The present method of "storing" these patterns in the computer is to set up data statements, one for each typical load pattern. Each data statement contains 24 numbers, one for each hour of the day. The hourly system load is then calculated by subtracting from the peak, the value in the data statement for the appropriate hour. For example, the data statement to define the load pattern for a summer weekday case might be

DATA SUMWD/2.3, 2.6, 2.8, 2.9, 2.9, 2.8, 2.3, 1.5, 0.8, 0.4,  
 0.2, 0.2, 0.3, 0.0, 0.0, 0.3, 0.4, 0.6, 0.8, 0.8, 0.8, 0.7, 0.7,  
 1.0, 1.8/ (in  $10^3$  MW).

If the peak load forecast from step 1 is 8500 MW, the 7 a.m. system load would be

$$8500 - 2300 = 6200 \text{ MW.}$$

3. Ideally, the system load at any time can be apportioned to the individual generating units within the system in the same manner in which they are actually dispatched, i.e., in order of least cost. However, the "incremental cost" of adding a piece of generating machinery is the decisive criterion, and this is determined on a real-time basis.

Alternatively, if the individual unit loads are plotted against the total system load when there are no major outages, a trend is easily established. Figure 7.10 shows a graph of unit load versus system load for several units in the Commonwealth Edison system. From this typical plot, functional relationships of the form

$$\left. \begin{array}{l} U = b_1 \\ U = b_1 + (b_2 - b_1) \frac{S - a_1}{a_2 - a_1} \\ U = b_2 \end{array} \right\} \begin{array}{l} S < a_1 \\ a_1 < S < a_2 \\ S > a_2 \end{array} \quad (7.1)$$

where

$U$  = individual unit load, MW,

and

$S$  = system load, MW,

can be formulated for each unit.

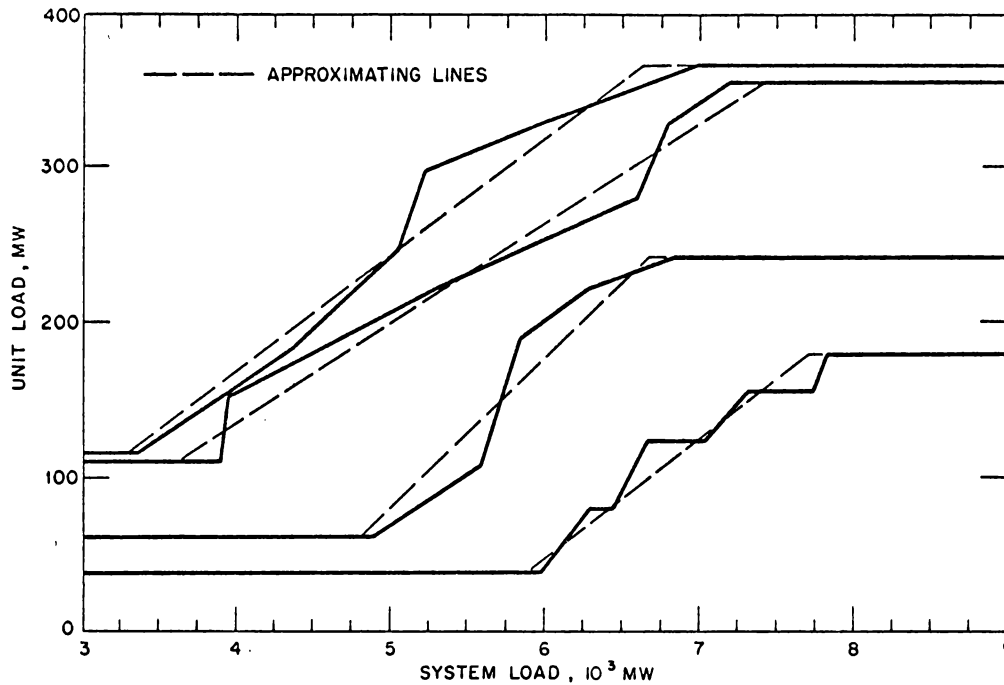


Fig. 7.10. A Typical Relation between Total System Load and Individual Unit Loadings. ANL Neg. No. 113-1176.

The values  $a_1$ ,  $a_2$ ,  $b_1$ , and  $b_2$  are input parameters (see Fig. 7.10).

The advantage to this approach is that the data for only the units of interest need be collected.

The electrical load on a generating unit can be converted to a thermal input using the relationship

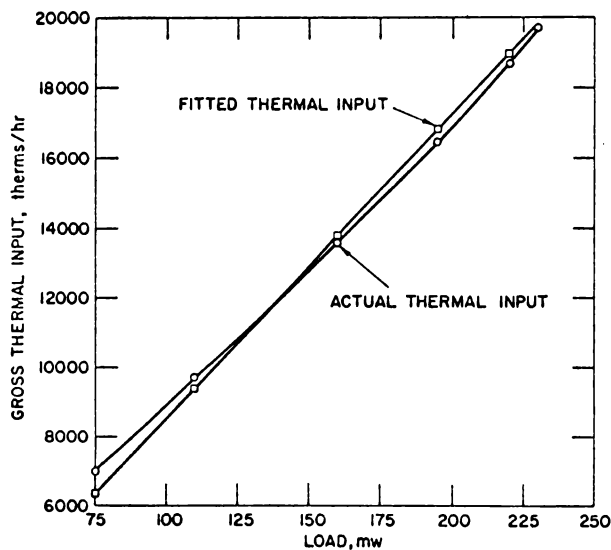


Fig. 7.11. Gross Thermal Input vs Load with Approximating Line. ANL Neg. No. 112-9796.

$$T = AL + B$$

where

$T$  = thermal input, therms/hr,

$L$  = unit load, MW,

and

$A$ ,  $B$  = coefficients (input).

This linear approximation can easily be fitted to the actual data the utility companies keep for each generating unit; a typical load curve is shown in Fig. 7.11.

Through a series of calculations using input data given on the power-plant source-description

cards (Fig. 7.12), the emission rates from each stack associated with the unit are determined.

$$\text{Thermal load: } T = AL + B \text{ (therms/hr);} \quad (7.2)$$

$$\text{Coal (tons/hr)} = \frac{(T \text{ therms/hr}) \times (10^5 \text{ Btu/therm})}{(12,000 \text{ Btu/lb}) \times (2000 \text{ lb/ton})} \times (\text{Avg annual \% coal used}); \quad (7.3)$$

$$\text{Oil (kgal/hr)} = \frac{(T \text{ therms/hr}) \times (10^5 \text{ Btu/therm})}{(18,000 \text{ Btu/lb}) \times (8000 \text{ lb/kgal})} \times (\text{Avg annual \% oil used}). \quad (7.4)$$

NOTE: If the temperature is above the assumed gas availability temperature, SO<sub>2</sub> emissions are reduced according to the percent gas conversion.

$$\text{SO}_2 \text{ from coal (lb/hr)} = \text{Coal (tons/hr)} \times 38.0 \times \% \text{ sulfur}; \quad (7.5)$$

$$\text{SO}_2 \text{ from oil (lb/hr)} = \text{Oil (kgal/hr)} \times 157 \times \% \text{ sulfur}; \quad (7.6)$$

$$\text{Total SO}_2 \text{ (lb/hr)} = \text{SO}_2 \text{ from coal} + \text{SO}_2 \text{ from oil}. \quad (7.7)$$

Plume-rise calculations are based on

$$\text{Thermal-emission rate (therms/hr)} = T \times 0.12. \quad (7.8)$$

Total thermal and SO<sub>2</sub> emission rates are divided among the stacks by multiplying by the percent of the effluent handled by each.

In some isolated cases, the emissions from two or more units will be directed up one stack. To be sure that the thermal emissions are correctly calculated in these cases, a set of cards must be included after the power-plant unit-description cards. The first of this set gives the number of stacks that handle emissions from more than one unit. This number (NCOUPL) is punched in columns 1-6. The following cards (one for each of the NCOUPL stacks) contain:

<u>Column</u>	<u>Description</u>
1-6	The stack number
7-12	The units that are feeding this stack (up to four)
13-18	
19-24	
25-30	





## 7.2 Industrial Sources

There are over 2500 relatively large coal- and oil-burning industrial plants in the City of Chicago. On an annual average basis, these are responsible for approximately 10% of the sulfur oxides emitted within the city limits. The largest 100 of these plants account for over 83% of the total industrial emissions, and the largest 50 plants account for over 77% of this total.

The inventory of industrial emissions was derived from four sources.

### 1. Department of Air Pollution Control Survey

A comprehensive annual average inventory compiled in 1963 by the Chicago Department of Air Pollution Control was computer-processed to establish industrial SO<sub>2</sub> emissions on a square-mile basis. Within any given square-mile sector, industrial emissions were assumed to be uniformly distributed. Emissions from major point sources were subtracted from the appropriate square-mile values. The results are displayed in Fig. 7.2.

### 2. Argonne National Laboratory Field Survey

Detailed fuel consumption and physical and operating cycle data for the 50 largest SO<sub>2</sub> sources were obtained through a field-survey system designed by Argonne and implemented by Laboratory and city engineers. This involved a program of site visitations and personal or telephone interviews with plant personnel.

### 3. Natural-gas Utility Records

The natural-gas consumption records for 1966-1967 and fuel costs for all dual fuel plants among the 50 largest SO<sub>2</sub> sources were obtained from the local, natural-gas supply utility.

### 4. Fuel-supply Records

The Midwest Coal Producers' Institute, an organization of wholesale coal suppliers, provided records of the annual average coal consumption by major industrial sources during 1966-1967.

Industrial sources that were not sufficiently large to be included among the largest 50 emitters were aggregated into uniformly distributed square mile area sources. All plants in this category were assumed to have a stack height of 150 feet.

### 7.2.1 Industrial-source Simulation Program

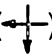
The 50 largest sources of SO<sub>2</sub> were treated as individual point sources. A detailed analysis of the diurnal, weekly, and seasonal operating pattern of each of these plants, in combination with fuel-consumption records, gas-use patterns, and such characteristics as process versus space-heating fuel-use practices was employed in an industrial-plant emission-simulation computer program (PLANTSIM) to generate an operating shift-oriented emission estimate for each plant.

The data file for large industrial sources is designed to include enough information about each plant to characterize its "expected" emission pattern by operating shifts for each day throughout the year. For this purpose, "shifts" are defined as follows:

Shift 1:	12 midnight to 8 a.m.	(0000) to (0800)
Shift 2:	8 a.m. to 4 p.m.	(0800) to (1600)
Shift 3:	4 p.m. to 12 midnight	(1600) to (2400)

Up to three daily emission patterns may be assigned to each plant. These are as follows:

- (1) W: weekday or normal operation
- (2) S: Saturday
- (3) H: Sunday or special holidays.

Finally, a monthly weighting is provided to allow for variation due to seasonal patterns, etc. Each plant requires three computer cards: a source-identification card, and two source-emission cards. Formats and an example of each are shown in Figs. 7.13\* and 7.14, respectively. Items on the cards are described in Tables 7.1 and 7.2. Data for 52 major sources in Chicago (excluding utilities) is presented in Table 7.3 according to the PLANTSIM formats. The origin of the coordinate system (+X west, +Y south) is designated by the crossed arrows () in Figs. 7.1 and 7.2.

The PLANTSIM code is completely general, in that large, individual space-heating sources or major institutional sources such as coal-fired water-pumping stations can be treated in exactly the same manner as industrial plants. For heating plants, the process-load portion of the operating cycle input is zeroed and emissions are calculated solely on the basis of temperature. A special-purpose plant such as a pumping station may be treated as an industrial plant which consumes fuel according to a characteristic processing cycle.

---

\*To allow more room for recording the name and address of each company, the card depicted in Fig. 7.13 was broken into two cards, as is evident by comparison with the actual PLANTSIM input shown in Table 7.3.





TABLE 7.1. Source Identification Card

No.	Item	Description
1	SOURCE NO.	Plant sequence number
2	NAME	Plant name (not to exceed 25 characters including blanks); address may be included if sufficient space is available
3	TYPE	Standard industrial code
4	GRID	City of Chicago square-mile number
5	COORDINATES	The x and y coordinates relative to standard City of Chicago coordinate system
6	STACK DATA	Four stacks maximum (1, 2, 3, 4) HGT: Stack height in feet %: The percent of total emission emitted from each stack
7	WORK SCHEDULE	Each day of the week is assigned to one of the following patterns; i. W: Weekday ii. S: Saturday iii. H: Sunday or Holiday

TABLE 7.2. Source Emission Card

No.	Item	Description
1	SOURCE NO.	Plant sequence number
2	MAX SPACE HTG LOAD	Maximum hourly thermal requirements for space heating
3	MAX PROCESS LOAD	Maximum hourly thermal requirements for process
4	MONTHLY FUEL USE WEIGHTING	Achieves monthly variation in process fuel use. Each month is assigned a weight (0, 1, ..., 9) which corresponds to the average percent (0, 10, ..., 90%) of maximum process fuel used during that month
5	SHIFT FUEL USE WEIGHTING	Within each daily pattern (W, S, H), a weight (0, ..., 99%) is assigned to each shift, which corresponds to the average percent of current monthly process fuel used during that shift
6	% SULFUR COAL	Average percent of sulfur in coal
7	AVG % COAL	Average percent of thermal load due to coal (Zero implies coal is not used.)
8	% SULFUR OIL	Average percent of sulfur in oil
9	AVG % OIL	Average percent of thermal load due to oil (Zero implies oil is not used.)
10	% GAS SP HTG	The percent of space-heating thermal requirements that can be supplied by gas
11	% GAS PROCESS	The percent of process thermal requirements that can be supplied by gas
12	AVG GAS TEMP	The average ambient temperature (°F) at which the dual fuel plant receives gas on an "interruptible" supply contract (varies among plants, but 45°F is representative).
13	GAS PRICE	The gas rate (\$/therm) for dual fuel plants (Much of this data was unobtainable; PLANTSIM disregarded this variable.)

TABLE 7.3. Computer Card Input to PLANTSIM  
for Major SO<sub>2</sub> Sources in Chicago, 1966-1967

```

SOURCES=52 ;
1 MARBHEAD MARELEHEAD LIME CO. 3245 E. 103 ST.
1 2819 26C1 C.9 -12.C 70101C0301C0301003C hhhhhhhh
1 10 2816 999999999999 999999999999999999 1.0 100 0. 0 100 30 45 .0325
2 CAMPBELL CAMPBELL'S SCUP CO. 255C W. 35 ST
2 2032 CEC9 8.2 -3.5 175251752525050C0000 hhhhhwh
2 0 C 666554246766 7099997C2C2030303C 2.9 100 0. 0 100 100 45 .0420
3 PRCC_GAM PROCTER AND GAMBLE 1232 W. NORTH AVE.
3 2841 03C7 6.5 2.0 225502255C0C0C0C0000 hhhhhwh
3 200 25C0 676655344567 60707C5C505C5C5C5C 2.7 100 0. 0 0 0 45 .0
4 SHER_WM SHERWIN-WILLIAMS 11541 SC. CHAMPLAIN
4 2851 28C5 4.1 -13.6 18099C00C0C0C0C0C0C0 hhhhhwh
4 0 3150 665531C0C046 999999999999999999 2.8 100 0. 0 100 100 45 100.
5 INTRLAK1 INTERLAKE STEEL CORP 13500 SO. PERRY
5 3441 32C6 5.2 -16.C 225502255C0C0C0C0000 hhhhhwh
5 0 1365 999999999999 999999999999999999 2.6 100 0. 0 100 100 45 .0000
6 INT_HAR1 INTERNATIONAL HARVESTER 26CC W. 31 BLVD
6 3522 C6C9 8.2 -2.3 100201C0201C0202044C hhhhhwh
6 0 C 655533133445 6599853C55403C554C 3.0 100 0. 0 100 90 45 .0267
7 CGN_1 CONTAINER CORP OF AMERICA 404 E. NORTH WATER ST.
7 2655 01C5 4.5 0.5 1965C1965C0C0C0C0000 hhhhhwh
7 40 1400 666666666666 6099996C9999609999 2.2 100 0. 0 100 100 45 .0262
8 US_STEEL U.S.STEEL CORP 3426 E. 89 ST
8 3441 28C1 0.7 -10.2 15C99C00C0C0C0C0C0C hhhhhwh
8 0 6970 999999999999 999999999999999999 0. 0 0.6 100 100 100 45 .0000
9 INT_HAR2 INTERNATIONAL HARVESTER 28CC E. 106 ST
9 3522 2602 1.5 -12.4 100501C05C0C0C0C0000 hhhhhwh
9 0 C 765533133445 6599853C55403C554C .97 95 1.7 5 100 0 45 .0
10 GEN_SOYA CENTRAL SCYA 1825 NO. LARAMIE
10 2042 0512 11.4 2.3 1674C1253C1253C0C000C hhhhhwh
10 120 30C0 666666555666 5090702C504C20504C 3.0 100 0. 0 0 0 45 .0
11 DARLING1 DARLING AND CO. 1251 W. 46 ST.
11 2013 1CC7 6.7 -4.9 6120 903015750C0000C0 hhhhhwh
11 100C 6CC 999999999999 509999377575377575 3.0 99 .94 1 100 100 45 .0262
12 INTRLAK2 INTERLAKE STEEL CO. 11236 SC. TCRRENCE
12 3441 28C2 1.5 -13.1 6099C0C0C0C0C0C0C0C0 hhhhhwh
12 0 648 999999999999 999999999999999999 3.0 78 1.5 22 0 0 45 .0
13 REP_STL REPUBLIC STEEL CO. 11236 SC. TCRRENCE
13 3441 28C2 1.0 -13.1 100501C05C0C0C0C0000 hhhhhwh
13 0 38C1 999999999999 999999999999999999 0. 0 0.8 100 100 80 45 .0000
14 CRANE CRANE CO. 4100 SC. KEDZIE
14 3433 101C 9.C -4.3 2255C2255C0C0C0C0C0C hhhhhwh
14 0 C 996531111159 2099332C202C2020 3.2 93 1.5 7 100 100 45 .0300
15 ARMOUR ARMOUR AND CO. 1355 W. 31 ST
15 2011 08C7 6.4 -3.C 12050 7025 7025C0C0C0 hhhhhwh
15 10 0 999C0C0C0099 999999999999999999 0. 0 0. 0 100 0 45 100.
16 CHI_MSC CHICAGO MET. SANITARY DIST. 5901 W. PERSHING RD.
16 4952 1C13 12.4 -4.C 17525175251752517525 hhhhhwh
16 0 8820 999999999999 999999999999999999 3.0 91 0.4 9 0 0 45 .0
17 INT_HAR3 INTERNATIONAL HARVESTER 1015 W. 120 ST.
17 3522 3CC7 6.3 -14.2 12C99C0C0C0C0C0C0C0C0C hhhhhwh
17 100C 13C0 765533133445 6599853C55403C554C 2.4 100 0. 0 100 100 45 .0640
18 GLIDDEN GLIDDEN CO. 2333 W. LCGAN
18 2033 07C6 7.9 3.3 15C6C 5020 5020C0000C hhhhhwh
18 75 7C7 999999999999 40707C4C505C4C505C 2.3 93 1.5 7 0 0 45 .0
19 WRIGLEY WILLIAM WRIGLEY CO. 410 NO. MICHIGAN
19 2073 01C5 4.7 C.5 12C99C0C0C0C0C0C0C0C0C hhhhhwh
19 800 4CC 999543333569 508C8C5C808C508C8C 0. 0 2.0 100 100 100 45 .0310
20 DARLING2 DARLING CO. 4210 SC. ASHLAND
20 2013 1CC6 7.C -4.4 28C99C0C0C0C0C0C0C0C0C hhhhhwh
20 0 C 999999999999 55998C102C15102C15 2.9 99 0.9 1 100 100 45 .0262
21 CONT_2 CONTAINER CORP OF AMERICA 900 W. CGDEN

```



TABLE 7.3 (Contd.)

42	2751	0711	10.8	3.6	19C990C00C0C0C000000	hwwwww													
42	500	15C0	886410CC0158	995959595959595959	0.	C	1.8	100	100	100	45	.0297							
43	GEN_REN	GENERAL	RENDERING	CO.	4200	SO.	HERMITAGE												
43	2013	1CC6	7.0	-4.3	12599C00C0C0C0C00000	hwwwww													
43	0	1441	666C00C0166	4059594C95554C9555	0.	0	2.5	100	100	100	45	100.							
44	GOR_BAKE	GCRDEN	PAKING	CO.	5234	FEDERAL													
44	2051	1206	5.1	-5.8	15C99C00C0C0C0C0C0C0C	hshwwsh													
44	0	338	595559595959	4059992C5050205C50	C.	0	1.2	100	0	0	45	.0							
45	CUNEO	CUNEO	PRESS	CANAL-22ND															
45	2751	06C6	5.8	-2.1	14C99C00C0C0C0C0000	hwwwww													
45	75	24C	7774C0C0C077	9959959595959595959	0.	0	2.6	100	100	90	45	.0850							
46	H_BUTTCN	HANDY	BUTTCN	CG.	2255	ROCKWELL													
46	3444	06C9	8.2	-2.2	18C99C00C0C0C0C0C0C0C	hwwwww													
46	541	C	888C0C0C0C88	995999959599909C90	2.5	96	0.8	4	0	0	45	.0							
47	AM_OIL	AMERICAN	OIL	CG.	910	N.MICHIGAN													
47	1301	02C5	4.5	-0.8	36099C00C0C0C0C0C0C0C	hwwwww													
47	120	C	666C0C0C0066	995995959599909C90	0.	0	2.6	100	0	0	45	.0							
48	CHGO_RAW	CHICAGO	RAWHIDE	13C1	AG.	ELSTON													
48	3199	03C6	5.5	1.6	13599C00C0C0C0C0C0C0C	hwwwww													
48	100	50C	666533333566	9959959595959595959	1.0	100	0.	0	100	100	45	.0720							
49	LIN_BELT	LINK	BELT	301	W.	35	ST.												
49	3569	C8C6	5.4	-4.0	15599C00C0C0C0C0C0C0C	hwwwww													
49	0	44	5959959595959	40303C4C3C3C40303C	2.5	100	0.	0	100	100	45	100.							
50	SQ_DINGE	SQUARE	DINGEE	1824	NC.	BEASLEY													
50	2042	05C7	6.5	2.1	4C99C00C0C0C0C0C0C0C	hwwwww													
50	40	35	595958EE8995	0	707C0	C	0	0	0	0	0	2.2	19	1.8	81	100	100	45	.0500
51	W_ELEC	WESTERN	ELECTRIC	CICERC-22ND															
51	3613	0611	10.7	-2.0	25C99C00C0C0C0C0C0C0C	hwwwww													
51	0	1474	5955959595959	9959959595959595959	2.1	99	1.5	1	100	100	45	100.							
52	INGERSCL	INGERSCLL	PRODUCTS	1000	W.	120	ST.												
52	3441	30C7	6.2	-14.0	8599C00C0C0C0C00000	hwwwww													
52	0	681	595993333959	9959996C6C606C6C6C	0.	0	1.7	100	100	100	45	.0300							

All sources treated in PLANTSIM are assigned individual physical stack heights based on the field-survey data.

### 7.2.2 PLANTSIM Computations

When the temperature,  $T$ , is between  $-10$  and  $55^{\circ}\text{F}$ , a linear relationship for the space-heating thermal load  $L^S$  is assumed. This is expressed as

$$L^S = L^S_{\text{MAX}} \frac{[55 - T]}{65}, \quad (-10 \leq T \leq 55). \quad (7.9)$$

Then the total thermal load is

$$L = L^S + L^P, \quad (7.10)$$

where  $L^P$ , the process load, is determined from the appropriate month, day, and shift factors. The amount of load due to coal,  $L^C$ , and due to oil,  $L^O$ , is then determined, and the  $\text{SO}_2$  emission due to each source is calculated as follows:



$$C \text{ (tons/hr)} = \frac{L^C(\text{therms/hr}) \times 10^5(\text{Btu/therm})}{12000(\text{Btu/lb}) \times 2000(\text{lb/ton})} \quad \left. \vphantom{\frac{L^C(\text{therms/hr}) \times 10^5(\text{Btu/therm})}{12000(\text{Btu/lb}) \times 2000(\text{lb/ton})}} \right\} (7.11)$$

$$SO_2^C(\text{lb/hr}) = C(\text{tons/hr}) \times 36.8 \times \%S^C;$$

$$O \text{ (kgal/hr)} = \frac{L^O(\text{therms}) \times 10^5(\text{Btu/therm})}{18000(\text{Btu/lb}) \times 8000(\text{lb/kgal})} \quad \left. \vphantom{\frac{L^O(\text{therms}) \times 10^5(\text{Btu/therm})}{18000(\text{Btu/lb}) \times 8000(\text{lb/kgal})}} \right\} (7.12)$$

$$SO_2^O(\text{lb/hr}) = O(\text{kgal/hr}) \times 157.0 \times \%S^O.$$

Thus, the total  $SO_2$  emission is

$$SO_2 = SO_2^C + SO_2^O. \quad (7.13)$$

When the ambient temperature is such that a dual-fuel interruptible plant is probably receiving natural gas, the amount of  $SO_2$  produced is correspondingly reduced.

To facilitate data storage according to a uniform and consistent format, each plant is assumed to have four stacks. For plants having less than four stacks, zeros are filled in for nonexistent stacks. The following parameters are associated with each stack:

1.  $SO_2$  emission in pounds per hour
2. Heat emission in therms per hour.

These parameters are determined by weighting the total  $SO_2$  and heat emissions for the plant by the percentage emitted from each stack. The heat emission,  $H$ , is assumed to be 15% of the thermal input.

### Example

Consider the example of the Campbell Soup Company shown in Figs. 7.13 and 7.14, and assume that emission data are required for the following set of conditions:

1. January
2. Temperature,  $30^\circ\text{F}$
3. Weekday pattern
4. First shift.

Then,

$$L^S = \left[ 500 \frac{55 - 30}{65} \right] = 200 \text{ therms/hr,}$$

$$L^P = (0.70)(0.60)5000 = 2100 \text{ therms/hr,}$$

$$L = 2300 \text{ therms/hr,}$$

$$L^C = 2300 \text{ therms/hr,}$$

$$L^O = 0,$$

$$C = \frac{2300 \times 10^5}{12000 \times 2000} \approx \text{tons/hr,}$$

$$\text{SO}_2 = 10 \times 36.8 \times 2.8 = 1000 \text{ lb/hr,}$$

and

$$H = (0.15)2300 = 345 \text{ therms/hr.}$$

For Stack 1

$$\text{SO}_2^{(1)} = (0.25)1000 = 250 \text{ lb/hr,}$$

and

$$H^{(1)} = (0.25)345 = 85 \text{ therms/hr.}$$

For Stack 2

$$\text{SO}_2^{(2)} = (0.25)1000 = 250 \text{ lb/hr,}$$

and

$$H^{(2)} = (0.25)345 = 85 \text{ therms/hr.}$$

For Stack 3

$$\text{SO}_2^{(3)} = (0.50)1000 = 500 \text{ lb/hr.}$$

and

$$H^{(3)} = (0.50)345 = 170 \text{ therms/hr.}$$

For Stack 4

$$\text{SO}_2^{(4)} = 0$$

and

$$H^{(4)} = 0.$$

### 7.3 Residential Space-heating Sources

Residential space-heating sources account for approximately 15% of the annual total emissions for the city. The inventory of coal- and oil-fired residential space-heating sources was derived primarily from data supplied by the market research organization of the local natural-gas-supply utility. This information was in the form of a citywide, field sampling survey of

space-heating sources categorized by fuel use and by the number of dwelling units per building surveyed. For the emission inventory, the survey data was aggregated into two groups--moderate-sized residential structures of 19 dwelling units or less, and large apartment complexes of 20 or more dwelling units (see Fig. 7.2).

Since residential sources are generally too small and too numerous to treat individually, the two building size categories described above were treated as uniformly distributed square-mile area sources. The source density per square mile for each category was assigned on the basis of the natural-gas-utility market-research data.

The operating cycle of the moderate-sized heating plants was based on a 65°F degree-day proration of a seasonal average fuel consumption, modified by an empirical function\* which represents the daily cycle of automatic stoking during waking periods, followed by a hold-fire and cooldown during sleeping periods. This cycle was simulated by a "Janitor Function," which maintains heating sources on an automatic stoking cycle between

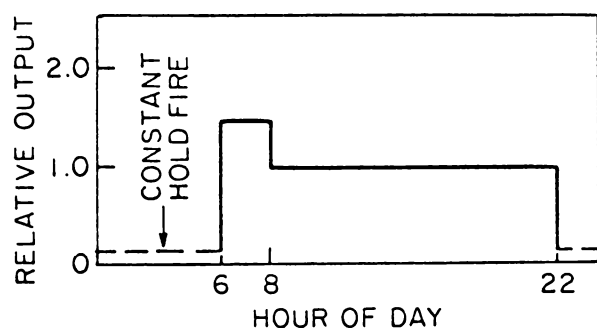


Fig. 7.15. Janitor Function for Low-rise Space Heaters

6 a.m. and 10 p.m. on days having a minimum night ambient temperature in excess of 5°F. For nights with a minimum temperature below 5°F, the automatic stoking period was assumed to begin at 3 a.m. The first heating hour of each day represents a building warmup period with approximately twice normal stoking requirements. In Fig. 7.15, this event is averaged over a 2-hr period to account for variability among buildings. This pattern was derived through an interview survey of building superintendents and heating-

plant operators. A hot-water-heating baseload equal to 20% of the annual fuel use was assumed for all residential buildings in this category. All moderate-sized residences were assigned a uniform physical stack height of 50 ft.

Large residential buildings were considered to operate on an automatic stoking cycle at all times. Fuel use and SO<sub>2</sub> emissions were based on a 65°F degree-day proration, and a hot-water-heating baseload equal to 20% of the annual fuel use was assumed. All buildings in this size category were assumed to have a 200-ft physical stack height.

#### 7.4 Commercial and Institutional Sources

Commercial and institutional sources account for about 8% of the total emissions in Chicago. Fuel use and SO<sub>2</sub> emission data for large

\*Croke et al., 1968b.

commercial and institutional sources such as office buildings and educational institutions were derived from a computer analysis of a comprehensive inventory developed in 1963 by the Chicago Department of Air Pollution Control (now the Chicago Department of Environmental Control), combined with the results of a field survey of major sources conducted in 1968 by Argonne National Laboratory and the Department of Air Pollution Control.

Virtually all sources in this category burn fuel primarily for space and hot-water heating and operate on an automatic stoking cycle. Emissions from these sources were therefore calculated in exactly the same way as for the large residential sources.


With a few notable exceptions, the commercial and institutional sources are too small and numerous to treat individually. They are therefore aggregated as area sources, uniformly distributed throughout each square mile, and, in the present study, combined with emissions from high-rise residential buildings (Fig. 7.2). The square-mile source density is based on the 1963 inventory.

#### 7.5 Additional Point Sources

Subsequent to the plant-by-plant survey of major point sources, it was realized that the 1963 Chicago DAPC inventory was deficient in certain source categories. Among these sources were:

1. All municipal fuel-burning sources, most notably Chicago public housing and pumping stations for water and sewage.
2. Institutional space-heating plants, such as universities.
3. Major industries which were either missed in or developed after the original survey.
4. Major emitters in surrounding counties, most notably large power plants 15-25 miles outside the city limits.

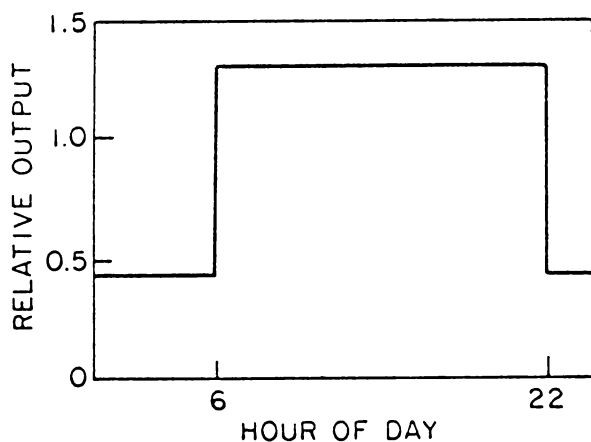
Although these additional point sources could have been added to PLANTSIM input (and, in retrospect, should have been), it was decided to treat them temporarily by storing annual emission information in subroutine ISPDV of the dispersion model (see Section 3.1) and prorating these by appropriate FORTRAN statements.

Twenty-seven additional point sources are described by DATA statements (see subroutine ISPDV listing in Appendix A) giving the following information: source coordinates (XPT, YPT, ZPT), number of stacks (NS), percent sulfur in fuel (SPCT), annual SO<sub>2</sub> emissions (QSO2, M-lb/yr), and a pattern identification. Data for these sources are listed in Table 7.4. The origin of the coordinate system (+X west, +Y south) is designated by the crossed arrows  in Figs. 7.1 and 7.2. Three source patterns are considered:

1. Uniform proration of annual output.
2. Twenty-four-hour degree-day response with 20% of annual fuel burn prorated uniformly for hot water.
3. A special diurnal pumping-station pattern (Fig. 7.16).

TABLE 7.4. Additional Point Sources in Chicago, 1966-1967

Source Name	XPT, mi	YPT, mi	ZPT, ft	NS	SPCT, %	QPTOT, 10 <sup>6</sup> lb/yr	NPAT
Central Park Pumping Station	9.8	0.8	242	1	2.2	2.34	3
Mayfair Pumping Station	11.0	-6.0	285	1	2.2	2.42	3
Roseland Pumping Station	5.5	12.0	265	1	2.2	2.10	3
Springfield Pumping Station	9.8	-2.0	240	1	2.2	2.02	3
Western Avenue Pumping Station	8.0	5.1	217	1	2.2	1.89	3
Union Station Powerhouse	5.6	0.3	110	0	3.4	8.00	2
Chicago & NW RR	10.3	-0.5	150	0	2.4	2.73	2
International Harvester	18.0	-2.0	150	1	2.2	4.12	1
Produce Terminal	6.0	4.5	150	0	2.9	4.26	2
Corn Products	15.1	7.0	150	1	2.7	31.90	1
Swift	6.7	4.5	150	1	3.2	4.59	1
Diamond Glue	7.2	2.8	150	1	3.2	1.88	1
Celotex	8.8	2.7	150	1	3.2	2.59	1
Municipal Heating Plant	8.8	2.8	150	1	2.7	2.38	2
Wyman Gordon	7.0	17.4	150	1	2.5	4.78	1
Reynolds	15.5	5.2	150	1	2.5	1.74	1
Standard Lime	16.2	5.9	150	1	2.5	4.78	1
Electromotive Division	16.7	6.0	150	1	2.5	4.32	1
Sears Roebuck	9.2	0.7	150	1	3.1	2.78	2
University of Illinois	6.0	0.3	150	1	3.2	3.53	2
Northwestern University	4.2	-0.8	150	1	2.7	2.06	2
Goldblatt Brothers	5.0	0.1	85	1	2.0	2.04	2
The University of Chicago	3.5	6.4	160	2	2.5	3.80	2
Merchandise Mart	5.4	-0.5	380	0	1.4	0.42	2
Will County Power Plant	29.2	16.0	450	4	3.2	397	1
Joliet Power Plant	30.4	24.8	500	8	3.5	560	1
Waukegan Power Plant	15.2	-35.2	400	4	2.9	232	1

Fig. 7.16  
Pumping-station Pattern

## 8. METEOROLOGICAL AND AIR QUALITY DATA

### 8.1 Chicago's TAM Network

In January 1966, the Chicago Department of Air Pollution Control began recording wind speed and direction and sulfur dioxide levels at eight telemetered air monitoring (TAM) stations (starred locations on the map, Fig. 7.1). These continuous measurements are integrated over 5-min periods; 15-min averages are then telemetered to the DAPC office, where they are recorded. Tape records of these 15-min observations have been edited and formed into hourly averages. Thus, although the accuracy of data from some of the aerovane sites is compromised by 15-30-ft masts and/or close proximity to taller buildings or smoke stacks, the procedure for developing hourly averages is excellent. This is in contrast to special airport data, where the aerovane sites are excellent, but only brief observations at the hour are recorded. Each TAM site is described in Section 9.

In the dispersion model, the wind speed and wind direction from the TAM aerovane nearest to the dose point are used to determine the trajectory of all puffs sensed at that point. The trajectory of a given puff is therefore defined by the sum of the hourly-average wind vectors at the reference aerovane during the lifetime of that puff. This temporary assumption will eventually be eliminated by using all eight stations to develop a wind field for the city. In contrast to single citywide values of wind speed and direction from the nearest airport, the data from a local aerovane are sensitive to special circulation patterns such as lake breezes.

### 8.2 Airport Data

Tapes containing standard weather hourly data from Midway Airport and Glenview Airport (15 miles north of Chicago) have been obtained from the National Weather Records Center.

### 8.3 Argonne Meteorological Data

The observing station at Argonne National Laboratory (25 miles southwest of Chicago) was specifically designed to measure those parameters controlling diffusion: atmospheric stability, wind speed and direction at five levels up to 150 ft, net and solar radiation, etc. Hourly averages are stored on magnetic tape. These are the only stability records available in the Chicago area. Unfortunately, the data are for a shallow layer and are taken in an open, grass-covered field. Studies are under way relating these data to the urban environment.

### 8.4 Upper-air Data

Radiosonde observations from the U.S. Weather Bureau RAWIN station at Peoria, Illinois (140 miles southwest of Chicago), and Green Bay, Wisconsin

(180 miles north of Chicago), have been obtained from the National Weather Records Center. These data have been extrapolated to estimate the height of the mixing layer in Chicago (see Section 8.6).

### 8.5 Atmospheric Stability

Turbulent diffusion of pollutant species is represented in the model by a Gaussian-puff kernel with dispersion coefficients  $\sigma_{x_i}(T)$ ,  $\sigma_{y_i}(T)$ , and  $\sigma_{z_i}(T)$ , where  $T$  is the travel time and  $i$  the atmospheric stability index. The choice of dispersion coefficient functions is discussed in Section 1.2.4.

### 8.6 Height of the Mixing Layer

The mixing layer defines a zone within which pollutants can be diluted. The height of this layer is one of the most critical parameters in determining ground-level  $\text{SO}_2$  concentrations resulting from emissions from tall stacks. With a high lid ( $>2000$  ft), plumes from power plants tend to travel far and disperse widely before touching ground. With a sharp temperature inversion beneath the physical stack height, plumes will travel in stable air which greatly inhibits vertical diffusion and therefore will touch ground far from the local urban area. High ground-level concentrations occur in the intermediate range of mixing-layer heights where the plumes are trapped beneath the lid and disperse rapidly to ground in unstable air. Figures 8.1 and 8.2 show vertical profiles of temperature and sulfur dioxide as measured by an instrumented helicopter at a point four miles downwind of a major industrial area in Chicago. The sharp inversion at 2300 ft (700 meters) has clearly defined a vertical mixing zone within which  $\text{SO}_2$  levels are nearly uniform.

Other than the low-level rural temperature profiles measured at Argonne, no vertical soundings are available for the Chicago area during the period from January 1966, when the TAM network became operational, to January 1969. This is the period during which meteorological air-quality and emission data have been accumulated at Argonne. It was therefore necessary to design a scheme for estimating the height of the mixing layer from historical weather data. [In July 1969, the Environmental Sciences Service Administration (ESSA) service bureau for the Chicago Air Quality Control Region began a program of daily balloon soundings at 0600 and 1200 from Midway Airport. These data will be available for future validation studies of the dispersion model and will also be used to validate the objective mixing-layer-height estimate described in this section.]

The computerized objective mixing-layer-height estimates are based on an interpolation scheme between two rawinsonde stations--Green Bay, Wisconsin, and Peoria, Illinois. The soundings are usually taken at 0600 and 1800 CST. The mandatory and significant levels for each station are

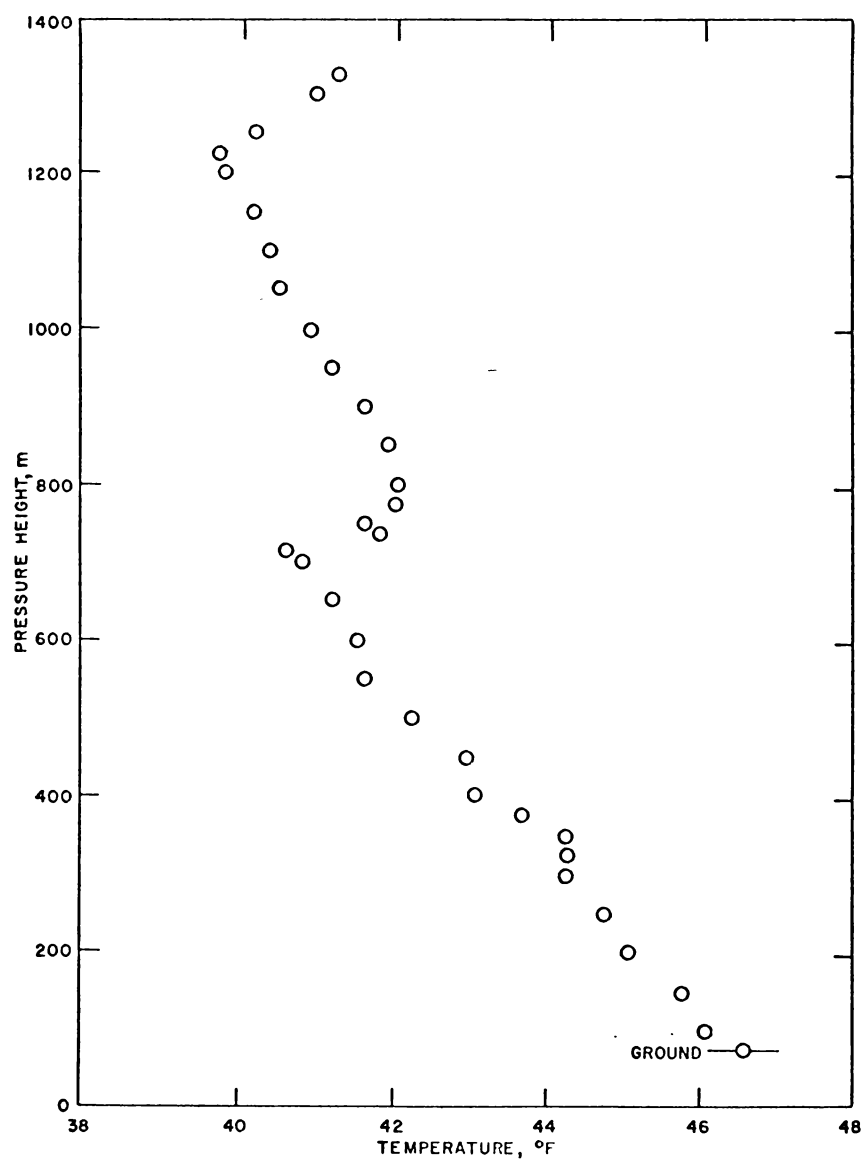


Fig. 8.1. Vertical Profile of Temperature, Hinsdale, Illinois, April 11, 1969, 10:20 a.m. (D. Nelson, Argonne National Laboratory)

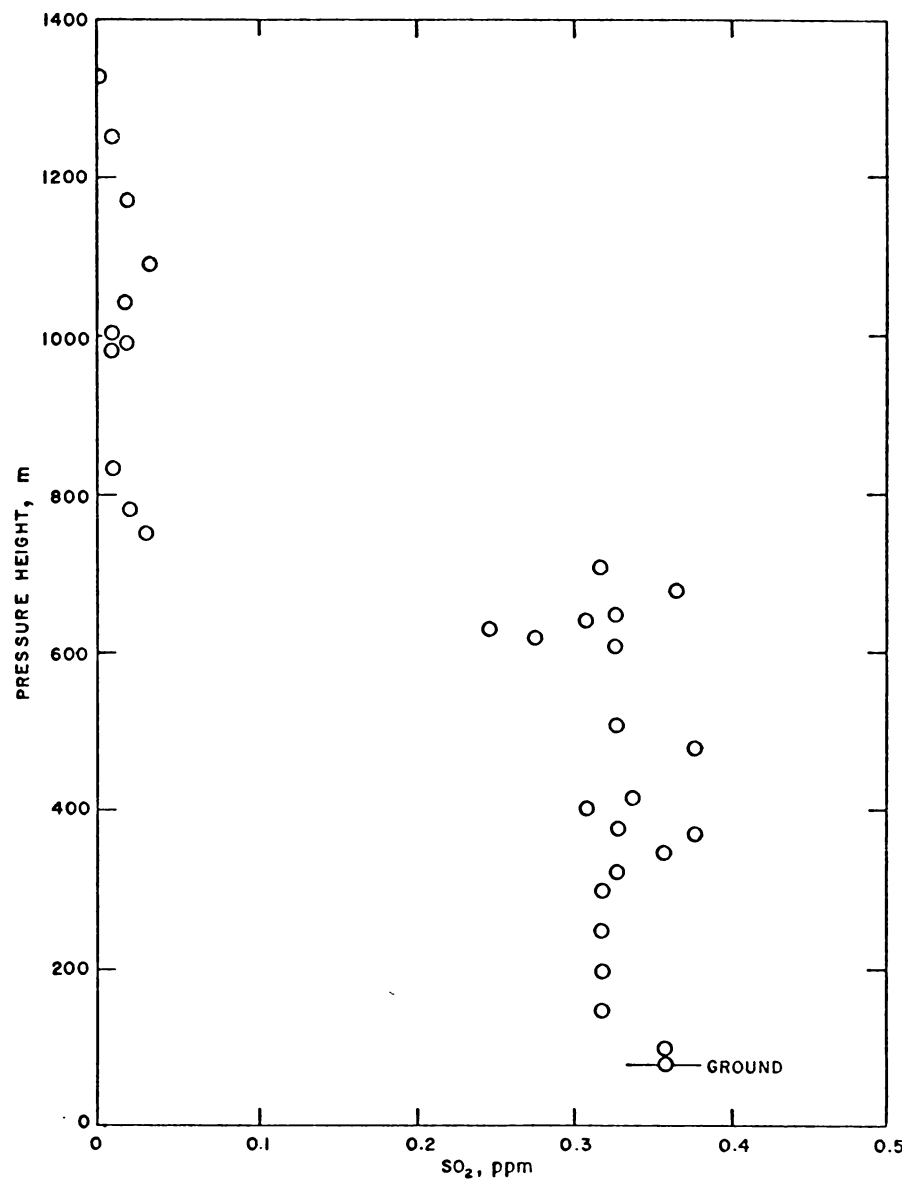


Fig. 8.2. Vertical Profile of SO<sub>2</sub>, Hinsdale, Illinois, April 11, 1969, 10:20 a.m. (D. Nelson, Argonne National Laboratory)



merged to form a single pressure-temperature array for each sounding. The Chicago rural (Argonne) temperature profile is formed either by "shifting" one of the two to the Argonne surface temperature or by interpolation between the Peoria and Green Bay soundings. If only one station is in the same air mass as Chicago, the sounding from that station is transposed, without changing its shape, to the Argonne surface temperature at sounding time. If both Peoria and Green Bay are in the same air mass as Chicago (as determined by inspection of the daily weather map), then a linear interpolation is performed. This procedure forms a pressure-temperature array for the 0600 and 1800 rural profiles.

The next step is to compute the hourly rural profiles using temporal weighting. The profile for any hour is linear interpolation in time between the bracketing 0600 and 1800 rural soundings.

The hourly urban mixing depth and mixing-depth indices are now computed. The height of the mixing layer is defined by the intersection of a dry adiabat from the urban surface temperature measured at Midway Airport with the constructed Argonne rural temperature profile. Mixing-layer heights calculated by this objective procedure were compared with more subjective estimates provided by a local meteorological consulting firm. Although actual magnitudes differed, diurnal trends were in good agreement. Calculated values agreed very closely with data from two helicopter soundings, but, in both cases, the inversions were above 2000 ft and therefore not in the critical range where plume trapping can occur.

## 9. THE CHICAGO AIR QUALITY MONITORING SYSTEM

Chicago operates a network of eight telemetered air monitoring (TAM) stations, which continuously and automatically record 5-min average SO<sub>2</sub> concentrations at 15-min intervals throughout the day. The data recorded by these stations during 1966 and 1967 are typical of a city characterized by a highly unhomogeneous SO<sub>2</sub> source distribution and density. Table 9.1 summarizes the air-quality situation of Chicago as recorded by the network of TAM stations.

TABLE 9.1. Total Number of Recorded  
1-hr SO<sub>2</sub> Dosages (1966-1967)

TAM Station	≥0.2 ppm	≥0.3 ppm	≥0.4 ppm	≥0.5 ppm
1	182	59	18	5
2	618	203	70	30
3	3210	1838	975	483
4	1990	966	491	268
5	525	207	84	45
6	364	169	94	65
7	934	332	122	35
8	206	51	15	6

Under certain meteorological conditions, the source density, type, and distribution in the immediate vicinity of a receptor may dominate the ambient air quality recorded. It is therefore of value to examine the record of the eight TAM stations from the standpoint of their proximity to Chicago's SO<sub>2</sub> sources. This exercise is particularly useful, since it indicates the types of sources likely to have the predominant effect on the recorded air quality, and therefore indicates the level of effort that should be expended to develop a detailed emission inventory. Moreover, an understanding of the distribution of sources relative to each monitoring station providing the data required to validate the Chicago atmospheric-diffusion model illuminates and explains certain of the results predicted by the model. Table 9.1 shows the distribution of 1-hr SO<sub>2</sub> dosages recorded at the eight TAM stations.

### 9.1 TAM Station 1

TAM station 1 is near the northwestern limits of Chicago in an area characterized by residential neighborhoods of relatively recent construction and a limited amount of light industrial development. Heating plants in this sector of the city are predominantly natural gas fired, and relatively little coal or oil is consumed by industrial or commercial sources. TAM 1 is thus sited in a relatively clean section of the city, insofar as sulfur oxide emissions are concerned. This conclusion is borne out by the fact that

TAM 1 has recorded high ambient SO<sub>2</sub> concentrations at least one order of magnitude less frequently than do monitoring stations located nearer to the urban core area. (See Table 9.1.)

## 9.2 TAM Station 2

TAM station 2, in the northeast sector of the city approximately 1.5 miles from the lakeshore, is in a mixed industrial-residential area containing a large concentration of high-rise gas-fired residential structures. The prevailing southwesterly flow tends to transport SO<sub>2</sub> from the central utility-industrial cluster into this area, but average dosages tend to be relatively low because of the comparatively large transport distances involved. This is evidenced by the relatively high ratio of low to high concentrations recorded at TAM 2 (Table 9.1) compared to the record for TAM 3 or TAM 4 where localized coal and oil burning sources are more significant. The nearest major SO<sub>2</sub> source to TAM 2 is a moderate-sized coal-fired power plant approximately 1.5 miles to the southwest.

## 9.3 TAM Station 3

TAM station 3 is centrally located atop a large office building in the Chicago loop business district. As such, it is not only surrounded by a cluster of large commercial and institutional space-heating sources, but is situated directly northeast of a major concentration of industrial plants and a line formed by the three largest power plants within the city limits. Since the prevailing flow is southwesterly, a high incident frequency due to this industrial-utility concentration and to local space-heating effects is to be expected at TAM 3. As indicated in Table 9.1, this station is, in fact, located in the most polluted sector of the city.

## 9.4 TAM Station 4

TAM station 4 is in the south-central Hyde Park area of Chicago within 1 mile of Lake Michigan. The immediate area is characterized by a row of high-rise apartments sited along the lakefront, a large concentration of old coal- or oil-fired, low-rise, six-flat apartment buildings and a single major source--The University of Chicago steam plant. TAM 4 is approximately 5 miles southeast of Chicago's central industrial-utility complex. As indicated in Table 9.1, the frequency of high, recorded SO<sub>2</sub> concentrations at TAM 4 is second only to that of TAM 3. Statistical analysis of TAM 4 air-quality data has indicated that the air quality in this area is strongly correlated with ambient temperature--a finding consistent with the likelihood that the Hyde Park area is largely self-polluted by local, residential space-heating sources.

### 9.5 TAM Station 5

TAM station 5 is approximately 6 miles inland in the south-central sector of the city. It is approximately 3 miles south of the central-industrial-utility complex, and is located atop a school building in a neighborhood of low-rise apartments and single-family dwellings. Residential buildings in the TAM 5 area are somewhat newer than for TAM 4, and gas tends to predominate over coal and oil for space-heating purposes. TAM 5 is nearer to the central industrial-utility cluster than any of the other monitoring stations; however, only a few large sources are located southwest of the site. This fact, combined with the relatively low residential emissions characteristic of its immediate vicinity, results in a comparatively modest number of high SO<sub>2</sub> concentrations recorded at this receptor (listed in Table 9.1).

### 9.6 TAM Station 6

TAM station 6, in the extreme southeast of the city, is in a residential area approximately 5 miles west of a second large concentration of Chicago industrial and power plants. Immediately adjacent to this Chicago source-cluster is the Gary-Hammond industrial complex. Since the receptor is also located within 1 mile of the southwest city limits of Chicago, it is exposed to emissions from two areas for which an emission inventory is not, at present, available. According to the data in Table 9.1, TAM 6 is located in one of the less frequently polluted areas of the city. This conclusion is consistent with the fact that the metropolitan region southwest of the city is relatively free of large SO<sub>2</sub> sources, and that east winds, which would bring in SO<sub>2</sub> from the south Chicago-Gary-Hammond area, are comparatively infrequent in the midwest Great Lakes region.

### 9.7 TAM Station 7

TAM station 7 is atop a school building within 0.5 mile of the western city limits and almost 7 miles directly west of the central business district. The immediate neighborhood is predominantly residential, although a few large industrial plants are located within 2 miles of the receptor in the north-east and southwest directions. The station is approximately 6 miles northwest of the central industrial-utility cluster.

A detailed emission inventory for the regions immediately west and south of this receptor is not now available, since these areas lie outside the Chicago city limits. It is, however, known that the area west of TAM 7 is a mixed residential, light-industrial sector in which gas heating predominates, while the highly industrialized city of Cicero, Illinois, lies immediately south of TAM 7, within 2 miles of the receptor.

Although the relative scarcity of southeasterly winds minimizes the influence of the central Chicago source cluster on TAM 7, the area experiences significant SO<sub>2</sub> concentrations with moderately high frequency, making it the third or fourth most frequently polluted site.

### 9.8 TAM Station 8

Like the TAM 6 receptor, TAM station 8 is in a residential neighborhood near one of the southwestern extremities of Chicago's irregular western border. Two relatively large industrial plants lie within 1 mile to the northeast of the site; however, the area is relatively free of significant SO<sub>2</sub> sources. Since the western city limits are within 0.5 mile and the southern city limits are within 1 mile, emission data for virtually the entire southwestern quadrant, relative to TAM 8, are not available.

As indicated in Table 9.1, the TAM 8 receptor is sited in one of the least polluted areas of the city.

## 10. STATISTICAL RESULTS

Over 2000 hourly averages of SO<sub>2</sub> levels at each of five monitoring stations (TAM's 1-5) were estimated for the periods December 1966-February 1967 and August 1967-September 1967. The five receptor locations represent a wide range of geographical and emission features, and all are far enough from the city limits so that the sources within the inventory dominate the measured pollutant concentrations. (See Section 9.) The 1967 season was chosen since it is closest to the 1968 residential and updated industrial inventories.

There are numerous statistical tests and formats for comparison of observed and estimated pollutant concentrations. The importance attached to any test depends upon the magnitude and range of the variables and, above all, upon the use to which the model is to be put (Moses, 1969). Seven criteria or display methods are used to compare observed and computed SO<sub>2</sub> data:

1. Mean values (monthly and seasonal):  $\mu_{\text{obs}}$  versus  $\mu_{\text{est}}$ .

$$2. \frac{\text{Standard deviation}}{\text{Mean}} \equiv \left[ \frac{1}{N_{\text{obs}} - 1} \sum_{i=1}^{N_{\text{obs}}} (X_{\text{obs}_i} - X_{\text{est}_i})^2 \right]^{1/2} / \mu_{\text{obs}}$$

$$= \sigma_{\text{oe}} / \mu_{\text{obs}}.$$

3. Percent of estimates within  $\pm 0.05$  ppm of corresponding observations (PCT05).
4. Percent of estimates within a factor of 2 of corresponding observations (PCTF2).
5. Contingency tables for 6-hr averages.
6. Percent reduction in variance ( $R^2 \times 100$ ).
7. Episode estimation: 2 x 2 contingency tables for prediction of levels above and below threshold.

Table 10.1 presents the data according to the first four criteria listed above. A glance down the columns of means ( $\mu_{\text{obs}}$  and  $\mu_{\text{est}}$ ) or at Fig. 10.1 indicates that, with the exception of TAM 4, February 1967, monthly and seasonal means for all and for individual TAM stations are accurately estimated over a wide range of values.

TABLE 10.1. Compilation of Validation Statistics

TAM's	Average Period	Data Period	N <sub>obs</sub>	$\mu_{obs}$ , ppm	$\mu_{est}$ , ppm	$\sigma_{oe}/\mu_{obs}$	PCT05	PCTF2
1-5	1	Winter-Summer 1967	10,800	0.11	0.11	1.1	62	47
	1s <sup>a</sup>		10,800			1.0	63	51
	6		1,800			0.9	65	55
	24		450			0.6	74	66
1-5	1	Winter 1967	8,300	0.14	0.13	1.0	56	52
	1s		8,300			0.9	58	56
	6		1,383			0.8	60	61
	24		345			0.5	69	75
1-5	1	Summer 1967	2,496	0.03	0.03	1.8	83	31
	1s		2,496			1.6	83	31
	6		416			1.4	83	33
	24		104			1.1	89	41
1-5	1	Dec 1966	2,876	0.13	0.15	1.2	60	52
	1s		2,876			1.1	61	57
	6		479			1.0	62	62
	24		119			0.6	71	77
1-5	1	Jan 1967	2,784	0.12	0.11	0.8	62	56
	1s		2,784			0.7	63	61
	6		464			0.6	66	67
	24		116			0.4	77	76
1-5	1	Feb 1967	2,712	0.16	0.12	0.9	48	49
	1s		2,712			0.8	49	51
	6		452			0.7	51	56
	24		113			0.5	58	68
1	1	Winter-Summer 1967	2,232	0.03	0.03	1.7	84	25
	1s		2,232			1.5	85	28
	6		372			1.3	86	32
	24		93			0.9	92	34
2	1		2,112	0.10	0.09	0.9	66	55
	1s		2,112			0.8	68	59
	6		352			0.7	71	62
	24		88			0.5	77	71
3	1		2,040	0.24	0.24	0.9	34	53
	1s		2,040			0.8	34	56
	6		340			0.7	35	62
	24		85			0.4	48	74
4	1		2,136	0.14	0.12	0.9	55	54
	1s		2,136			0.8	55	58
	6		356			0.7	57	62
	24		89			0.6	64	74
5	1		2,280	0.07	0.07	1.1	70	50
	1s		2,280			1.0	72	53
	6		380			0.8	75	58
	24		95			0.5	85	80

<sup>a</sup>Smoothed 1-hr averages ( $X_{1s}$ ):  $X_{1s}(N) = \frac{X_1(N-1) + 2X_1(N) + X_1(N+1)}{4}$ .

TABLE 10.1 (Contd.)

TAM's	Average Period	Data Period	N <sub>obs</sub>	$\mu_{obs}$ , ppm	$\mu_{est}$ , ppm	$\sigma_{oe}/\mu_{obs}$	PCT05	PCTF2
1	1	Winter 1967	1,776	0.03	0.03	1.7	81	23
	1s		1,776			1.5	83	27
	6		296			1.3	83	32
	24		74			0.9	91	37
2	1		1,656	0.12	0.10	0.8	62	63
	1s		1,656			0.7	64	68
	6		276			0.6	68	71
	24		69			0.4	74	80
3	1		1,392	0.34	0.31	0.8	18	62
	1s		1,392			0.7	19	68
	6		232			0.6	19	75
	24		58			0.4	33	90
4	1		1,584	0.17	0.16	0.8	45	64
	1s		1,584			0.7	45	68
	6		264			0.7	47	71
	24		66			0.5	55	85
5	1		1,896	0.07	0.07	1.1	66	52
	1s		1,896			0.9	68	56
	6		316			0.8	70	63
	24		79			0.5	82	84
1	1	Dec 1966	576	0.02	0.02	2.1	90	19
	1s		576			2.0	91	26
	6		96			1.8	92	33
	24		24			1.4	92	38
	1	Jan 1967	648	0.03	0.05	2.0	77	25
	1s		648			1.7	79	31
	6		108			1.4	79	37
	24		27			1.1	85	33
	1	Feb 1967	552	0.04	0.03	1.3	77	24
	1s		552			1.2	78	22
	6		92			1.0	79	24
	24		23			0.6	96	39
1	Summer 1967	456	0.03	0.02	1.5	95	35	
1s		456			1.3	94	33	
6		76			1.2	95	30	
24		19			0.9	100	26	
2	1	Dec 1966	432	0.08	0.10	1.2	63	53
	1s		432			1.1	65	57
	6		72			0.9	72	61
	24		18			0.8	72	72
	1	Jan 1967	576	0.12	0.10	0.7	64	64
	1s		576			0.6	67	69
	6		96			0.6	71	71
	24		24			0.4	75	83
	1	Feb 1967	648	0.15	0.11	0.6	58	70
	1s		648			0.6	60	74
	6		108			0.5	62	77
	24		27			0.4	74	82



TABLE 10.1 (Contd.)

TAM's	Average Period	Data Period	N <sub>Obs</sub>	$\mu_{\text{Obs}}$ , ppm	$\mu_{\text{est}}$ , ppm	$\sigma_{\text{oe}}/\mu_{\text{Obs}}$	PCT05	PCTF2
2 (Contd.)	1	Summer 1967	456	0.04	0.02	1.9	81	29
	1s		456			1.9	81	26
	6		76			1.7	80	32
	24		19			1.3	79	37
3	1	Dec 1966	600	0.34	0.36	0.8	17	62
	1s		600			0.7	19	68
	6		100			0.7	17	73
	24		25			0.5	32	96
	1	Jan 1967	432	0.33	0.25	0.6	23	68
	1s		432			0.5	26	73
	6		72			0.4	26	83
	24		18			0.3	50	83
	1	Feb 1967	360	0.35	0.30	0.6	15	56
	1s		360			0.6	13	62
	6		60			0.5	13	68
	24		15			0.3	13	87
	1	Summer 1967	648	0.03	0.06	2.1	67	32
	1s		648			1.8	67	31
	6		108			1.6	69	32
	24		27			1.3	82	41
4	1	Dec 1966	648	0.13	0.17	1.2	55	65
	1s		648			1.1	55	69
	6		108			1.0	55	69
	24		27			0.7	70	85
	1	Jan 1967	432	0.15	0.14	0.5	59	81
	1s		432			0.5	60	85
	6		72			0.4	65	90
	24		18			0.3	78	100
	1	Feb 1967	504	0.25	0.15	0.6	19	49
	1s		504			0.5	18	51
	6		84			0.5	23	57
	24		21			0.5	14	71
	1	Summer 1967	552	0.03	0.01	1.3	86	23
	1s		552			1.2	86	29
	6		92			1.1	84	35
	24		23			0.9	91	44
5	1	Dec 1966	552	0.06	0.06	1.1	74	56
	1s		552			0.9	77	62
	6		92			0.7	79	69
	24		23			0.4	96	96
	1	Jan 1967	696	0.06	0.07	1.1	71	55
	1s		696			1.0	71	60
	6		116			0.8	74	66
	24		29			0.6	86	90
	1	Feb 1967	648	0.09	0.09	1.0	52	44
	1s		648			0.9	55	47
	6		108			0.8	58	54
	24		27			0.6	67	67

TABLE 10.1 (Contd.)

TAM's	Average Period	Data Period	N <sub>obs</sub>	μ <sub>obs</sub> , ppm	μ <sub>est</sub> , ppm	σ <sub>oe</sub> /μ <sub>obs</sub>	PCT05	PCTF2
(Contd.)	1	Summer 1967	384	0.03	0.02	1.2	92	40
	1s		384			1.1	93	39
	6		64			0.8	95	38
	24		16			0.6	100	63

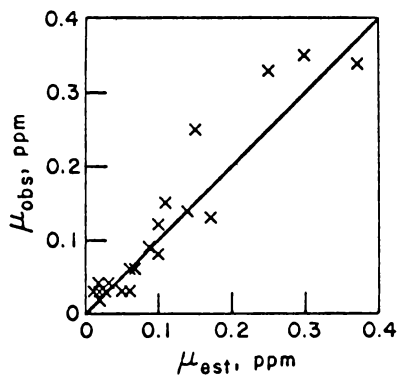


Fig. 10.1. Individual TAM Stations Monthly Means, Winter 1967

Although the ratio of the standard deviation (observed-estimated) to the observed mean ( $\sigma_{oe}/\mu_{obs}$  in Table 10.1) is not a true statistic, in that it cannot be related by, for example, a confidence level to a random distribution of uncorrelated pairs of values, it is a ratio commonly used to evaluate the success of models. Marsh and Withers (1969) indicate that, for their Reading, England, model as well as for others in the literature, the ratios  $\sigma_{oe}/\mu_{obs}$  are all higher than 1.1 for 6- and 24-hr averages during the heating season. From Table 10.1, the corresponding values are 0.5 for 24-hr averages and 0.8 for 6-hr averages. For low SO<sub>2</sub> values (<0.05 ppm) such as those at TAM 1 in winter and all TAM's in summer, the accuracy of the instrumentation ( $\pm 0.01$  ppm under laboratory conditions) and the heterogeneity of local sources lead to short-term errors and thus larger values of  $\sigma_{oe}/\mu_{obs}$ .

Figures 10.2-10.9 show contingency tables for 6- and 24-hr averages. The 6-hr time period was chosen since it is the minimum practical time step for implementation of episodal control strategies (Croke and Booras, 1969). The heavy "staircase" lines bracket a zone of successful estimations defined in terms of the accuracy required of a model used for planning episodal control strategies as well as for evaluating regional air-quality statistics. On a citywide basis, the 6-hr averages are estimated with a skill score\* (based on chance) of 0.55. Also listed are the R<sup>2</sup> values for the original data set. This statistic, defined by  $(\sigma_{obs}^2 - \sigma_{oe}^2)/\sigma_{obs}^2$ , is the fractional reduction in the variance of the original observed data set about the observed mean ( $\sigma_{obs}^2$ ) when the model is employed. This figure is 0.43 for 6-hr averages and 0.71 for 24-hr averages when all TAM stations are considered in the same data set. Results (6-hr values) for individual TAM stations vary widely from R<sup>2</sup> = 0.53 at TAM 2 to R<sup>2</sup> ≈ 0 at TAM 5. The significant discrepancy between the skill score (0.35) and R<sup>2</sup> (~0) values for TAM 5 occurs

\*Skill scores are defined by the ratio  $(V - V^1)/(T - V^1)$  where V is the number of correct estimates (within the heavy lines), T the total number of cases, and V<sup>1</sup> the value of V expected by some means other than the model under evaluation. For example, instead of chance, a simpler plume model might be used.

because the former considers a band of acceptable error, whereas the latter is based on actual calculated and observed values (e.g., if  $X_{\text{Obs}} = 0.03$  ppm and  $X_{\text{Est}} = 0.01$  ppm, the skill score considers this pair a "success," whereas, for the purposes of calculating  $R^2$ , this pair represents an error of 0.02 ppm).

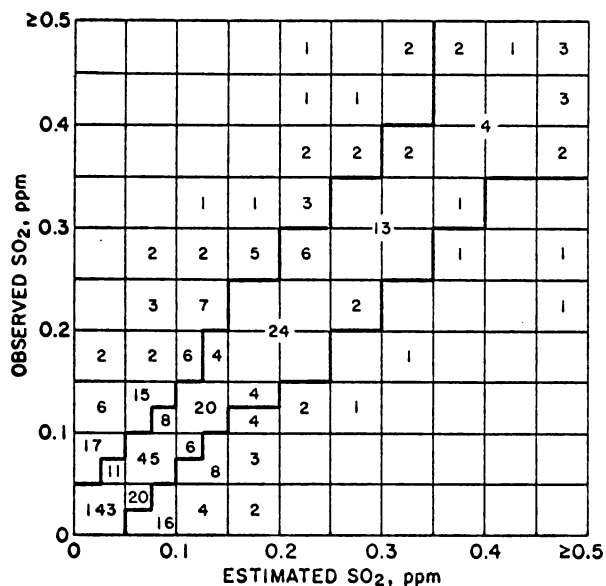


Fig. 10.2. Twenty-four-hour Averages for TAM's 1-5, All Seasons.  $R_{24\text{-hr}}^2 = 0.71$ .

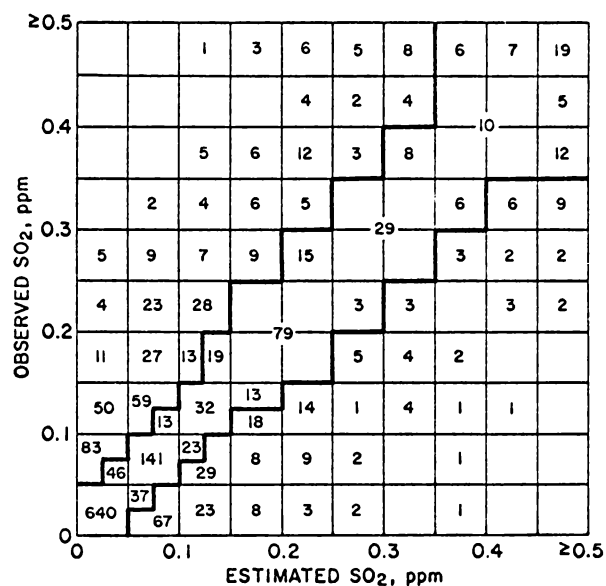


Fig. 10.3. Six-hour Averages for TAM's 1-5, All Seasons.  $R_{6\text{-hr}}^2 = 0.48$ . Skill score<sub>6-hr</sub> = 0.55.

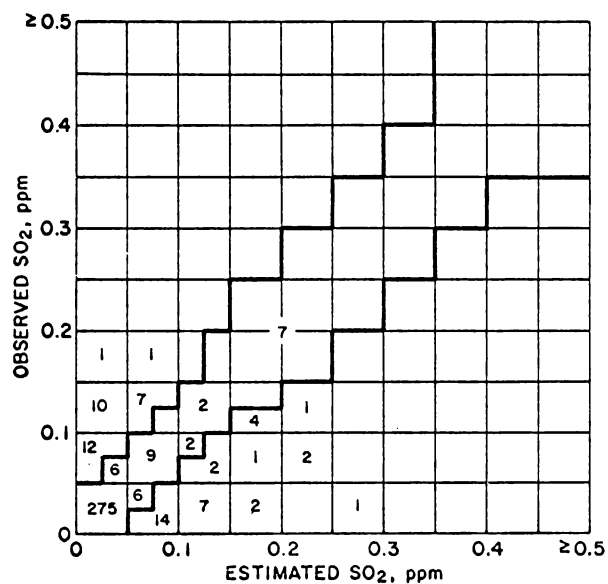


Fig. 10.4. Six-hour Averages for TAM 1, All Seasons.  $R_{6\text{-hr}}^2 = 0.19$ .  $R_{24\text{-hr}}^2 = 0.28$ .

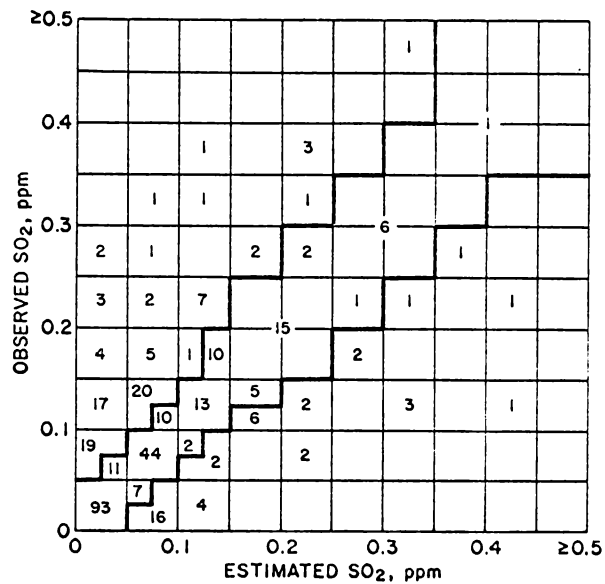


Fig. 10.5. Six-hour Averages for TAM 2, All Seasons.  $R_{6\text{-hr}}^2 = 0.46$ .  $R_{24\text{-hr}}^2 = 0.53$ .



3. If the observed average is greater than the threshold less a tolerance, then an incident is said to have occurred.

4. If the observed average is less than the threshold plus a slight tolerance, then an incident is said not to have occurred.

TABLE 10.2. Stations 1-5: 6-hr Incidents--Winter 1967

Symbol	Threshold, ppm	Tolerance, ppm	Skill Score (based on chance)
x	0.2	0.05	0.81
y	0.3	0.05	0.77

O c c u r	Yes	x 56	x 247
		y 42	y 109
	No	x 1052	x 29
		y 1222	y 21
		No	Yes

Predict

TABLE 10.3. Stations 1-5: 24-hr Incidents--Winter 1967

Symbol	Threshold, ppm	Tolerance, ppm	Skill Score (based on chance)
x	0.2	0.025	0.84
y	0.3	0.025	0.77

O c c u r	Yes	x 13	x 58
		y 11	y 30
	No	x 271	x 4
		y 301	y 4
		No	Yes

Predict

When compared to chance, the model is significant at better than 99.9% confidence level and the skill scores for this air-pollution war game range from 0.77 to 0.84. In terms of incident-control policies, taking serious actions such as temporarily curtailing industrial production is costly. Air-pollution cost-benefit studies at Argonne show that as much as \$10 million per day can be involved in lost wages and production for a city such as Chicago. Thus, in practice, the tolerance used above would be enlarged sufficiently to ensure that the model scores significantly better than shown in Tables 10.2 and 10.3.

## APPENDIX A

FORTTRAN Listings for Integrated-puff Dispersion Model  
(Excluding PL1 links to APICS system)

ISPDVAV

```

SUBROUTINE ISPDVAV(EMIS,HEFF)
C
C11111
  COMMON/KTRCUE/KTRG
  DIMENSION KTRM(8)      , JSSAVE(12)
  COMMON/MXC/MX
  DIMENSION A(12,8),B(12,8),C(12,8),WABAR(12,8)
  REAL*4 EMIS(12,4,1),HEFF(12,4,1)
  DIMENSION WD(8),WS(8)
  REAL*4 XS(1),YS(1),ZS(4,1),QSC2(1),QHEAT(1),
1 SQ2VAL(1),WCA(1),WSA(1),PERCENT(4,1)  ,SOBS(1)
C
  COMMON/TIME/ MMAX,NMAX,M,N
  COMMON/KERNEL/X,Y,Z,U(24),V(24),W(24),JS(24),HMIX(24),WSBAR(24),WL
  COMMON/RISE/ZSS
  COMMON/PLUT/I
  COMMON/XTRAN/KSTAB
  COMMON/SUEDO/TX,TY,TZ,DX,CY,CZ
  COMMON/HALF/THALF
  DIMENSION TEM(12)
  DIMENSION KSTAF(6,100)
  DIMENSION TXX(6,6),TZZ(6,6,3),DXX(6,6),CYY(6,6),
2  EMIT(6,3,1000)
  DIMENSION PP(7),LSAVE(24),VSAVE(24)
  DIMENSION NDW(12,4,100)
  DIMENSION WSSAVE(24)
  DATA PP/.2,.2,.2,.3,.4,.5,.5/
  DATA KPS/1/
  DATA NCLID/1/
C
  DIMENSION NTMP(4,8),NHRP(4),MPU(4),PREC(4,8)      , OBSC(4,8)
  DATA NCOUNT/1/
  DIMENSIONXPT(30),YPT(30),ZPT(30),CPTGT(30),
XQPHR(12,30),HEFPT(12,30),NPAT(30),NS(30),HKEE(12),
XEKEE(12),SPCT(30)
  DATA NPTS/27/
  DATA XPT/9.8,11.0,5.5,9.8,8.0,5.6,10.3,18.,6.0,15.1,6.7,7.2,8.8,
X8.8,7.0,15.5,16.2,16.7,9.2,6.0,4.2,5.0,3.5,5.4,15.2,29.2,30.4/
  DATA YPT/0.8,-6.0,12.0,-2.0,5.1,0.3,-0.5,-2.0,4.5,7.0,4.5,2.8,2.7
X,2.8,17.4,5.2,5.9,6.0,0.7,0.3,-0.8,0.1,6.4,-0.5,-35.2,16.0,24.8/
  DATA ZPT/242.,285.,265.,240.,217.,110.,150.,150.,150.,150.,150.,
X150.,150.,150.,150.,150.,150.,150.,150.,150.,85.,160.,380.,
1400.,450.,500./
  DATA NS/1,1,1,1,0,0,1,0,1,1,1,1,1,1,1,1,1,1,1,2,0,4,4,8/
  DATA SPCT/2.2,2.2,2.2,2.2,2.2,3.4,2.4,2.2,2.9,2.7,3.2,3.2,3.2,
X2.7,2.5,2.5,2.5,2.5,3.1,3.2,2.7,2.0,2.5,1.4,2.9,3.2,3.5/
C
  CPTGT UNITS ARE M LBS.SC2/YR.
  DATA CPTOT/2.34,2.42,2.10,2.02,1.89,8.00,2.73,4.12,4.26,31.89,4.59
X,1.88,2.59,2.38,4.78,1.74,4.78,4.32,2.78,3.53,2.06,2.04,3.80,.42,
X232.,357.,560./
C
  ADDITIONAL POINT SOURCES INCLUDE:

```

ISPDAY (Contd.)

```

C      PUMPING STATIONS(CENTRAL PK.,MAYFAIR,ROSELAND,SPRINGFIELD,WESTERN AVE.),
C      UNICN STATION POWER PLANT,CHICAGO-NORTHWESTERN RR,INTERNATIONAL HARVESTER,
C      PRODUCE TERMINAL,CCRN PRODUCTS,SWIFT,DIAMOND GLUE,CELCTEX,MUN.HEATING PL.,
C      WYMAN GORDON,REYNOLDS, STANDARD LIME,ELECTROMOTIVE DIV.,SEARS ROEBUCK,
C      UNIV.OF ILL.,NC.WESTERN UNIV.,GOLDBLATT BROS.,UNIV.OF CHICAGO,
C      MERCHANDISE MART.,POWER PLANTS(WAUKEGAN,WILL COUNTY,JOILET).
C      DATA NPAT/3,3,3,3,3,2,2,1,2,1,1,1,1,2,1,1,1,1,2,2,2,2,2,2,1,1,1/
C      EACH ADDITIONAL POINT SOURCE IS IDENTIFIED BY A
C      PATTERN OF EMISSION. 1=UNIFORM, 2=TEMP DEPENDENT, 3=PUMPING STA.
C      DIMENSION IIND(100)
C      EACH ADDITIONAL POINT SOURCE MUST BE
C      IDENTIFIED BY A CLASSIFICATION NUMBER.
C      1=UTILITY, 2=INDUSTRY, 3=RES/COML.
C      DATA IIND/2,2,2,2,2,3,3,2,3,2,2,2,2,3,2,2,2,2,3,3,3,3,3,3,1,1,1/
C      DIMENSION NOSTK(50)
C      DATA NCSTMX/9/
C      DATA NCSTK/25,28,30,31,40,41,43,45,50/

C      DATA NPPP/C/, NPRINT/1/
C      RESULTS FOR GRID PRINTED EVERY NPRINT HOURS.
C      CCMPCN/AREAS/QTOT(3,1004),HAVG(3),DGRID,XSCRIG,YSORIG,
2  NSXMAX,NSYMAX,EMAX(5,3)
C      CCMPCN/QHWWW/PCTH,DDAVG
C      CCMPCN/NUMEPT/NPCH,NIND
C      CCMPCN /SO2DAT/RECDAT(4,500)
C      CCMPCN/RGR/XRGRID,YRORIG,NWEST,NSTH,CRGRID,ZREC
C      CCMPCN/MINC/EMINPT
C      CCMPCN/ASGRID/NSGRID,XSGRID(100),YSGRID(100)
C      DIMENSIONCCUP(100,3,6)
C      DIMENSION VQ(6,3)
C      CCMPCN/METREF/ZWS
C      ZWS IS HEIGHT(FT)OF AERCVANE

C
C      DATA VALOP,NRTAM/1.,43/
C      IF VALOP.GT.0 THEN SC2VAL=RECDAT(4,NRTAM) IS RETURNED TO
C      APCDATA FOR EVENTUAL PRINTOUT ALONGSIDE SO2 DATA FROM
C      TAM STATION SPECIFIED AS OUTSTATION ON INPUT CARDS
C      DATA FNCHOP/C/
C      IF FNCHOP.GT.0, SO2VAL AND SCBS ARE PUNCHED ON CARDS FOR
C      USE WITH STATISTICS CODES.
C      INITIALIZATION OF STORAGE IN TRAN.
C      CALL ITRAN(EMIS,FEFF)
C      MMAX=0
C      NMAX=6
C      NMAX MUST BE .LE.6 HOURS
C      CALL ACAT2
C      ACAT2 READS IN RECEPTOR AND AREA SOURCE DATA.
C      NTEST=0
C      NTEST=1
C      IF(NTEST.GT.0 )
1  PRINT 401,QTOT(1,50),QTOT(3,300),HAVG(2),DGRID,XSCRIG,
2  YSCRIG,NSXMAX,NSYMAX,EMAX(2,2)
401 FORMAT(10X,6E10.2,2I10,E10.2)
C      IF(NTEST.GT.0 )
1  PRINT 402,XSGRID(20),YSGRID(20),ZWS
402 FORMAT(10X,3E10.2 //)
C      LLL=1
C      RETURN

```



ISPDAY (Contd.)

```

C      CODE COORDINATES, PLUS FOR X LEFT AND Y DOWN
      ENTRY      PUFF(NR,TEMP,WSA,WDA,STAB,HLID,NSRC,XS,YS,ZS,
      1 PERCENT,QSO2,QHEAT,
      2 SO2VAL,MM,KTAM,SCBS)
C22222
C      SCBS IS THE ACTUAL OBSERVED SO2. USED HERE ONLY IN PUNCHED
C      OUTPUT FOR STATISTICAL COMPARISON WITH CALCULATED VALUES
      KTRC=C
C      UNITS ARE F,CEG,MFH,,FT,,MI,MI,FT,FRACTION,LB/HR,TH/HR,,MI,MI,FT,,
C*****
C      ONLY ONE AERGVANE READING IS USED PER PROBLEM.
C      THIS IS SPECIFIED BY RECEPTOR CARD IN DATA DECK.
C$$$$$
C      ZERC THE EMIT ARRAY
      CC 2 L=1,6
      DC 2 I=1,3
      DC 2 K=1,1000
      2 EMIT(L,I,K)=C.
      I=1
      IRR=1
      WD(I)=WDA(IRF)
      WS(I)=WSA(IRR)
      IF(WS(I).LT..01)          WS(I)=.1
      3 CCNTINUE
      M=MM
      MX=MINC(NMAX,M)
      JSM=JSLB(M)
      IRR=C
C
      TEM(JSM      )=TEMP
      WZ=1.
      HR=NR
      IR=C
      TX=C.
      TY=0.
      TZ=0.
      DX=0.
      DY=0.
      DZ=0.
      I=1
      WCRAC=WD(I)*.01745
      A(JSM,I)=WS(I)*SIN(WCRAC)
      B(JSM,I)=WS(I)*COS(WCRAC)
      C(JSM,I)=0.
      5 WABAR(JSM,I)=WS(I)
      JSTAB=STAB
      JS(JSM      )=JSTAB
C      CORRECTION FOR MISSING MIXING HT IN MASTER FILE.
      IF(M.EQ.1.AND.(HLID.GT.1000..OR.FLID.LT.0.))HLID=9999.
      IF(M.GT.1.AND.(HLID.GT.1000..OR.FLID.LT.0.))HLID=HMIX(JSUB(M-1))
      HMIX(JSM      )=FLID
C33333
      DC 8 J=1,NSRC
      DC 8 K=1,4
      IRR=C
      ZSS=ZS(K,J)
      EMIS(JSM,K,J)=CSC2(J)*PERCENT(K,J)
      WSSSS=WSA(1)          +.1

```

## ISPDV (Contd.)

```

      KSTAE=C
      DHMIN=PRISE(WSSSS,5,QHEAT(J)*PERCENT(K,J))
      IF(HLIC.LT.ZSS)KSTAB=1
C IF KSTAB.GT. 0 ,WE HAVE CASE CF STACK ABOVE LIC OR PENETRATION
C INTO LIC. USE JSTAB=5 FCR PRISE AND SIGMAS.
C UNTIL LIC RISES TC HEFF. THEN TREAT AS A PLUME
C REFLECTED AS USUAL.
      IF(HLIC.LT.(ZSS+CHMIN).AND.KSTAB.EQ.0)KSTAB=2
      HEFF(JSM,K,J)=ZSS+CHMIN
      IF(KSTAB.GT.C)GO TC 7
      HEFF(JSM,K,J)= ZSS + AMIN1(PRISE(WSSSS,JSTAB,QHEAT(J)*PERCENT(K,J)
1 ) , HLIC-ZSS)
      GC TC 58
      7 CONTINUE
      98 NDW(JSM,K,J)=0.
      WDW=15.1
C DCWNWASH ASSUMTICN FOR TAM WINDS GT WDW
      IF(WSSSS.LT.WDW) GO TO 8
      NDW(JSM,K,J)=1
      HEFF(JSM,K,J)=ZSS
      8 CCNTINUE
      IF(WSSSS.LE.6.) GC TO 501
      IF(NCSTMX.EQ.0) GC TC 501
C TABULATED STACK HEIGHTS ARE OFTEN SIMPLY BUILDING HEIGHTS WHERE
C EMISSIONS ARE FROM STLBBY STACKS. FGR THESE CASES WHEN WS.GT.
C 6 MPH, CCNSIDER DCWNWASH.
      J=1
      NC=1
      NCS=NCSTK(1)
      503 IF(J.EQ.NCS) GO TO 502
      J=J+1
      GC TC 503
      502 DC 504 K=1,4
      NDW(JSM,K,J)=1
      504 HEFF(JSM,K,J)=ZS(K,J)
      NC=NC+1
      IF(NC.GT.NCSTMX) GO TO 501
      NCS=NCSTK(NC)
      J=J+1
      GC TC 503
      501 CONTINUE
C44444
C RECEPTOR GRID DEFINED BY XRCRIG,YRORIG,NWEST,NSTH
      I=1
C CALCULATE PCINT SOURCE CCNTRIBUTICN AT EACH DCSE POINT
C IN RECEPTR GRID. AREA SOURCES EVALUATED MORE EFFICIENTLY.
C PCWER PLANTS TREATED SIMILAR TC INDUSTRIAL POINT SOURCES.
C RECCAT(1,NR)-POWER PLANTS, (2,NR)-INDUSTRY,(3,NR)-RES/CCML
C (4,NR)-TOTAL PCLLUTANT CCNCENTRATIUN AT POINT NR
      NRMAX=(NWEST+1)*(NSTH+1)
C NRMAX MUST BE .LE. 500
      NRWEST=NWEST
      NRSTH=NSTH
      CG 21 NRCP=1,NRMAX
      IWSI=NXF(NRCP,NRWEST+1)
      ISTH=NYF(NRCP,NRWEST+1)
      CALL RGRID(IWSI,ISTH,XRG,YRG)
      IF(NTST.GT.C.ANC.NRCP.LE.2)PRINT 403,XRG,YRG,ZREC
      403 FORMAT(10X,'XRG,YRG ,ZREC=',3E10.2)

```

ISPDVAV (Contd.)

```

C   XRG,YRG ARE CCCRDS. OF DOSE POINT NUMBER NRCP
      DC 88 JJJJ=1,4
C   ZERC THE CONCENTRATION ARRAY FOR HOUR M AT DOSE POINT NRCP
88  RECDAT(JJJJ,NRCP)=C.
      ZT=ZREC
C   UNIFORM HEIGHT FOR ALL RECEPTOR POINTS IN GRID
      Z=ZT/5280.
      NLIM=NMAX
      IF(WSSSS.GT.6.) NLIM=4
      IF(WSSSS.GT.10.) NLIM=2
      NLIM=MINO(NLIM,M)
      NLIMA=NLIM
      DO 20 N=1,NLIM
      JJX=JSUB(M-N+1)
      JJJ=JS(JJX)
C   POINT SOURCES      INITIAL DIMENSIONS SIGX=SIGY=100 FT,SIGZ=100 FT
      DSS=100.*2.4/5280.
      CALL FSEUDC(      CSS,0.,C.,TX,TY,TZ,DX,DY,JJJ,100.,0)
      TX1=TX
      TZ1=TZ
C   BUILDINGS WITHOUT STACKS OR STACKS IN DOWNWASH
C   APPROXIMATED BY INITIAL DIMENSIONS SIGX=SIGY=750 FT,SIGZ=150
      DSS=750.*2.4/5280.
      CALL FSEUDC(      CSS,0.,C.,TX,TY,TZ,DX,DY,JJJ,150.,0)
      TX2=TX
      TZ2=TZ
      THALF=100.
C   THALF IN HOURS
C   SO2 HALF LIFE HERE ONLY A CRUDE FCT. OF TEMP.
      L=N
      DC9NT=1,L
      IF(TEM(JSUB(M-NT+1)).GT.6C.) THALF=4.
9  CONTINUE
C
      XSAVE=-1.
      YSAVE=-1.
      KSTABB=-1
      DC 20 J=1,NSRC
      KM=4
      CHI=C.
      DO 10 K=1,KM
      IF(EMIS(JJX,K,J).LE.EMINPT) GO TO 10
C   EMISSIONS IN LB/HR. PROGRAM CONSIDERS EACH STACK SEPARATELY AND
C   UP TO 6 STACKS PER PLANT. EMISSIONS LESS THAN EMINPT ARE
C   DISREGARDED.      FOR TWO FOR MORE STACKS PER PLANT,
C   CALCULATIONAL SHORTCUTS ARE AVAILABLE. NTRAN IS A FLAG FOR THIS
      NTRAN=C
      IF(NCH(JJX,K,J).GT.0) GO TO 1001
      TX=TX1
      TY=TX
      TZ=TZ1
      GO TO 1002
1001 TX=TX2
      TY=TX
      TZ=TZ2
1002 CONTINUE
99  CONTINUE
      X=XRG-(XS(J)-A(JJX,1)*TX)

```

## ISPDV (Contd.)

```

      Y=YRG+(YS(J)+B(JJX,1)*TY)
C     NCTE PLANTSIM STCRS +Y UP
C     CGCRD SYSTEM IS +X(LEFT), +Y(CCW)
C     CONSIDERS UP TO 6 STACKS PER PLANT
      KSTAB=C
      IF(ZS(K,J).GE.HMIX(JJX)) KSTAB=1
      IF(KSTAB.EQ.C.AND.HEFF(JJX,K,J).GT.HMIX(JJX))KSTAB=2
      IF(XSAVE.EQ.X.ANC.YSAVE.EQ.Y.AND.KSTABB.EQ.KSTAB) NTRAN=1
      IF(NTRAN.EQ.1) GO TO 11
      KSTABB=KSTAB
      XSAVE=X
      YSAVE=Y
      IF(ZT.LT.1.) ZT=1.
C     ZT IN FEET
      WZ=1.
      HEF=HEFF(JSUB(M-N+1),K,J)
      IF(KSTAB.GE.1)JJJ=5
      IF(HEF.GT.ZWS ) WZ=((HEF      )/ZWS )**PP( JJJ
      IF(WZ.GT.3.)WZ=3.
C     WIND FRCFILE LAW
      DG12Ih=1,MX
      WSBAR(IW)=WABAR(Ih,I)*WZ
      U(Ih)=A(IW,I)*WZ
      W(IW)=C(IW,I)
      JSSAVE(IW)=JS(IW)
12  V(IW)=B(Ih,I)*WZ
11  CHI=CHI+EMIS(JSUB(M-N+1),K,J)*TRAN(N,M,K,J,NTRAN)*.38122E-4
10  CCNTINUE
      IXPT=1
      IF(J.GT.NPCW)IXPT=2
      IF(J.GT.NIND) IXPT=3
      RECDAT(IXPT,NRCP)=RECDAT(IXPT,NRCP)+CHI
      RECDAT(4,NRCP)=RECDAT(4,NRCP)+CHI
      IF(CHI.GT..0001)PRINT 407,M,N,J,X,Y,CHI
407  FORMAT(10X,'PT.SCS.  M,N,J,X,Y,CHI =' ,3I6,3E12.3)
20  CCNTINUE
21  CCNTINUE
      IF(NTEST.LT.1 )      'GC TC 405
      PRINT 404
404  FORMAT(15X,'PRCUT FOR PLANTSIM SCURCES ONLY')
      CALL PROUT(MM,RECDAT,NWEST,NSTh)
405  CCNTINUE
C
C     ADDITIONAL POINT SCURCES
      JSM=JSUB(M)
      DG20Ih=1,MX
      HKEE(Ih)=HEFF(IW,1,1)
201  EKEE(Ih)=EMIS(IW,1,1)
C     ESTIMATE HCURLY EMISSIONS
      DG22CJ=1,NPTS
      NPATTJ=NPAT(J)
      GCTC(209,211,213),NPATTJ
209  QPHR(JSM,J)=CPTOT(J)/8760.
      CPHR(JSM,J)=CPHR(JSM,J)*1.E6
      GCTO22C
211  TE=0.
      IF(TEMP.LT.65.)TE=1.
      QPHR(JSM,J)=CPTOT(J)*(.2/8760.+ .8*TE*(65.-TEMP)/1.68E5
      CPHR(JSM,J)=CPHR(JSM,J)*1.E6

```

## ISPDVAV (Contd.)

```

      GCTG22C
213 TPUMP=.429
      IF(HR.GT.6.9.AND.+R.LT.23.1)TPUMP=1.29
C     PUMPING STATIC PATTERN
      QPHR(JSM,J)=CPTOT(J)*TPUMP/876C.
      QPHR(JSM,J)=CPR(JSM,J)*1.E6
      GGTG22C
220 CCNTINLE
C     EMISSIONS FOR ADDITIONAL SCS. STORED AS M LBS SO2/YR
C     ESTIMATE PLUME RISE IF NS=0, ASSUME EMISSION AT
C     XBUILDING HEIGHT. ASSUME PLUME RISE PROP. TO 1/(NS**.5)
      DC225J=1,NPTS
      ZSS=ZPT(J)
      KSTAE=C
      DH=0.
      IF(NS(J).EQ.C.CR.WSSSS.GT.WDh)GOTC224
      DN=NS(J)
      QHEATT=QPHR(JSM,J)*.12/ (.C2*SPCT(J)*SQRT(DN))
C     ALLOW FOR 20 PERCENT GREATER PLUME RISE FROM STACK INTERACTION
      IF(DN.GT.1.1)QHEATT=1.4*QHEATT
      IF(HLID.LT.ZPT(J))KSTAB=1
      DHMIN=PRISE(WSSSS,5,QHEATT)
      IF(KSTAB.EQ.C.ANC.(DHMIN+ZPT(J)).GT.HLID) KSTAB=2
      IF(KSTAB.GE.1)GOTC222
      DH=AMIN1(PRISE(WSSSS,JSTAE,QHEATT),HLID-ZPT(J))
      GCTC224
222 DH=DHMIN
224 HEFPT(JSM,J)=ZPT(J)+DH
      KSTAF(JSM,J)=KSTAE
225 CCNTINLE
      IR=0
      I=1
      IR=IR+1
      Z=ZREC/528C.
      DC27CJ=1,NPTS
C     SOME ADDITIONAL POINT SOURCES ARE 20 MILES FROM CITY.
      NLIMA=MINO(NMAX,M)
      DC27CN=1,NLIMA
      JJJ=JS(JSUB(M-N+1))
      JSN=JSLB(M-N+1)
      HEFF(JSN,1,1)=HEFFT(JSN,J)
      EMIS(JSN,1,1)=CPR(JSN,J)
      IF(EMIS(JSN,1,1).LT.EMINPT) GC TC 27C
      KSTAB=KSTAF(JSN,J)
      IIN=IIND(J)
      IF(KSTAB.GT.C) JJJ=5
      HEF=HEFF(JSN,1,1)
      WZ=1.
      IF(HEF.GT.ZWS) WZ=(HEF/ZWS)**PP(JJJ)
      IF(WZ.GT.3.)WZ=3.
      DC205Ih=1,MX
      U(Ih)=A(Ih,I) *WZ
      V(Ih)=E(Ih,I) *WZ
      W(Ih)=C(Ih,I) *WZ
205 WSBAR(IW)=WABAR(Ih,I) * WZ
      IF(WSSSS.GT.WDh.CR.NS(J).EQ.0) GC TC 230
      DSS=1CC.*2.4/528C.
      CALL FSEUDC( CSS,0.,C.,TX,TY,TZ,DX,DY,JJJ,100.,0)

```

ISPDAY (Contd.)

```

GC TC 231
230 CCNTINLE
DSS=75C.*2.4/528C.
C DCWASH CR BUILDINGS WITHOUT STACKS CX=DY= 750. FT DZ=150.FT
CALLPSEUDC( CSS,0.,C.,TX,TY,TZ,DX,DY,JJJ,150.,0)
KSTAB=KSTAF(JSN,J)
231 CCNTINLE
DC 269 NRCP=1,ARMAX
IWSI=AXF(NRCP,ARWEST+1)
ISTH=NYF(NRCP,ARWEST+1)
CALL RGRID(IWSI,ISTH,XRG,YRG)
X=XRG-(XPT(J)-TX*L(JSN))
Y=YRG-(YPT(J)-TY*V(JSN))
CC=.381E-4
CHI=EMIS(JSN,1,1)*CO*TRAN(N,M,1,1,0)
IF(CHI.GT..0001)PRINT 408,M,N,J,X,Y,CHI
408 FCRMAT(10X,'AC.SCS. M,N,J,X,Y,CHI =',3I6,3E12.3)
RECCAT(IIN,NRCP)=RECCAT(IIN,NRCP)+CHI
RECCAT(4,NRCP)=RECCAT(4,NRCP)+CHI
269 CCNTINLE
270 CCNTINLE
IF(NTEST.LT.1) GC TO 289
PRINT 406
406 FORMAT(10X,'FCUT FOR ALL POINT SOURCES')
CALL PROUT(MM,RECCAT,NWEST,NSTF)
289 CCNTINLE
DC291IW=1,MX
HEFF(IW,1,1)=HKEE(IW)
EMIS(IW,1,1)=EKEE(IW)
291 JS(IW)=JSSAVE(IW)
C55555
C EVALUATE AREA SOURCE CONTRIBUTIONS
C ADJUST NIGHTTIME STABILITY FOR CITY ROUGHNESS
IF(FLID.GT.100..AND.WSSSS.GT.6.)GC TO 90
GC TC 95
90 IF(JSTAB.EQ.5) JSTAB=4
DC 91 J=1.MX
JSSAVE(J)=JS(J)
91 IF(JS(J).EQ.5)JS(J)=4
95 CCNTINLE
C PRORATE ANNUAL SOURCES
NSMAX=NSXMAX*NSYMAX
DC 1000J=1,NSMAX
DC 100 NCL=1,3
IF(QTCT(NCL,J).LT..01) GO TO 100
GO TO (101,102,106),NCL
101 CCNTINLE
C LGW RISE ANNUAL FUEL USE -HOURLY PRORATION
C SOURCES ON AT 6 AM, OFF AT 10 PM AND IDLE IN BETWEEN
TCN=5.9
C HOUR 0 IS MIDNIGHT
TGFF=22.1
IF(TEMP.LT.5.0) TCN=3.9
C FIRE BOILERS EARLY WHEN TEMP.LE. 5 DEG.F
TE=1.C
IF(HR.GT.TCN.AND.FR.LT.(TCN+2.1)) TE=1.5
C JANITOR FUNCTION FOR LGW RISE RESIDENTIAL BUILDINGS
TCNGFF=TCFF-TCN+1.
GC TC 105

```

## ISPDV (Contd.)

```

102 CCNTINLE
C   HIGH RISE- TWENTY-FOUR HOUR SOURCE
   TCN=-.C01
   TGFF=24.001
   TE=1.C
   TONGFF=24.
105 CCNTINLE
   QIND=C.
   QHT=C.
   IF(TEMP.GE.65.)TE=0.
C PCTHW IS FRACTION OF ANNUAL FUEL USE FOR HOT WATER.
   QHW=QTOT(NCL,J)*PCTHW/(24.*365.)
   FR=1.-PCTHW
   IF(NCL.EQ.1.AND.(FR.GT.TOFF.CR.HR.LT.TCN)) TE=0.
   QHT=QTCT(NCL,J)*FR*TE*(65.-TEMP)/(DDAVG*TONOFF)
   GO TO 107
106 QHW=C.
   QHT=C.
   QIND=QTOT(NCL,J)/(24.*365.)
107 EMIT(JSUB(M),NCL,J)=QHW+QHT+QIND
100 CCNTINLE
1000 CCNTINLE
C66666
C
C   EACH AREA SOURCE HAS HOURLY SC2 IN 3 CLASSES.
C   DEPENDING ON NSIDE, THE COORD OF UPWIND PSEUDO PT SOURCE
C   IS KNOWN.
C   EACH MUST BE EVAL.BY TRAN.FIRST EVAL. LCM RISE AND IF
C   POSSIBLE USE EXPONENTIAL CORRECTIONS FOR OTHER CLASSES.
C   NSIDE NOW LIMITED TO 1,2,4,8,AND 16 MILES.
C
   JSU=JSUB(M)
   I=1
   DS=.5
   DO 110 IS=1,5
   DS=2.*DS
   DO 110 NCL=1,3
   CALL PSEUDG(DS,A(JSU,I),B(JSU,I),TXX(JSU,IS),TY,
2     TZZ(JSU,IS,NCL),DXX(JSU,IS),DYY(JSU,IS),JSTAB,HAVG(NCL),NCL)
110 CCNTINLE
C   DISTINCTION BETWEEN TZZ(.,NCL) VALUES IMPORTANT ONLY FOR
C   AREAS ADJACENT TO RECEPTOR POINT.
   NLIMA=NLIM
   DO 111 IW=1,MX
   U(IW)=A(IW,I)
   V(IW)=B(IW,I)
   W(IW)=C(IW,I)
111 WSBAR(IW)=WABAR(IW,I)
C
C   A STANDARD RECEPTOR-ORIENTED SOURCE GRID SYSTEM WITH
C   GRID SQUARES NUMBERED SEQUENTIALLY FROM 1-NSGRID IS DEFINED.
C   THE COORDINATES OF LOWER LEFT CORNER OF EACH SQUARE RELATIVE TO
C   THE REFERENCE RECEPTOR AT 0.0 ARE INPUTS.
C   PLACED SYMMETRICALLY ABOUT RECEPTOR, THE FIRST 16 SQUARES
C   ARE OF SIDE LENGTH DGRID, SQUARES 17-48 OF SIDE
C   LENGTH 2*DGRID,ETC.
C   WIND SPEED AND DIRECTION
C   ARE REPRESENTED BY SINGLE HOURLY-CONSTANT
C   FUNCTIONS OF TIME.

```

ISPDVAV (Contd.)

```

C      COUPLING COEFFICIENTS CCUP(JSUB(M-N+1),NSQ,NCL) BETWEEN RECEPTOR
C      AND EACH GRID SQUARE ARE CALCULATED BASE ON A
C      REFERENCE EMISSION FOR EACH SIZE GRID SQUARE.
C              RESULTS ARE TRANSLATED AND ACTUAL
C      EMISSIONS USED TO CALCULATE CONCENTRATIONS AT EACH
C      PCINT OF THE CITY GRID.
C
C      EVALUATE COUPLING COEFFICIENTS FOR SQUARES ADJACENT TO RECEPTOR.
C      FOR THESE SQUARES, A DISTINCT SIGZO
C      AND COUPLING CCEF. SET IS USED FOR EACH SOURCE CLASS.
C      CCEFS. FOR AREAS FURTHER CUT ARE NOT SENSITIVE TO THIS
C      DISTINCTION.
C
C      FOR EACH SIZE AREA(E.G.1X1,2X2,4X4) AND EACH SOURCE
C      CLASS THERE IS A
C      MAXIMUM AVG. EMISSION RATE(LB/HR)
C      THESE VALUES ARE INPUTS. COUPLING COEFFICIENTS
C      ARE EVALUATED FOR THESE EMISSION MAXIMA (TO TEST FOR
C      SIGNIFICANCE).
C
C      DO 31 N=1,NLIMA
C      JSM=JSUB(M-N+1)
C      EMSAV=EMIS(JSM,1,1)
C      HKEEP=HEFF(JSM,1,1)
C      ONLY ONE LID HEIGHT CONSIDERED FOR WHOLE CITY
C      AREA SOURCE REFERENCE GRID. X AND Y VALUES IN MILES.
C      DC30NSG=1,NSGRID
C      NSIDE=1
C      IF(NSG.GT.16)NSIDE=2
C      IF(NSG.GT.48)NSIDE=3
C      IF(NSG.GT.88)NSIDE=4
C      RSIDE=NSIDE
C      IF(NSIDE.GT.2)RSIDE=4.
C      IF(NSIDE.GT.3)RSIDE=8.
C      RECEPTOR AT 0,0
C      X=-XSGRID(NSG)+DXX(JSM,NSIDE)+RSIDE/2.
C      Y=-YSGRID(NSG)+DYY(JSM,NSIDE)+RSIDE/2.
C      Z=ZREC/5280.
C
C      TX=TX(X(JSM,NSIDE))
C      TY=TY(Y)
C      DCWNWASH RULES. WS.GE.WSCRIT, THEN HEFF=HAVG
C      WS.LT.WSCRIT, THEN HEFF=HAVG+PRI
C      NCL=1
C      PRI=C.
C      ZSS=FAVG(1)
C      WSCRIT=6.
C      DF=ZSS
113 IF(WSEAR(JSM).LT.WSCRIT)PRI=DF
C      KSTAB=C
C      HLI=FMIX(JSM)
C      IF(HLI.LT.ZSS)KSTAB=1
C      HEFF(JSM,1,1)=ZSS+AMIN1(PRI,HLI-ZSS)
C      HEFF IN FEET.
116 CCNTINLE
C      GCTC(117,118,119),NCL
117 CCNTINLE
C      LCW RISE SPACE HEATERS
C      TZ=TZZ(JSM,NSIDE,NCL)

```



## ISPDAV (Contd.)

```

      EMIS(JSM,1,1)=EMAX(NSIDE,NCL)
      COUP(NSG,NCL,JSM)=EMAX(NSIDE,NCL)*TRAN(N,M,1,1,0)*.381E-4
      KSTABB=KSTAB
C     LCM RISE CCNE. HIGH RISE CHECK IF KSTAB IS SAME FOR
C     THIS CASE AND IF NSG.GT.4. IF SO CAN SIMPLIFY CALCULATION
C     IN SUBROUTINE TRAN.
C
      NCL=2
      WSCRIT=6.
      PRI=C.
      ZSS=F.AVG(2)
      DH=ZSS/2
      GCTC113
118  CONTINUE
      NTRAN=C
      IF(KSTAB.EQ.KSTABE)NTRAN=1
      IF(NSG.LE.4)NTRAN=C
      TZ=TZZ(JSM,NSICE,NCL)
      EMIS(JSM,1,1)=EMAX(NSIDE,NCL)
      COUP(NSG,NCL,JSM)=EMAX(NSIDE,NCL)*TRAN(N,M,1,1,NTRAN)*.381E-4
      KSTABE=KSTAB
C     INDUSTRY
      NCL=3
      WSCRIT=15.
      PRI=C.
      ZSS=F.AVG(3)
      DH=ZSS
      GC TC 113
119  CONTINUE
      NTRAN=C
      IF(KSTABB.EQ.KSTABE)NTRAN=1
      IF(NSG.LE.4)NTRAN=C
      TZ=TZZ(JSM,NSICE,NCL)
      EMIS(JSM,1,1)=EMAX(NSIDE,NCL)
      COUP(NSG,NCL,JSM)=EMAX(NSIDE,NCL)*TRAN(N,M,1,1,NTRAN)*.381E-4
30   CONTINUE
      IF(NTTEST.LT.1.CR.LLL.GT.2) GO TO 1112
      NT=NSGRID
      PRINT 1011
1011  FCRMAT(10X,'((COUP(NSG,NCL,JSM),NSG=1,NT) ,NCL=1,3)  ')
      PRINT 1111,((COUP(NSG,NCL,JSM),NSG=1,NT),NCL=1,3)
1111  FCRMAT(5X,11E1C.2)
      LLL=LLL+2
1112  CONTINUE
C77777
C     THE ARRAY OF COUPLING COEFFICIENTS FOR FOUR M AND CLASSES 1-3
C     HAS BEEN FORMED. NOW PLACE ORIGIN OF GRID ON EACH POINT OF
C     RECEPTOR GRID: EVALUATE ACTUAL AREA SOURCES. EVALUATE POLLUTANT
C     CONCENTRATION.
C
      EMIS(JSM,1,1)=EMSAV
31   HEFF(JSM,1,1)=FKEEP
      DC 50 NRCP=1,NRMAX
      IWST=NXF(NRCP,NRWEST+1)
      Isth=NYF(NRCP,NRWEST+1)
      CALLRGRID(IWST,Isth,XRG,YRG)
      DC49NSG=1,NSGRID
      XALL=XRG+XSGRID(NSG)
      YALL=YRG+YSGRID(NSG)

```

## ISPDAV (Contd.)

```

      IAX=(XALL-XSCRIG+.1)/DGRIC
      IAY=(YALL-YSCRIG+.1)/CGRIC
      NX=1
      IF(NSG.GT.16)NX=2
      IF(NSG.GT.48)NX=4
      IF(NSG.GT.88)NX=8
      NSIDE=NX
      IF(NSG.GT.48)NSIDE=3
      IF(NSG.GT.88)NSIDE=4
C     IF GC UP TO LARGER AREAS, MUST MODIFY CODE HERE.
      DC 35 NCL=1,3
      DC 35 N=1,NLIMA
      JSM=JSLB(M-N+1)
35    VQ(JSM,NCL)=0
      DC 45 NSIX=1,NX
      DC 45 NSIY=1,NX
      IAXX=IAX-(NSIX-1)
      IAYY=IAY-(NSIY-1)
      IF(IAXX.LT.1.CR.IAXX.GT.NSXMAX.CR.
2     IAYY.LT.1.CR.IAYY.GT.NSYMAX) GO TO 45
      NAREA=NSXMAX*(IAYY-1)+IAXX
      DC 44 NCL=1,3
      DC 44 N=1,NLIMA
      JSM=JSLB(M-N+1)
44    VQ(JSM,NCL)=VQ(JSM,NCL)+EMIT(JSM,NCL,NAREA)
45    CONTINUE
      IF(NTEST.LT.1.CR.LLL.GT.2) GO TO 1115
      PRINT 1016,NRCP,XRG,YRG,NSG
1016  FORMAT(10X,'VQ ARRAY FOR NRCP,XRG,YRG,NSG=',I10,2E10.2,I10 /)
      PRINT 1116,(VQ(JSM,NCL), NCL=1,3)
1116  FORMAT(10X,3E10.2)
1115  CONTINUE
      CHI1=0
      CHI2=0
      CHI3=0
      DC 47 N=1,NLIMA
      JSM=JSLB(M-N+1)
      CHI1=CHI1+COLP(NSG,1,JSM)*VQ(JSM,1)/EMAX(NSIDE,1)
      CHI2=CHI2+COLP(NSG,2,JSM)*VQ(JSM,2)/EMAX(NSIDE,2)
47    CHI3=CHI3+COLP(NSG,3,JSM)*VQ(JSM,3)/EMAX(NSIDE,3)
      RECCAT(3,NRCP)=RECCAT(3,NRCP)+CHI1+CHI2
      RECCAT(2,NRCP)=RECCAT(2,NRCP)+CHI3
49    RECCAT(4,NRCP)=RECCAT(4,NRCP)+CHI1+CHI2+CHI3
50    CONTINUE
C8E888
C     POLLUTANT CONCENTRATIONS CALCULATED FOR EACH POINT ON RECEPTOR
C     GRID. CONTRIBUTIONS FROM MAJOR SOURCE CLASSES IS KNOWN.
      IR=1
      I=1
C     PRINT 469,M,I,RECCAT(4,NRTAM),HLID
C 469  FORMAT(10X,'SC2 AT HOUR N=',I5,10X,'FOR TAM',I4,10X,'=',E12.3,
C     X 10X,'HLID=',E10.2)
      NPFP=NPFP+1
      IF(NPFP.LT.NPRINT) GO TO 6666
      NPPP=0
C     IN ORDER TO USE SUBROUTINE PROUT TO PRINT CONCENTRATIONS
C     IN GRID FORMAT, MUST LIMIT NREST+1 .LE.12
      CALL PROUT(M,RECCAT,NWEST,NSTH)
6666  CONTINUE

```

ISPDVAV (Contd.)

```

C      PUNCHED OUTPUT . ONE TAM STATION AT A TIME. FOUR HOURS PER CARD
      IF (VALCP.GT.C) SC2VAL(1)=RECCAT(4,NRTAM)
      IF (FNCHOP.EC.C) GC TO 513
      NHRP(NCOUNT)=NR
      NTMP(NCOUNT,IR)=I
      PREC(NCOUNT,IR)=SC2VAL(1)
      GBSC(NCOUNT,IR)=AMIN1(9.959,SOBS(IR))
295  MPU(NCOUNT)=M
      NCCLNT=NCCLNT+1
      IF(NCCUNT.LT.5) RETURN
      NCCLNT=1
      DG 258 IR=1,1
      PUNCH 470,(NTMP(NC,IR),NHRP(NC),MPU(NC),PREC(NC,IR),OBSC(NC,IR),
X      NC=1,4)
298  CONTINUE
470  FORMAT(4(I1,I3,I4,2F5.3,2X))
513  CONTINUE
293  CONTINUE
      RETURN
      END

```

ADAT2

```

      SUBROUTINE ACAT2
C      ZERC QTOT ARRAY
      DIMENSION TITLE(20)
      COMMON/ASGRID/NSGRID,XSGRID(100),YSGRID(100)
      COMMON/QHWWW/PCTHW,DDAVG
C      DDAVG IS AVG NUMBER OF DEG.DAYS/YEAR(7000 IN CHICAGO).
C      PCTHW IS FRACTION OF ANNUAL FUEL USED FOR HOT WATER
C      CHICAGO HOT WATER REQ. =20 PCT OF ANNUAL FUEL
      COMMON/NUMBPT/NPCW,NIND
C      POINT SOURCES SHOULD BE LISTED WITH POW PLANTS J=1,NPOW,
C      INDUSTRY FROM J=NPCW+1 TO NINC, FOLLOWED BY RES/COML.
      COMMON/METREF/ZWS
C      ZWS IS HEIGHT(FT)CF AEROVANE
      COMMON/RGR/XRGRID,YRGRID,NWEST,NSTH,DGRID,ZREC
      COMMON/AREAS/QTOT(3,1004),HVG(3),DGRID,XSGRID,YSORIG,
2  NSXMAX,NSYMAX,EMAX(5,3)
      COMMON/MINC/EMINPT
C      THE AREA SOURCE GRID COORDINATE SYSTEM HAS BEEN FORMED WITH +X
C      WEST AND +Y SCLTH.
C      THE GRID SYSTEM CRIGIN XSCRIG,YSORIG NEED NOT BE 0,0.
C      DGRID IS THE GRID SPACING IN MILES.
C      NSXMAX AND NSYMAX DEFINE MAX GRID COORDINATES. THE COORDINATES
C      CF THE LOWER LEFT CORNER CF GRID SQUARE NX,NY ARE
C      (XSCRIG+NX*DGRID),(YSORIG+NY*DGRID).
C      CRIGIN OF GRID SYSTEM SHOULD BE LOCATED SO THAT WHOLE
C      REGION LIES IN THIRD QUADRANT (HERE +X,+Y).
C      EACH AREA OF SIZE DGRID**2 MUST BE ASSIGNED A POLLUTANT
C      EMISSION RATE (LB/YR) FOR THREE TYPES CF EMISSIONS.
C      LOW PRESSURE SPACE HEATERS,HIGH RISE SPACE HEATERS AND
C      INDUSTRIAL. COMMERCIAL EMISSIONS CAN BE INCLUDED IN
C      EITHER OF THE FIRST TWO CATEGORIES.QTCT(NCL,NAREA) IS THE ARRAYNAME
C      A SINGLE STACK HEIGHT IS INPUT FOR EACH CLASS CF AREA SOURCES

```

ADAT2 (Contd.)

```

      NSGRIC=88
      EGRIC=1
      XSGRIG=-2.
      YSGRIG=-12.
      NSXMAX=20
      NSYMAX=50
      DO 2 I=1,1000
      DO 2 NCL=1,3
2     QTGT(NCL,I)=C.
C     READ IN EMISSION DATA BASED ON JJR GRID
C     DATA DECK MUST BE FOLLOWED BY A CARD WITH 99999. PUNCH IN CULMS. 1-6
      K=0
      L=1
      M=4
3     K=K+1
      READ 15,TITLE
      GC TC (10,11,12,13,17),K
10    READ 5, ((QTCT(I,NA),I=1,3),NA=L,M)
      IF(QTCT(1,L).GT.10000.) GC TC 20
      L=L+4
      M=M+4
      GC TC 10
20    CONTINUE
      GC TC 3
11    READ 450,(XSGRID(IX),YSGRID(IX),IX=1,16 )
      GCTC3
12    READ 450,(XSGRID(IX),YSGRID(IX),IX=17,48)
      GCTC3
13    READ 450,(XSGRID(IX),YSGRID(IX),IX=49,88)
      GCTC3
17    READ 16,((EMAX(I,J),I=1,3),J=1,3)
30    CONTINUE
      5 FCRMAT(12F6.0)
      15 FCRMAT(20A4)
      16 FCRMAT(3F8.0)
450   FCRMAT(12F6.1)
      DO 40 J=1,1000
      DO 40 I=1,3
40    QTGT(I,J)=QTCT(I,J)*1.E4
C     QTGT(I,J) HAS UNIT LBS/YR.
      PCTHh=.2
      CDAVG=7000.
      NPCW=24
      NINC=72
      ZREC=75.
      EMINFT=10.
      ZWS= 75.
      HAVG(1)=100.
      HAVG(2)=200.
      HAVG(3)=150.
C     DEFINE 6X11 RECEPTOR GRID FOR TEST PROBLEM.
      XRCRIG=3.
      YRCRIG=-7.
      NWEST=5
      NSTE=10
      CRGRIC=2.
      RETURN
      END

```

PROUT

```

SUBROUTINE PROUT(MM,RECDAT,NWEST,NSTH)
DIMENSION RECDAT(4,500)
C   IN CRDR TC USE SUBROUTINE PROUT TO PRINT CONCENTRATIONS
C   IN GRID FORMAT, MUST LIMIT NWEST+1 .LE.12
DIMENSION REC(4,12)
PRINT 400,MM
400 FORMAT(1H1,///,1CX,'MM= ',I4///)
C   REMEMBER STD.RECEPTR GRID IS +XLEFT WHEREAS PRINTOUT IS
C   FRGM LEFT TO RIGHT.
Nk=NWEST+1
IMULT=1
10 DO 11 NR=1,Nk
IR=Nk*IMULT+1-NR
DC11K=1,4
11 REC(K,NR)=RECDAT(K,IR)
IMULT=IMULT+1
DC 15 K=1,4
15 PRINT 402,(REC(K,I),I=1,Nk)
402 FORMAT(5X,12(F7.2,3X))
PRINT 401
401 FCRMAT(/ )
IF(IMULT.GT.NSTH+1) RETURN
GO TC 10
END

```

PSEUDO

```

SUBROUTINE PSEUDC(CS,U,V,TX,TY,TZ,DX,DY,MSTB,HS,NCL)
EXTERNAL SIGGX,SIGGZ
C   CALLING SEQ.UNITS ARE MPH,HRS,MI.,      HS IN FEET.
CCMPCN/STABIL/NSTB,SIGXO,SIGZC
CCMPCN/WDUN/WSAVE
WSAVE=SQRT(U*U+V*V)
NSTB=MSTB
IF(NCL.GE.2) GO TC 9
SIGXC=CS/2.4
EPP=.001
CALLGUESS2(SIGGX,.1,.3,TX,EPP,1C,NF1,0,I)
TY=TX
9 SIGZC=HS/5280.
18 CALLGUESS2(SIGGZ,.1,.01,TZ,EPP ,1C,NF1,C,1)
40 DX=U*TX
DY=V*TY
RETURN
END

```

RGRID

```

SUBROUTINE RGRID(I,J,XR,YR)
CCMCMC/RGR/XRCRIG,YRCRIG,NWEST,NSTH,DRGRID,ZREC
C IT IS ASSUMED THAT AREA SOURCE GRID SIZE DSGRID.LE.
C RECEPTOR DRGRID AND THAT RECEPTOR POINTS COINCIDE
C WITH GRID LINE INTERSECTIONS. FUTURE MODIFICATIONS SHOULD
C ELIMINATE THIS AND PERHAPS INCLUDE ARBITRARY GRID POINTS
C ALONG CENTER LINES OF MAJOR PLUMES.
C THE RECEPTOR GRID HAS NORTHEAST ORIGIN A POINT
C (XRCRIG,YRCRIG) AND (NWEST+1)*(NSTH+1)POINTS IN ALL
C WITH GRID SPACING DRGRID (MILES) WITH DRGRID
C A MULTIPLE (1,2,ETC.) OF DSGRID.
XR=XRCRIG+(I-1)*DRGRID
YR=YRCRIG+(J-1)*DRGRID
RETURN
END

```

NXF

```

FUNCTION NXF(NC,NY)
NXXX=NYF(NC,NY)
NXF=NC-NY*(NXXX-1)
RETURN
END

```

NYF

```

FUNCTION NYF(NC,NY)
NYF=(NC-1)/NY + 1
RETURN
END

```

PRISE

```

C FUNCTION PRISE(WS,JSTAB,QFEAT)
REAL A(7)
REAL XF(7)
CCMCMC/RISE/ZSS
CCMCMC/METREF/ZWS
DATA A/2.65,2.65,2.65,1.0E,.68,.68,.68/
DATA XF/.3,.3,.2,.3,.4,.5,.6/
DATA KPR/1/
JST=JSTAB
IF(ZSS.GT.200..AND.JST.LE.3) JST=4
C STABILITY CONDITIONS HAVE BEEN LIMITED TO NEUTRAL AND STABLE
C FOR STACKS ABOVE 200 FEET (THIS INCLUDES ALL CECO PLANTS)
C
C
WSMPS=WS*1609.3/3600.
WZ=1.
IF(ZSS.GT.ZWS)WZ=(ZSS/ZWS)**XP(JST)
IF(WZ.GT.3.)WZ=3.
WSMPS=WSMPS*WZ
C A WIND SPEED PROFILE HAS BEEN APPROXIMATED BY POWER LAW

```

PRISE (Contd.)

```

C      AFTER BROCKHAVEN WCRK
C      ALL TAMS ARE TRARILY ASSUMED AT 50 FEET< CORRECTION
C      SHOULD BE MADE FOR TAM 3 AT 120 FEET
C
C      NC DOWNDASH EFFECTS OR LOOPING HAVE BEEN INCLUDED.
C
C      IF(WSMPS.LT.2.C) WSMPS=2.0
C      TVA DATA INDICATES CARSON MOSES AND OTHER FORMULAE
C      OVERPREDICT PLUME RISE FOR WS .LT.2 OR 3 M/S
C      THUS A MINIMUM WINDSPEED OF 2 M/SEC HAS BEEN SET FOR PRISE
C      QKCS=QHEAT*7.0
C      . QHEAT IN TH/HR
C      PRISE=A(JST )*5.35*3.281*SQRT(QKCS)/WSMPS
C      PRISE IS IN FEET
C      IF (KPR.GT.0) GO TO 500
C      KPR=KPR+1
C      WMFS=WSMPS
C      PRINT 401, JST,WMFS,QHEAT,PRISE
401  FORMAT(15X,'IN PRISE. JST,WMPS,QHEAT,PRISE= ', I2,5X,3E12.2)
500  CONTINUE
C      RETURN
C      END

```

ITRAN

```

C      FUNCTION ITRAN(EMIS,HEFF)
C
C      COMMON/KTRCUE/KTRFC
C      CUT CFF ON N
C
C      REAL*4 EMIS(12,4,1),HEFF(12,4,1)
C
C      COMMON/MXC/MX
C      COMMON/KERNEL/X,Y,Z,U(24),V(24),W(24),JS(24),HMIX(24),WSBAR(24),WZ
C
C      EXTERNAL KERN
C
C      COMMON/SUECO/TX,TY,TZ,DX,CY,CZ
C      COMMON/XTRAN/KSTAB
C      IF(KSTAB.GT.0)HAVE PLUME INITIALLY ABOVE LID.
C      COMMON/POLT/I
C      DIMENSION JSSS(24)
C      DATA NCUT/4/
C      DATA KPR/1/
C      DATA KI/O/,KMAX/1CC/
C
C      COMMON/WDUN/WSAVE
C      ITRAN=C
C      ACC1=C.
C      QSS=C.
C      CH1MAX=0.
C      E5=C.
C      EPS=.001
C      EPS=.001
C      RETURN
C
C      ENTRY TRAN(N,M,K,J,ATRAN)
C11111

```

## ITRAN (Contd.)

```

C     TIN=ILEFT(YYYY)
C     IF(NTRAN.EQ.C) USE KERN TC EVALUATE POINT CR AREA SOURCE.
C           OTHERWISE USE PREVIOUS AREA SOURCE CALC. WITH NEW HEFF
C     MULTIPLE IMAGES
C     Z AND ZKEEP IN MILES
      JSUBX=JSUB(M-N+1)
      DO 51C IK=1,MX
510   JSSS(IK)=JS(IK)
C     NOW CAN PLAY AROUND WITH THE JS ARRAY
C
      WSAVE=C.
      DO 308 IN=1,N
308   WSAVE=WSAVE+WSEAR(JSUB(M-N+IN))
      WSAVE=WSAVE/N
      KFUME=10
      ZKEEP=Z
      IF (NTRAN.EQ.0) GO TO 10C1
      TEST=CHIMAX*E5*EMIS(JSUBX,K,J)/QSS
      IF(NTRAN.EQ.1.AND.TEST.LT.EPS) GO TO 76
      IF(NZERO.EQ.1) NTRAN=0
      IF(NTRAN.GT.C) GO TO 1
1001  CONTINUE
      NZERC=C
      QSS=EMIS(JSUBX,K ,J)
      ACC1=C.
      ACC2=C.
      ACC3=C.
      1  CONTINUE
      ACC4=C.
      ACC5=C.
      ACC6=C.
      ACC7=C.
      ACC8=C.
      ACC9=C.
      Z1=HEFF(JSUBX ,K ,J)/52E0.-ZKEEP
      Z2=HEFF(JSLBX , K ,J)/52E0.+ZKEEP
C
C     ESTIMATE AN EFFECTIVE HMIX FOR THE LIFETIME OF THE PUFF
C
      MN=M-N+1
      NT=N-1
      ZSS=HEFF(JSUBX,K ,J)
      IF(KSTAB.GT.C)GO TC 121
      DO10C IK=1,N
      JIK=JSLB(M-N+IK)
100   IF(JS(JIK).EQ.5)JS(JIK)=4
      IF(N.EQ.1) HLID=FMIX(JSLB(M))
      IF(N.EQ.1) GO TO 120
C     RISING LID CHECK
      DO 1C1 IN=1,NT
      IF(HMIX(JSLB(MN-1+IN)).GT.HMIX(JSUB(MN+IN))) GO TO 105
101  CONTINUE
      HLID=FMIX(JSLB(M))
      GO TC 120
C
C     105 CONTINUE
C     FALLING LID
      DO 1C6 IN=1,NT
      IF(HMIX(JSLB(MN-1+IN)).LT.HMIX(JSUB(MN+IN))) GO TO 110

```



## ITRAN (Contd.)

```

106 CCNTINLE
  IN=0
  HLID=FMIX(JSLB(M))
  L=JS(JSUB(MN))
  T=1.+TZ
  IF((ZSS+SIGZ(L,T)).GE.HMIX(JSLB(MN))) GO TO 109
  DO 108 IN=1,N
  T=IN      + TZ
  L=JS(JSUB(MN+IN))
  IF((ZSS+2*SIGZ(L,T)).GE.HMIX(JSUB(MN+IN)))GO TO 109
108 CCNTINLE
  GC TO 120
109 HLID=FMIX(JSLB(MN+IN))
  GC TO 120
110 CCNTINLE
C   RIGHT NOW I DO THE PROBLEMS OF RISING-FALLING AND
C   FALLING-RISING LIDS. FOR NOW, MAKE HLID THE MAX VALUE
C   OF HMIX DURING THE PLFF LIFETIME.
C
  HLID=FMIX(JSLB(MN))
  DO 115 IN=2,N
  HL=HMIX(JSLB(M-N+IN))
115 IF(HL.GT.HLID) HLID=HL
120 CCNTINLE
  GC TO 140
121 KFUME=C
C   PLUME IS INITIALLY ABOVE LIC. AS LONG AS HLID.LT.HEFF
C   USE UNREFLECTED STABLE PLUME. IF AT HOUR NFUME,HLID.GT.HEFF,HAVE
C   FUMIGATION AND SET HLID=MAX OF LIDS. CALCULATE CHI AS
C   FOLLOWS*REFLECTED PLUME ABOUT LID HEIGHT.JSTAB=5 FOR HOURS
C   BEFORE HOUR NFUME. STAB=MASTER FILE VALUE FOR HOURS.GT.NFUME
C   IF STACK BELOW LIC AND PLUME RISE ABOVE,ASSUME INFINITE LIC
C   AND MIXING ACCORDING TO STABILITY CLASS 4
  NFUME=N
  JSSS=4
  IF(KSTAB.EQ.2) GC TO 130
  JSSS=5
  IF(N.EQ.1) GC TO 130
  DO 123 IK=1,N
  MN=M-N+IK
123 IF(ZSS.LT.FMIX(JSLB(MN))) GC TO 124
  GC TO 130
124 KFUME=1
C   FIND MAX LID AFTER FUMIGATION BEGINS
  HLID=FMIX(JSLB(MN))
  DO 125 IX=IK,N
  HL=HMIX(JSLB(M-N+IX ))
125 IF(HLIC.LT.HL) HLID= HL
  NFUME=IK-1
130 DO 131 IK=1,NFUME
131 JS(JSLB(M-N+IK))=JSSS
  IF(KFUME.EQ.C)HLID=1.E4
140 CCNTINLE
  Z3=(2.*HLID -HEFF(JSUBX ,K ,J))/5280.-ZKEEP
C   IF PLUME BELOW LIC AND RECEPTOR ABOVE,CHI=0.AND GC TO 61
  IF(528C.*ZKEEP.GT.HLIC.AND.KSTAB.EQ.O)GCTC61
  HLI=HLID/528C.

```

ITRAN (Contd.)

```

      IF(KFLME.GT.C.ANC.ZKEEP.GT.HLI ) GO TO 61
      IF(NIRAN.GT.C) GO TO 998
      ZA=Z1
      ZB=Z2
      ZC=Z3
      TY=TX
C22222
C CHECK BY COMPARISON WITH FLUME IN STEADY STATE
  XPP=C.
  YPP=C.
  XK=X
  YK=Y
  X=X-TX*U(JSUEX      )
  Y=Y-TY*V(JSUEX      )
  JLIM=M-N+2
  IF(JLIM.GT.M)GO TO 7
  DO 6 JJ=JLIM,M
  JSUBJ=JSUB(JJ)
  XPP=XPP+U(JSLEJ)
  YPP=YPP+V(JSLEJ)
6 CONTINUE
7 CONTINUE
  XP=XPP+U(JSUEX      )
  YP=YPP+V(JSUEX      )
  DL=SQRT((X-XP)*(X-XP)+(Y-YP)*(Y-YP))
  DT=SQRT((X-XPP)*(X-XPP)+(Y-YPP)*(Y-YPP))
  SLC=(YF-YPP)/(XP-XPP+.0001)
  BC=YF-SLC*XP
  SLOR=-1./(SLC+.0001)
  BR=Y-SLOR*X
  XI=(BC-BR)/(SLC-SLOR)
  XI=-XI
  YI=BC+SLC*XI
  DMIN=SQRT((XI-X)*(XI-X) + (YI-Y)*(YI-Y))
  D1=SQRT((XI-XPP)*(XI-XPP) + (YI-YPP)*(YI-YPP))
  D2=SQRT((XI-XP)*(XI-XP) + (YI-YP)*(YI-YP))
  D3=HSEAR(JSUBX      )
  X=XK
  Y=YK
  NDTL=C
  IF(D1.GT.D2.ANC.D1.GT.D3) GO TO 302
  IF(D2.GT.D1.ANC.D2.GT.D3) GO TO 303
  DMIN=DMIN
  TMIN=(N-1) + D1/D3
  GO TO 305
302 DMIN=D1
  NDTL=1
  TMIN=N
  GO TO 305
303 DMIN=D2
  NDTL=1
  TMIN=N-1
305 CONTINUE
  JSTAE=JS(JSUE(M))
  IF(TMIN.LE..001) TMIN=.01
  T=TMIN
  SY=SIGY(JSTAB,T+TY)
  SZ=SIGZ(JSTAB,T+TZ)
  E1=.000001

```

## ITRAN (Contd.)

```

E2=.CCCC0C1
E3=.CCCC0C1
EXPZ1=(-.5*(Z1/SZ)*(Z1/SZ))
EXPZ2=(-.5*(Z2/SZ)*(Z2/SZ))
EXPZ3=(-.5*(Z3/SZ)*(Z3/SZ))
IF(EXPZ1.GT.-2C.) E1=EXP(EXPZ1)
IF(EXPZ2.GT.-2C.) E2=EXP(EXPZ2)
IF(EXPZ3.GT.-2C.) E3=EXP(EXPZ3)
DENGM=6.284*WSAVE*SY*SZ
CHIMAX=EMIS(JSLBX ,K ,J)*(E1+E2+E3)*.38122E-4/DENGM
E4=DMIN/SY
TTT=N-1 +TY
TT=N +TY
IF(N.LT.2) GC TC 9
E5=DT/SIGY(JSTAB,TTT)
IF(E5.LT.E4) E4=E5
9 E5=DL/SIGY(JSTAB,TT)
IF(E5.LT.E4) E4=E5
E5=0.
IF(E4.LT.4.) E5=EXP(-.5*E4*E4)
CHIME5=CHIMAX*E5
IF(CHIME5.LT.EPS)NZERO=1
CY=2.*SY
IF(NDTL.EQ.1.AND.WSBAR(JSLB(M-N+1)).GT.3..AND.DT.GT.CY
X .AND.DL.GT.CY) NZERO=1
C DCWNWIND SCURCES NEGLECTED UNDER SPECIAL CONDITIONS. CHECK FOR
C SENSITIVITY
IF(NZERO.EQ.1) GC TC 61
IF(KPR.GT.KMAX) GC TO 311
KPR=KPR+1
PRINT 404,M,N,I,HLID ,KFUME,NTRAN
404 FORMAT(3X,'IN TRAN. M,N,I=',3I5,5X,'HLIC=',E12.3,
X 3X,'KFUME=',I4,3X,'NTRAN=',I3)
PRINT 999,N,M,Z1,Z2,Z3,WSAVE,X,T,JSTAB,SY,SZ
999 FORMAT(3HON=I5,3H M=I5,4H Z1=E10.1,4H Z2=E10.1,4H Z3=E10.1/
17H WSAVE=F10.1,3H X=F10.1,3H T=F10.2/
27H JSTAB=I5,4H SY=E15.5,4H SZ=E15.5)
PRINT 410,CHIME5,QSS,E1,E2,E3
410 FORMAT(10X,'CHIMAX*E5=',E10.2,5X,'QSS=',E12.2,5X,'E1,E2,E3=',
X 3E10.2)
PRINT 413,KSTAE,U(1),V(1),X,Y,TX
413 FORMAT(10X,'KSTAB,U,V,X,Y,TX=',I5,5E10.2)
PRINT 401,CMIN,TMIN,E5,CL,DT
401 FORMAT(5X,'IN TRAN. DMIN,TMIN,E5,DL,DT=',5E12.2)
C33333
311 CCNTINUE
A=N-1
B=N
XINT=.1
AMAG=.C01
EPSIL=1.
EPSIL=.1
Z=Z1
CALL INTEG1(KERN,A,B,XINT,AMAG,EPSIL,ACC1)
GC TC 20
20 CCNTINUE
ACC2=ACC1*E2/E1
IF( E2/E1.GT..7)GC TC 40
Z=Z2

```

ITRAN (Contd.)

```

      CALL INTEG1(KERN,A,B,XINT,AMAG,EPSIL,ADC2)
40  CCNTINLE
      IF(E3/E1.LT..05)GC TO 60
      ADC3=ACD1*E3/E1
      IF(E3/E1.GT..7 )GC TO 60
      Z=Z3
      CALL INTEG1(KERN,A,B,XINT,AMAG,EPSIL,ADC3)
598 CCNTINLE
60  CCNTINLE
      SYY=SIGY(JSTAB,TMIN+TY)
      SZZ=SIGZ(JSTAB,TMIN+TZ)
      SZQ=SZZ*SZZ
      HLI=HLID/528C.
      IF(KPR.LT.KMAX)PRINT 407,Z1,ZA,Z2,ZB,Z3,ZC,ACD1,ADC2,ADD3,SZQ
407 FCRMAT(3X,10E12.2)
      IF(NTRAN.EC.C) GC TO 660
      EXPC=-.5*(Z1*Z1-ZA*ZA)/SZC
      IF(EXPC.LE.-20) EXPC=-10.
      ACCA=ACD1
      ADD1=ACD1*EXP(EXPC)
      EXPO=-.5*(Z2*Z2-ZE*ZB)/SZC
      IF(EXPC.LE.-20) EXPC=-10.
      ACCB=ACD2
      ACC2=ACD2*EXP(EXPC)
      EXPC=-.5*(Z3*Z3-ZC*ZC)/SZC
      IF(EXPC.LE.-20) EXPC=-10.
      ACCC=ACD3
      IF( ACC3.LT.1.E-4) GC TO 66C
      ACC3=ACD3*EXP(EXPC)
      KU=KMAX
      IF(KPR.LE.KU)PRINT 408,ACC1,ACC2,ADD3
408 FCRMAT(75X,3E12.2 /)
660 CCNTINLE
C44444
      IF(ACC3.LT.1.E-5) GC TO 61
      ZLBG=Z3+2.*ZKEEP
      ZGAL=Z2+2.*(HLI -ZKEEP)
      ZL3=ZLBG+2*HLI-2.*ZKEEP
      G3=ZGAL+2.*ZKEEP
      ZL4=G3+2.*(HLI-ZKEEP)
      G4=ZL3+2.*ZKEEP
      IF(ACC3.LE..00001) GO TO 61
      EXPC= .5*(Z3*Z3- ZLBG**2)/SZC
      IF(EXPC.LE.-20.) GO TO 61
      ACC4=ACD3*EXP(EXPC)
      EXPC= .5*(Z3*Z3- ZGAL**2)/SZC
      IF(EXPC.LE.-20.) GO TO 61
      ACC5=ACD3*EXP(EXPC)
      EXPC= .5*(Z3*Z3- ZL3 **2)/SZC
      IF(EXPC.LE.-20.) GO TO 61
      ACC6=ACD3*EXP(EXPC)
      EXPO= .5*(Z3*Z3- G3**2)/SZQ
      IF(EXPC.LE.-20.) GO TO 61
      ACC7=ACD3*EXP(EXPC)
      EXPO= .5*(Z3*Z3- ZL4**2)/SZQ
      IF(EXPC.LE.-20.) GO TO 61
      ACC8=ACD3*EXP(EXPC)
      EXPO= .5*(Z3*Z3- G4**2)/SZQ
      IF(EXPC.LE.-20.) GO TO 61

```

ITRAN (Contd.)

```

      ADD9=ACD3*EXP(EXFC)
    61 CONTINUE
C55555
      TRAN=ACD1+ACC2+ACC3+ACD4+ADC5+ACC6+ADC7+ADC8+ACD9
C      IF(KPR.GT.KMAX)GCTC 416
C      ANSW=TRAN*.38E-4*EMIS(JSUB(M-N+1),K,J)
C      TIN=(TIN-TLEFT(YYYY))/100.
C      IF(ANSW.EQ.0.) GC TO 416
C      PRINT 415,ANSW,K,J,TIN
C 415 FGMAT(10X,'IN TRAN. CONCENTRATICN,PPM,=',E10.2,2I10,
C      2 10X,'TIME IN TRAN(SEC)=',E10.2)

    416 CONTINUE
      IF(CHIMAX*E5.LT.EPS) GC TO 70
      IF(ACC3.LT.1.E-5) GC TO 7C
C
      IF(KPR.GT.KU) GC TO 7C
      PRINT 409,ADC4,ACC5,ADD6,ADD7,ACC8,ADC9
    409 FGMAT(3X,6E12.2)
    7C CONTINUE
    700 CONTINUE
      DC 71 IK=1,MX
    71 JS(IK)=JSSS(IK)
C      JS ARRAY AS BEFCRE.
      Z=ZKEEP
      IF(NTRAN.EQ.0) GC TO 75
      ADD1=ACDA
      ACC2=ACDB
      ACC3=ACDC
    75 CONTINUE
      RETURN
    76 TRAN=C.
      ACDA=ACD1
      ACCB=ACD2
      ACCC=ACD3
      GC TO 700
      END

```

SIGY

```

      FUNCTION SIGY(J,THCUR)
C
      COMMON/WDUN/MSAVE
      DIMENSION A(7),B(7)
      DIMENSION C(5),D(5)
C
      DATA C/155.,100.,68.,50.,34./, C/.91,.92,.93,.90,.93/
      DATA A/2.1511,1.5454,1.0606,.68465,.59366,.59366/
      DATA B/.87326,.88261,.89031,.88866,.89138,.89138/
      DATA CCNV/.000621371/
C      J=1,2,3,4,5 ARE CLASSES B,C,D,E,F
C      XX AND SIGXY ARE IN MILES
      TSEC=THOUR*3600.

```

SIGY (Contd.)

```

C      SIGY=(A(J)*TSEC**B(J))*CONV
C  WSAVE IS MEAN WIND SPEED UP TO TIME T.
      XX=WSAVE*THCUR*1.609
      JJ=MAXC(J-1,1)
      SIGXY=C(JJ)*(XX**C(JJ))*0.000889
C  .000889=(1/1609.)*(6**.2)
      SIGY=AMAX1(SIGY,SIGXY)
C
C  DISPERSION COEFFICIENTS BASED ON TURNER WORKBOOK.
C  WHERE THE SIGMAS GIVEN IN THE WORKBOOK FOR
C  TEN MINUTE SAMPLINGS ARE SCALED TO 1 HOUR
C  AVERAGES BY A FACTOR OF 1.43
      RETURN
      END

```

SIGZ

```

      FUNCTION SIGZ(J,THCUR)
C
C  COMMON/WDCN/WSAVE
C  DISPERSION COEF. BASED ON TURNER WORKBOOK
C  J=1,2,3,4,5 ARE CLASSES B,C,C,E,F
C  X AND SIGZ ARE IN MILES
      DIMENSION C(3,5),D(3,5)
      REAL TIME(7),A(7,6),B(7,6)
C
      DATA TIME/C.,300.,1000.,3000.,10000.,30000.,172000./
      DATA A/.17122,.27668,.41219,.51921,.50963,.47639,.52140,
1      .11062,.39953,.41219,.57145,.76485,.71936,.88886,
2      .01338,.16640,.41219,1.0813,1.9467,2.3901,1.8877,
3      .01338,.16640,.41219,2.2830,2.9850,3.8684,6.7452,
3      .01338,.16640,.41219,2.3333,5.7990,16.897,20.673,
3      .01338,.16640,.41219,5.6801,14.599,64.577,54.149/
      DATA B/1.2098,1.0572,.92365,.84130,.79689,.76308,.69839,
1      1.2864,.95275,.92365,.82449,.72571,.69082,.60486,
2      1.5922,1.1195,.92365,.73217,.59047,.51700,.49583,
3      1.5922,1.1195,.92365,.63883,.53708,.45686,.33677,
4      1.5922,1.1195,.92365,.63646,.46497,.29621,.21517,
5      1.5922,1.1195,.92365,.55016,.37541,.16667,.12177/
      DATA C/110.,110.,110.,60.,60.,60.,33.,33.,40.,21.5,21.5,36.,14.,
114.,23.5/
      DATA D/1.,1.09,1.09,.92,.92,.92,.80,.61,.53,.70,.56,.35,.78,.53,
1.30/
      DATA CCNV/.000621371/
      DATA KPR/0/

      TSEC=THOUR*3600.
      DO 10 N=2,7
      IF(TSEC.LE.TIME(N))GO TO 20
10  CONTINUE
20  CONTINUE
      N=N-1
      KMAX=C
      IF(KPR.GT.KMAX) GO TO 1
      KPR=KPR+1
      TIN=TLEFT(YYYY)

```

SIGZ (Contd.)

```

      SIGZ=(A(J,N)*TSEC**B(J,N))*CONV
      TIN=(TIN-TLEFT(YYYY))/100.
      PRINT 401,TIN
401  FCRMAT(10X,' IN SIGZ.TIN=', E12.2)
      RETURN
1   CONTINUE
      SIGZ=(A(J,N)*TSEC**B(J,N))*CCNV
C   TURNER TEST EQUATION
C   SIGZ=(1.17518*TSEC**.72012)*CONV
      XX=HSAVE*THOUR*1.6C9
      I=1
      IF(XX.GT.1.) I=2
      IF(XX.GT.1C.) I=3
      JJ=MAXC(J-1,1)
C
C
C   SIGTZ=(C(I,JJ)*XX**D(I,JJ))*0C0889
C   .000889=(1/1609*(6C/10)**.2
      SIGZ=AMAX1(SIGZ,SIGTZ)
      RETURN
      END

```

SIGX

```

      FUNCTION SIGX(J,THCUR)
C
      SIGX=SIGY(J,THCUR)
C
      RETURN
      END

```

SIGGZ

```

      FUNCTION SIGGZ(THCUR)
      CCMCN/STABIL/NSTB,SIGXC,SIGZC
      SIGGZ=SIGZ(NSTB,THOUR)-SIGZC
      RETURN
      END

```

SIGGX

```

      FUNCTION SIGGX(THCUR)
      CCMCN/STAEIL/NSTB,SIGXC,SIGZC
      SIGGX=SIGX(NSTB,THCUR)-SIGXC
      RETURN
      END

```

JSUB

```

      FUNCTION JSUB(J)
C
      CCMCN/TIME/ MMAX,NMAX,M,N
C
      JSUB=MCD(J-1,NMAX)+1
      RETURN
      END

```

ABSF

```

      FUNCTION ABSF(X)
      ABSF=ABS(X)
      RETURN
      END

```

KERN

```

      SUBROUTINE KERN(T,FT)
C
      CCMCN/KTRCUE/KTRC
      CCMCN/SUECO/TX,TY,TZ,DX,DY,DZ
      CCMCN/HALF/THALF
      CCMCN/TIME/ MMAX,NMAX,M,N
      CCMCN/KERNEL/X,Y,Z,U(24),V(24),W(24),JS(24),HMIX(24),WSBAR(24),WZ
C
      DATA CCEF/15.748/
      DATA KPK/0/
C
      KMAX=1000
      IF(T.EQ.0.)GO TO 30
      USUM=C.
      VSUM=C.
      WSUM=C.
      SXSUM=C.
      SYSUM=C.
      SZSUM=C.
      JLIM=M-N+2
      IF(JLIM.GT.M)GO TO 20
      DO 10 J=JLIM,M
      JSUBJ=JSUB(J)
      TIME1=J-(M-N+1)+(T-(N-1))
      TIME2=TIME1-1.
      USUM=USUM+L(JSUBJ)
      VSUM=VSUM+V(JSUBJ)
      WSUM=WSUM+W(JSUBJ)
      SXSUM=SXSUM+(SIGX(JS(JSUBJ),TIME1)-SIGX(JS(JSUBJ),TIME2))
      SYSUM=SYSUM+(SIGY(JS(JSUBJ),TIME1)-SIGY(JS(JSUBJ),TIME2))
      SZSUM=SZSUM+(SIGZ(JS(JSUBJ),TIME1)-SIGZ(JS(JSUBJ),TIME2))
10 CONTINUE
20 CONTINUE
      JSUBJ=JSUB(M-N+1)
      TDIF=T-(N-1)
      TDX=TDIF+TX
      TCY=TDIF+TY
      TCZ=TDIF+TZ

```



KERN (Contd.)

```

      JSK=JS(JSUBJ)
      IF(KTRC.EQ.1) PRINT 400,T,TX,TDIF,TDX,JSK
400  FCRMAT(10X,'KERN. T,TX,TDIF,TDX,JSK=',4E12.2,I4)
      SX=SXSUM+SIGX(JS(JSUBJ),TCX)
      SY=SYSUM+SIGY(JS(JSUBJ),TCY)
      SZ=SZSUM+SIGZ(JS(JSUBJ),TCZ)
      T1=(X-LSUM-U(JSUBJ)*TDX )/SX
      T2=(Y-VSUM-V(JSUBJ)*TDY )/SY
      T3=(Z-WSUM-W(JSUBJ)*TDZ )/SZ
      EXPCN=-(T1*T1+T2*T2+T3*T3)*.5
      IF(ABS(EXPCN).GT.20)GO TO 30
      TGF=EXP(EXPCN)
      BCT=CCEF*SX*SY*SZ
      FT=TCP/BOT
      FT=FT*EXP(-.693*T/THALF)
      RETURN
30  CONTINUE
      FT=C.
      RETURN
      END

```

INTEG1

SUBROUTINEINTEG1 (FFUNC,XL,XU,DXINT,AMAG,EPS,VALU)

C		2
C	ROUTINE TO EVALUATE INTEGRAL OF F(X) BETWEEN	2
C	THE LIMITS XL AND XU BY VARIABLE SIMPSCNS	2
C	RULE.	2
C		2
	JDB	2
	VALU=C.	3
	XZERC=XL	4
	DX=DXINT	5
	CALLFFUNC(XZERC,FZERC)	6
10	CONTINUE	7
	IF(XU-(XZERO+4.*DX))20,30,30	8
20	CONTINUE	9
	DX=(XL-XZERO)/4.	10
30	CONTINUE	11
	CALLFFUNC(XZERC+DX,F1)	12
	CALLFFUNC(XZERC+2.*DX,F2)	13
	CALLFFUNC(XZERC+3.*DX,F3)	14
	CALLFFUNC(XZERC+4.*DX,F4)	15
	S1=2.*DX*(FZERC+4.*F2+F4)/3.	16
	S2=DX*(FZERC+4.*F1+2.*F2+4.*F3+F4)/3.	17
	RATIC=ABS(S2-S1)/(AMAX1(ABS(S2),AMAG*1.E-4)*EPS)	
	IF(RATIC-1.)60,40,40	19
40	CONTINUE	20
C		20
C	CYCLE REJECTED. REDUCE DX AND TRY AGAIN	20
C		20
	DX=DX/1.5	21
	GO TO 30	22
60	CONTINUE	23
C		23
C	CYCLE ACCEPTED.	23
C		23
	ADD=S2+(S2-S1)/15.	24

INTEG1 (Contd.)

VALU=VALU+ACC	25
XZERC=XZERC+4.*DX	26
FZERC=F4	27
IF(XZERO.GE.XU)RETURN	
IF(ABS(XZERO-XL).LE.1-E-4)RETURN	
IF(RATIO-.5)100,90,90	32
90 CCNTINLE	33
DX=DX/1.5	34
GOTG1C	35
100 CCNTINLE	36
IF(RATIO-.01)110,10,10	37
110 DX=DX*1.5	38
GOTG10	39
END	

GUESS2

SUBROUTINE GUESS2(FCTN,PGGA,PGGB,PZERC,TOL1, 1 NITMAX,NFLAG1,NFLAG3,NFLAG4)	
C	
C      CCCC   MODIFIED FOR PZERC .GT.0.   ONLY	
C                          SEE STATEMENT 16	
C	
C      THIS PROGRAM HAS BEEN TRANSLATED FOR THE      360/50	2
C      WITH RELEASE 1-A OF THE MCD-50 TRANSDECK	
C	
C  JDB	2
C      DIMENSION PGG(50),ERR(50)	3
C      THIS SUBROUTINE FINDS A ZERO OF THE FUNCTION FCTN(X)	3
C      FCTN MUST BE DEFINED BY AN EXTERNAL FUNCTION STATEMENT.	3
C                          PGGA AND PGGB ARE TWO INITIAL GUESSES	3
C                          TOL1 = ALLOWABLE DEVIATION FROM ZERO IF NFLAG4=1	3
C                          = ALLOWABLE DIFFERENCE BETWEEN LAST TWO PZERO	3
C                          VALUES IF NFLAG4 = -1	3
C                          NITMAX = MAX NO. OF ITERATIONS	3
C                          NFLAG3 = 1 IF WANT PRINT OUT VIA THE SUBROUTINE	3
C                          NFLAG3 = 0 IF NO PRINT OUT DESIRED	3
C                          INITIALLY CODE SETS NFLAG1=0      IF	3
C      A DIVIDE CHECK OR EXCESS NO. OF ITERATIONS OCCURS, SETS NFLAG1=1	3
C	
C      DELTP=ABS(PGGA-PGGB)	
C      NFLAG1=0	4
C      NIT=2	5
C      PGG(1)=PGGA	6
C      PGG(2)=PGGB	7
C      I=3	8
C      IA=1	9
C      IB=2	10
C      ERRA=FCTN(PGGA)	11
C      ERR(1)=ERRA	12
C      IF(NFLAG4) 2,2,4	13
2 GC TC 5	14
4 VALUE=ABSF(ERRA)	15
IF(VALUE-TCL1)400,400,5	16
400 PGGB=PGG(1)	17
NIT=1	18
ERRKB=ERRA	19

GUESS2 (Contd.)

	GC TC 100	20
5	ERRB=FCTN(PGGB)	21
	IF(NFLAG4) 6,6,8	22
6	VAL=PGG(IA)-PGG(IE)	23
	VALUE=ABSF(VALUE)	24
	GC TC 9	25
8	VALUE = ABSF(ERRE)	26
9	IF(VALUE-TCL1) 100,100,10	27
10	CONTINUE	28
	VALUE=ABSF(ERRA-ERRB)	29
	IF(VALUE-1.E-28) 75,75,15	30
15	PGG(I)=PGG(IE) - ERRB*(PGG(IA)-PGG(IE))/(ERRA-ERRB)	31
16	IF(PGG(I).LE.C.)PGG(I)=.001*DELTF	
20	ERRA=ERRB	32
	ERR(IE)=ERRB	33
	PGGB=PGG(I)	34
	I=I+1	35
	IA=I-2	36
	IB=I-1	37
	NIT=NIT+1	38
	IF(NIT-NITMAX) 5,5,70	39
C		39
	70 PRINT 71,NITMAX	40
	71 FORMAT(1H1,45H MAX. NO. ITER. FOR PZERO EXCEEDED,NITMAX = I5 ///	41
	NFLAG1 = 1	42
	GC TC 100	43
C		43
	75 CONTINUE	
	NFLAG1=1	46
	GC TC 100	47
C		47
	100 IF(NFLAG3) 80,80,101	48
	80 J=I-1	49
	ERR(J)=ERRE	50
	PZERC=PGGB	51
	GC TC 125	52
C		52
	101 PZERC=PGGB	53
	J=I-1	54
	ERR(J)=ERRE	55
	104 FORMAT ( ///// )	56
	105 FORMAT( 22F NC.OF ITERATIONS = I5 /// )	57
	115 FORMAT( 4X, 4H NIT ,9X, 6F GUESS , 16X, 6H ERRCR // )	58
	120 FORMAT(I8,2E20.8)	59
	125 RETURN	60
	END	

## APPENDIX B

Sample Problem

Sulfur dioxide values are estimated at 66 points on a 2 x 2-mi grid for January 15, 1967, in order to demonstrate the input/output aspects of the program. Figure titles are self-explanatory and refer to the basic text where applicable (Figs. B.1-B.7). Run time on the IBM 360/75 was 80 min.

A comment is worthwhile on Fig. B.7, which presents strip charts for observed and estimated SO<sub>2</sub> levels at TAM's 2-5. Two types of estimates are shown: (1) That from the nearest grid point in the sample problem for which all SO<sub>2</sub> values are calculated using TAM 4 winds with all receptors at 75 ft, and (2) values based on separate calculations employing actual receptor location and wind data for TAM's 2, 3, and 5. Although the wind field for the sample day is relatively uniform, calculations based on individual TAM data are superior to estimates derived from a single city-wide wind and receptor height. This is particularly noticeable for TAM 3, where the receptor is 180 ft high and 0.6 mile north of the nearest grid point in the sample problem. The effect of localized sources, particularly Union Station and the Merchandise Mart, is quite apparent when the wind is WNW. Furthermore, when the TAM 4 wind shifts to the direction band 253-266° at 7 mph after 8 p.m. (hour 20), the TAM 3 aerovane indicates slightly more southerly winds (236 to 263°) at 6 mph, which bring in large point sources along the southwest industrial corridor.

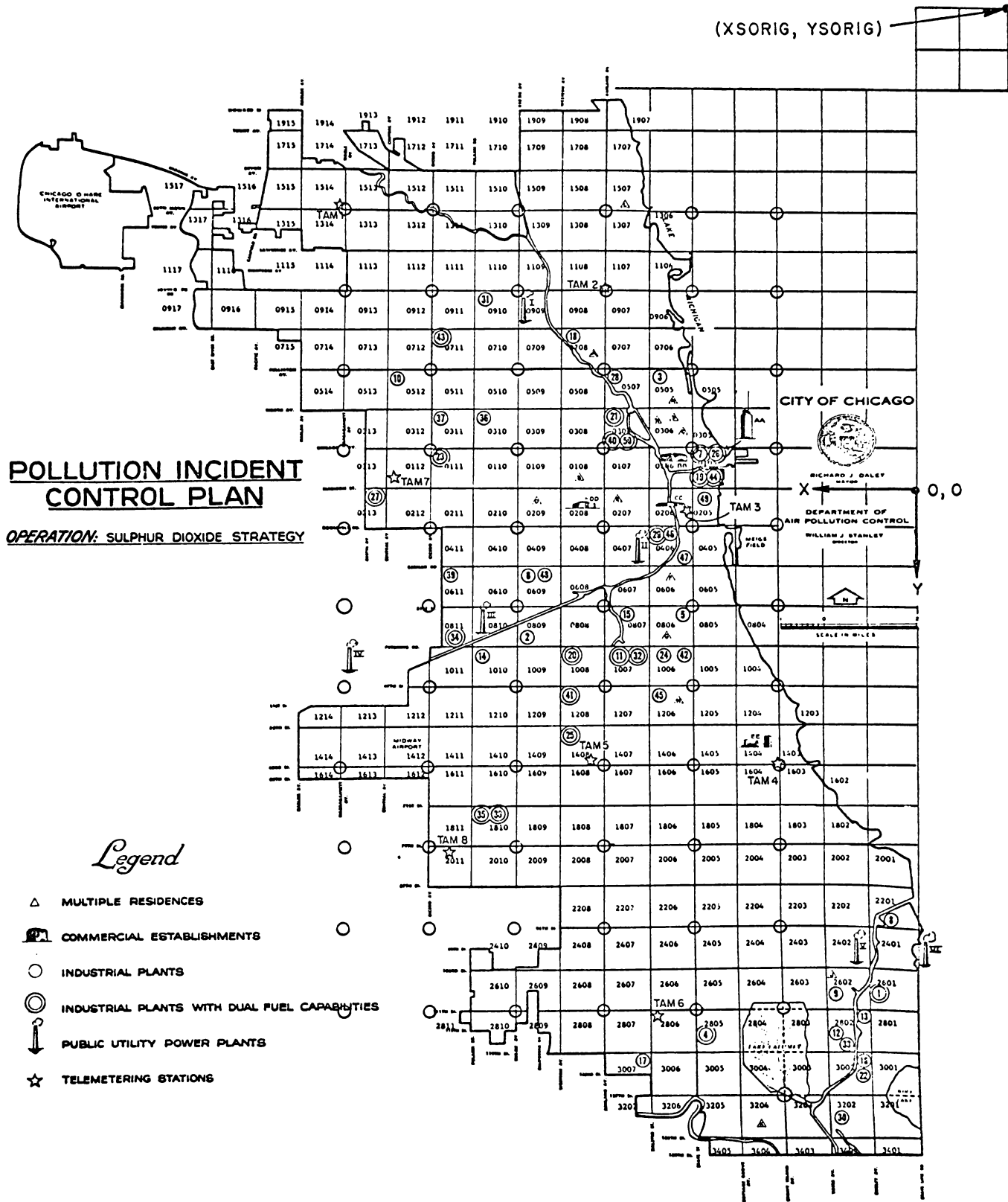


Fig. B.1. Chicago Map Showing Origin of Cartesian-coordinate System (0,0), Origin of Area-source Array (XSORIG, YSORIG) = (-2,-12), and 6 x 11 Receptor Grid Denoted by ⊕. TAM stations indicated by ☆. ANL Neg. No. 112-8979 Rev. 1.

```

JJR2 SAMPLE PROBLEM FOR TAM 4 JAN 15,1967
CPTLIST='PRINT';
DATE_LIMITS=1;
'67/01/15','67/01/15'
RECEPTCRS=1;
RECEPTOR='TAM_4'    X=7.4          , Y= -1.          , Z=0.;
CUT_STATIONS=11;
STATION='MIDWAY'    PARAMS=3;
PARAM='TEMP';
PARAM='WIND_DIR';
PARAM='WIND_VEL';
STATION='TURNER'    PARAMS=1;
PARAM='TURNER_C';
STATION='NGRCO'    PARAMS=1;
PARAM='MIX_HT';

STATION='TAM_1'    PARAMS=1;
PARAM='SO2';
STATION='TAM_2'    PARAMS=1;
PARAM='SO2';
STATION='TAM_3'    PARAMS=1;
PARAM='SO2';
STATION='TAM_5'    PARAMS=1;
PARAM='SO2';
STATION='TAM_6'    PARAMS=1;
PARAM='SO2';
STATION='TAM_7'    PARAMS=1;
PARAM='SO2';
STATION='TAM_8'    PARAMS=1;
PARAM='SO2';
STATION='TAM_4'    PARAMS=3;
PARAM='WIND_VEL';
PARAM='WIND_DIR';
PARAM='SO2';
END
STCP

```

Fig. B.2. Sample Problem: Input to APICS System. TAM 4 wind speed and wind direction selected for citywide grid.

//GO.FTC5FC01 DD \*

PGLC EMISSION DATA BASED ON JJR GRID											
0.	C.	C.	C.	0.	C.	0.	C.	C.	0.	C.	0.
0.	C.	C.	C.	0.	0.	0.	0.	0.	0.	0.	0.
0.	C.	C.	C.	0.	C.	0.	0.	0.	0.	0.	0.
0.	C.	0.	C.	0.	0.	0.	0.	0.	0.	0.	0.
0.	C.	C.	C.	0.	0.	0.	0.	0.	0.	0.	0.
0.	C.	C.	C.	0.	0.	0.	C.	C.	0.	0.	0.
0.	C.	C.	C.	0.	C.	0.	C.	C.	0.	0.	0.
0.	C.	C.	C.	0.	C.	0.	0.	0.	0.	0.	0.
0.	C.	C.	C.	0.	0.	0.	0.	0.	0.	0.	0.
0.	C.	0.	C.	0.	C.	0.	0.	0.	0.	C.	0.
57.	97.	C.	68.	141.	C.	0.	15.	1.	0.	0.	0.
0.	C.	C.	C.	0.	C.	0.	0.	1.	0.	0.	0.
0.	13.	C.	C.	0.	0.	0.	C.	0.	0.	0.	0.
0.	C.	C.	C.	0.	C.	0.	C.	0.	0.	0.	0.
0.	C.	C.	C.	0.	C.	0.	C.	0.	0.	0.	0.
122.	246.	8.	96.	151.	1.	40.	55.	1.	0.	0.	0.
0.	C.	C.	C.	0.	C.	0.	5.	0.	1.	7.	0.
0.	8.	C.	C.	0.	C.	0.	C.	0.	0.	0.	0.
0.	0.	C.	C.	0.	C.	0.	0.	0.	0.	0.	0.
0.	C.	C.	C.	0.	C.	0.	C.	0.	0.	0.	0.
148.	229.	C.	48.	93.	C.	93.	61.	0.	16.	41.	0.
4.	32.	5.	C.	11.	2.	8.	10.	0.	11.	20.	1.
0.	17.	C.	C.	0.	C.	0.	0.	0.	0.	0.	0.
0.	C.	C.	C.	0.	C.	0.	0.	C.	0.	0.	0.
0.	C.	0.	0.	0.	0.	C.	0.	0.	0.	0.	0.
190.	288.	1.	87.	102.	3.	108.	91.	3.	92.	81.	1.
8.	21.	2.	8.	19.	5.	3.	13.	1.	0.	7.	0.
0.	14.	C.	C.	1.	C.	C.	C.	0.	0.	0.	0.
0.	C.	C.	C.	0.	C.	0.	0.	0.	0.	0.	0.
0.	C.	C.	C.	0.	C.	0.	0.	0.	12.	67.	0.
328.	390.	3.	117.	166.	7.	150.	74.	4.	105.	113.	2.
44.	77.	2.	19.	315.	1.	7.	10.	0.	0.	0.	0.
0.	C.	C.	C.	6.	C.	0.	C.	0.	0.	0.	0.
0.	C.	C.	C.	0.	0.	0.	C.	0.	0.	0.	0.
0.	C.	C.	C.	0.	0.	C.	C.	0.	74.	206.	0.
150.	180.	5.	68.	64.	5.	40.	47.	7.	38.	55.	54.
34.	47.	5.	55.	33.	1.	10.	27.	C.	1.	11.	0.
5.	5.	C.	C.	2.	0.	0.	C.	0.	0.	0.	0.
0.	C.	C.	C.	0.	C.	0.	0.	0.	0.	0.	0.
0.	C.	0.	C.	0.	C.	0.	C.	0.	90.	233.	1.
101.	115.	42.	5.	113.	240.	81.	63.	12.	112.	102.	2.
35.	72.	69.	57.	36.	C.	25.	23.	C.	10.	29.	6.
0.	C.	C.	C.	0.	C.	0.	0.	0.	0.	0.	0.
0.	C.	C.	C.	0.	C.	C.	C.	C.	0.	0.	0.
0.	C.	C.	C.	0.	0.	0.	C.	C.	74.	212.	24.
33.	110.	720.	11.	62.	88.	64.	96.	21.	74.	72.	4.
31.	95.	82.	36.	40.	102.	27.	42.	4.	8.	52.	24.

Fig. B.3. Sample Problem: Input of Emissions from Area Sources. Read by Subroutine ADAT2. (See Section 3.1 and Figs. 7.2 and B.1). Units are  $10^4$  lb  $\text{SO}_2/\text{yr}$ . Three source classes: (NCL = 1, 2, 3) per square mile: low-rise residential/commercial, high-rise residential/commercial, industry. Origin of citywide Cartesian coordinate system shown in Fig. B.1. Origin of  $20 \times 50$  area-source grid is (XSORIG, YSORIG) = (-2, -12).

0.	C.	C.	C.	0.	C.	0.	C.	0.	0.	0.	0.
0.	C.	C.	C.	0.	0.	0.	0.	0.	0.	0.	0.
0.	0.	C.	C.	0.	0.	15.	220.	0.	37.	222.	50.
3.	116.	820.	82.	74.	7.	115.	58.	7.	63.	50.	55.
39.	87.	96.	67.	45.	9.	24.	24.	0.	0.	0.	0.
0.	C.	0.	0.	0.	C.	C.	0.	C.	0.	C.	0.
0.	C.	0.	C.	0.	0.	0.	0.	C.	0.	C.	0.
0.	C.	C.	0.	0.	C.	0.	440.	27.	13.	286.	1060.
16.	181.	82.	49.	98.	23.	54.	140.	81.	85.	97.	8.
54.	127.	50.	62.	144.	7.	40.	121.	1.	0.	0.	0.
0.	C.	C.	0.	0.	0.	0.	0.	0.	0.	0.	0.
0.	C.	C.	C.	0.	0.	0.	0.	0.	0.	0.	0.
0.	C.	C.	C.	0.	C.	0.	284.	60.	0.	315.	22.
16.	294.	12.	58.	224.	17.	94.	108.	16.	192.	126.	1.
117.	127.	69.	57.	113.	79.	23.	92.	82.	0.	0.	0.
0.	C.	C.	C.	0.	0.	0.	0.	0.	0.	0.	0.
0.	C.	C.	C.	0.	0.	0.	0.	0.	0.	0.	0.
0.	0.	C.	C.	0.	0.	11.	203.	11.	1.	102.	2.
8.	145.	20.	14.	56.	17.	49.	97.	61.	316.	86.	4.
76.	61.	91.	0.	0.	0.	0.	C.	0.	0.	0.	0.
0.	C.	C.	C.	0.	0.	0.	0.	0.	0.	0.	0.
0.	C.	C.	C.	0.	0.	0.	0.	0.	0.	0.	0.
0.	C.	C.	C.	0.	0.	0.	0.	0.	0.	0.	0.
0.	55.	222.	C.	53.	21.	4.	94.	29.	11.	36.	4.
11.	58.	63.	C.	0.	C.	0.	0.	C.	0.	0.	0.
0.	C.	C.	C.	0.	0.	0.	0.	0.	0.	0.	0.
0.	C.	C.	C.	0.	0.	0.	0.	0.	0.	0.	0.
0.	C.	C.	19.	172.	C.	64.	66.	0.	11.	192.	2.
7.	184.	68.	14.	66.	180.	4.	66.	640.	0.	42.	10.
0.	19.	3.	C.	0.	C.	0.	0.	0.	0.	0.	0.
0.	C.	0.	C.	0.	0.	0.	C.	0.	0.	0.	0.
0.	C.	C.	C.	0.	0.	0.	0.	0.	0.	0.	0.
0.	C.	C.	56.	179.	0.	264.	280.	70.	5.	63.	150.
0.	127.	946.	C.	93.	158.	5.	25.	280.	5.	56.	58.
0.	61.	64.	C.	12.	0.	0.	0.	0.	0.	0.	0.
0.	C.	C.	C.	0.	0.	0.	0.	0.	0.	0.	0.
0.	C.	0.	C.	0.	0.	0.	0.	0.	0.	0.	0.
10.	94.	C.	121.	239.	1.	219.	250.	0.	18.	41.	6.
11.	169.	4.	10.	60.	58.	4.	66.	31.	10.	67.	9.
9.	20.	2.	C.	17.	0.	0.	12.	C.	0.	3.	0.
0.	C.	C.	C.	0.	C.	0.	0.	C.	0.	0.	0.
0.	C.	C.	C.	0.	C.	0.	0.	C.	0.	0.	0.
18.	24.	C.	185.	248.	1.	146.	193.	1.	75.	44.	7.
79.	34.	7.	23.	38.	1.	84.	13.	88.	27.	13.	0.
3.	22.	C.	C.	21.	C.	1.	5.	0.	0.	21.	1.
0.	C.	C.	C.	0.	C.	0.	0.	0.	0.	0.	0.
0.	C.	C.	C.	0.	C.	C.	0.	C.	0.	5.	0.
101.	160.	C.	268.	186.	1.	102.	69.	2.	188.	81.	2.
107.	51.	C.	44.	28.	3.	76.	31.	0.	3.	9.	0.
1.	8.	0.	C.	14.	3.	0.	95.	0.	0.	4.	0.
0.	C.	0.	C.	0.	0.	0.	0.	0.	0.	0.	0.
0.	0.	0.	C.	0.	0.	C.	0.	0.	70.	172.	0.
114.	139.	1.	43.	75.	4.	122.	17.	1.	104.	60.	5.
54.	77.	5.	42.	26.	7.	7.	21.	72.	2.	20.	3.
0.	55.	C.	C.	0.	C.	0.	0.	C.	0.	0.	0.

Fig. B.3 (Contd.)



0.	C.	C.	C.	0.	0.	C.	0.	C.	0.	C.	0.
0.	C.	C.	C.	0.	C.	0.	1.	0.	59.	16.	6.
49.	85.	C.	114.	62.	36.	129.	56.	1.	12.	41.	2.
106.	37.	1.	62.	58.	1.	0.	6.	0.	0.	12.	0.
0.	11.	C.	C.	0.	C.	C.	C.	0.	0.	0.	0.
0.	C.	C.	C.	0.	0.	0.	0.	0.	0.	0.	0.
0.	C.	C.	C.	0.	0.	5.	9.	70.	36.	46.	2.
9.	11.	C.	28.	26.	5.	28.	9.	0.	11.	8.	0.
35.	14.	1.	7.	11.	C.	C.	0.	C.	0.	0.	0.
C.	C.	C.	C.	0.	C.	0.	0.	C.	0.	0.	0.
0.	C.	C.	C.	0.	C.	0.	0.	C.	0.	0.	0.
0.	C.	C.	C.	0.	C.	3.	11.	6.	5.	17.	5.
0.	5.	C.	C.	36.	5.	6.	20.	0.	10.	5.	0.
9.	12.	C.	C.	14.	C.	C.	7.	C.	0.	47.	0.
0.	C.	C.	C.	0.	0.	C.	0.	0.	0.	0.	0.
0.	C.	C.	C.	0.	C.	0.	0.	0.	0.	0.	0.
0.	C.	C.	0.	0.	C.	18.	17.	1.	1.	182.	52.
0.	C.	C.	C.	25.	8.	18.	25.	0.	20.	13.	0.
10.	19.	15.	20.	22.	C.	5.	8.	C.	3.	6.	0.
0.	C.	C.	C.	0.	0.	0.	0.	0.	0.	0.	0.
0.	C.	C.	C.	0.	C.	0.	0.	0.	0.	0.	0.
0.	C.	C.	C.	0.	C.	0.	26.	39.	0.	0.	404.
C.	1.	C.	C.	0.	C.	33.	65.	C.	13.	15.	0.
1.	13.	1.	3.	28.	1.	3.	11.	C.	0.	5.	0.
0.	34.	C.	C.	0.	C.	0.	0.	0.	0.	0.	0.
0.	C.	C.	C.	0.	0.	0.	0.	0.	0.	0.	0.
0.	C.	C.	C.	0.	0.	0.	10.	2.	0.	0.	490.
0.	C.	1.	C.	0.	0.	0.	7.	3.	12.	8.	0.
0.	33.	224.	C.	0.	0.	0.	0.	C.	0.	0.	0.
0.	C.	C.	C.	0.	C.	C.	C.	C.	0.	0.	0.
0.	C.	0.	C.	0.	C.	0.	0.	0.	0.	0.	0.
0.	C.	C.	C.	0.	C.	4.	2.	0.	2.	3.	0.
0.	4.	5.	C.	29.	C.	C.	2.	0.	0.	0.	0.
0.	3.	C.	C.	0.	0.	0.	0.	0.	0.	0.	0.
0.	C.	C.	C.	0.	0.	C.	C.	0.	0.	0.	0.
0.	C.	C.	C.	0.	0.	0.	0.	C.	0.	0.	0.
0.	C.	0.	C.	0.	0.	0.	2.	0.	0.	26.	69.
0.	C.	C.	C.	1.	C.	C.	44.	C.	0.	0.	0.
0.	C.	0.	C.	0.	0.	C.	0.	C.	0.	C.	0.
0.	C.	C.	C.	0.	0.	0.	0.	C.	0.	0.	0.
0.	C.	C.	C.	0.	C.	C.	C.	C.	0.	0.	0.
0.	C.	C.	C.	0.	C.	0.	0.	0.	0.	0.	0.
0.	C.	C.	C.	0.	C.	C.	0.	0.	0.	0.	0.
0.	C.	C.	C.	0.	C.	C.	0.	0.	0.	0.	0.
0.	C.	C.	C.	0.	C.	C.	0.	0.	0.	0.	0.

Fig. B.3 (Contd.)

```

SOURCE GRID DATA XSGRIC(IX),YSGRIC(IX),IX=1,16
1. 0. C. C. 1. 1. C. 1. 2. -1. 1. -1.
C. -1. -1. -1. 2. 0. -1. 0. 2. 1. -1. -1.
2. 2. 1. 2. C. 2. -1. 2.
SOURCE GRID DATA XSGRIC(IX),YSGRIC(IX),IX=17,48
6. -4. 4. -4. 2. -4. C. -4. -2. -4. -4. -4.
6. -2. 4. -2. 2. -2. C. -2. -2. -2. -4. -2.
6. 0. 4. C. -2. 0. -4. 0. 6. 2. 4. 2.
-2. 2. -4. 2. 6. 4. 4. 4. 2. 4. 0. 4.
-2. 4. -4. 4. 6. 6. 4. 6. 2. 6. 0. 6.
-2. 6. -4. 6.
SOURCE GRID DATA XSGRIC(IX),YSGRIC(IX),IX=49,88
14. -10. 10. -10. 6. -10. 2. -10. -2. -10. -6. -10.
-10. -10. 14. -6. 10. -6. 6. -6. 2. -6. -2. -6.
-6. -6. -10. -6. 14. -2. 10. -2. -6. -2. -10. -2.
14. 2. 10. 2. -6. 2. -10. 2. 14. 6. 10. 6.
-6. 6. -10. 6. 14. 10. 10. 10. 6. 10. 2. 10.
-2. 10. -6. 10. -10. 10. 14. 14. 10. 14. 6. 14.
2. 14. -2. 14. -6. 14. -10. 14.
MAX. EMISSION DATA ((EMAX(I,J),I=1,3),J=1,3)
1300. 2900. 7200.
1700. 5300. 13040.
1060. 2012. 3278.

```

Fig. B.4. Sample Problem: Input to Subroutine ADAT2. Coordinates of standard area-source overlay of Fig. 3.3 read by three separate statements in ADAT2. For example, coordinates of lower left-hand corner of square 48 (a 2 x 2-mi square) relative to central reference receptor are (-4,6). EMAX array is discussed in Sections 3.1 and 3.6. For example, maximum hourly industrial emission (NCL = J = 3) from 2 x 2-mi square in Chicago is 2012 lbSO<sub>2</sub>/hr.

JJR2 SAMPLE PROBLEM FOR TAM\_4 JAN 15,1967

	MIDWAY TEMP	MIDWAY WIND_DIR	MIDWAY WIND_VEL	TURNER TURNER_C	NORCO MIX_HT
67/01/15 0	29.000	300.000	13.000	4.000	3629.000
67/01/15 1	27.000	270.000	12.000	4.000	3339.000
67/01/15 2	25.000	280.000	10.000	4.000	3022.000
67/01/15 3	24.000	290.000	10.000	4.000	2909.000
67/01/15 4	22.000	320.000	10.000	4.000	2642.000
67/01/15 5	19.000	300.000	12.000	4.000	2339.000
67/01/15 6	17.000	310.000	9.000	4.000	2213.000
67/01/15 7	14.000	310.000	12.000	4.000	989.000
67/01/15 8	12.000	310.000	18.000	4.000	989.000
67/01/15 9	12.000	290.000	14.000	4.000	540.000
67/01/15 10	14.000	270.000	15.000	4.000	1191.000
67/01/15 11	15.000	270.000	12.000	4.000	1466.000
67/01/15 12	15.000	270.000	11.000	4.000	1485.000
67/01/15 13	16.000	280.000	11.000	4.000	1768.000
67/01/15 14	16.000	250.000	12.000	4.000	1749.000
67/01/15 15	17.000	280.000	10.000	4.000	1997.000
67/01/15 16	17.000	280.000	13.000	4.000	1959.000
67/01/15 17	16.000	270.000	13.000	4.000	1706.000
67/01/15 18	14.000	270.000	8.000	5.000	1381.000
67/01/15 19	13.000	270.000	7.000	5.000	1154.000
67/01/15 20	12.000	260.000	8.000	5.000	843.000
67/01/15 21	12.000	260.000	8.000	5.000	679.000
67/01/15 22	13.000	250.000	10.000	5.000	746.000
67/01/15 23	13.000	240.000	6.000	5.000	622.000

Fig. B.5. Tabular Printout of Meteorological and Air Quality Data. Missing mixing height at hour 8 (9 a.m.) is automatically set at previous value of 989 ft. TAM 4 wind speed and wind direction are used in this problem.

TAM_1 SO2	TAM_2 SO2	TAM_3 SO2	TAM_5 SO2	TAM_6 SO2
0.0	0.010	0.170	0.150	0.0
0.0	0.020	0.170	0.120	0.0
0.0	0.010	0.200	0.090	0.0
0.0	0.010	0.160	0.030	0.0
0.0	0.010	0.150	0.040	0.0
0.0	0.040	0.170	0.050	0.0
0.0	0.060	0.250	0.030	0.0
0.0	0.050	0.280	0.030	0.0
0.0	0.040	0.260	0.040	0.0
0.0	0.040	0.310	0.050	0.0
0.0	0.040	0.330	0.070	0.0
0.0	0.040	0.310	0.120	0.0
0.0	0.040	0.290	0.090	0.0
0.0	0.040	0.300	0.110	0.0
0.0	0.030	0.300	0.110	0.0
0.0	0.040	0.310	0.060	0.0
0.0	0.040	0.300	0.090	0.0
0.0	0.040	0.360	0.120	0.0
0.0	0.060	0.350	0.080	0.0
0.0	0.100	0.480	0.080	0.0
0.0	0.090	0.560	0.070	0.0
0.0	0.110	0.470	0.050	0.0
0.0	0.090	0.530	0.050	0.0
0.010	0.070	0.390	0.040	0.020

Fig. B.5 (Contd.)

	TAM_7 SO2	TAM_8 SO2	TAM_4 WIND_VEL	TAM_4 WIND_DIR	(OBS) TAM_4 SO2	(EST) TAM_4 SO2
67/01/15 0	0.0	0.010	10.800	279.000	0.100	0.074
67/01/15 1	0.010	0.020	10.300	285.000	0.080	0.106
67/01/15 2	0.010	0.030	9.900	290.000	0.080	0.116
67/01/15 3	0.010	0.030	8.900	303.000	0.090	0.155
67/01/15 4	0.010	0.030	9.900	296.000	0.110	0.149
67/01/15 5	0.020	0.020	9.500	289.000	0.130	0.229
67/01/15 6	0.030	0.010	9.900	291.000	0.110	0.241
67/01/15 7	0.030	0.020	10.900	286.000	0.110	0.219
67/01/15 8	0.030	0.040	12.300	284.000	0.170	0.207
67/01/15 9	0.030	0.040	11.900	284.000	0.150	0.296
67/01/15 10	0.030	0.040	11.700	281.000	0.150	0.186
67/01/15 11	0.030	0.040	12.400	278.000	0.120	0.147
67/01/15 12	0.030	0.040	11.800	277.000	0.120	0.148
67/01/15 13	0.030	0.040	10.300	278.000	0.130	0.159
67/01/15 14	0.030	0.040	10.200	282.000	0.130	0.197
67/01/15 15	0.020	0.040	10.200	274.000	0.160	0.139
67/01/15 16	0.030	0.040	10.300	283.000	0.170	0.215
67/01/15 17	0.040	0.040	8.800	285.000	0.190	0.241
67/01/15 18	0.050	0.020	7.900	280.000	0.270	0.226
67/01/15 19	0.060	0.010	7.100	265.000	0.230	0.171
67/01/15 20	0.080	0.020	7.300	261.000	0.150	0.180
67/01/15 21	0.070	0.040	7.200	266.000	0.160	0.199
67/01/15 22	0.070	0.050	8.000	266.000	0.150	0.085
67/01/15 23	0.070	0.040	6.600	253.000	0.110	0.092

Fig. B.5 (Contd.)

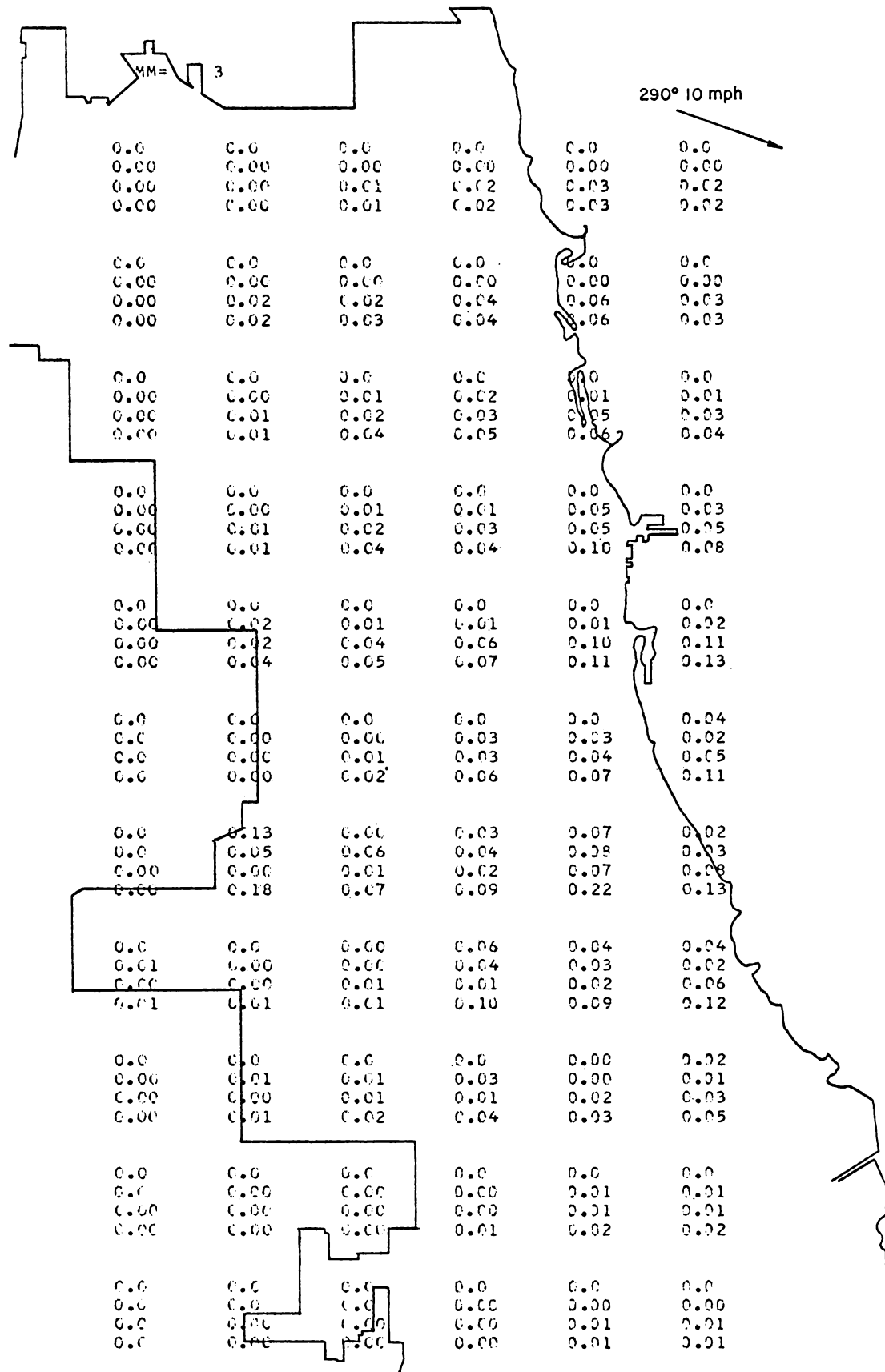


Fig. B.6. Printout of Estimates of SO<sub>2</sub> on 2 x 2-mi Grid according to Subroutine PROUT with Chicago Map Overlay and TAM4 Wind Speed and Direction. (Compare with Fig. B.1.)

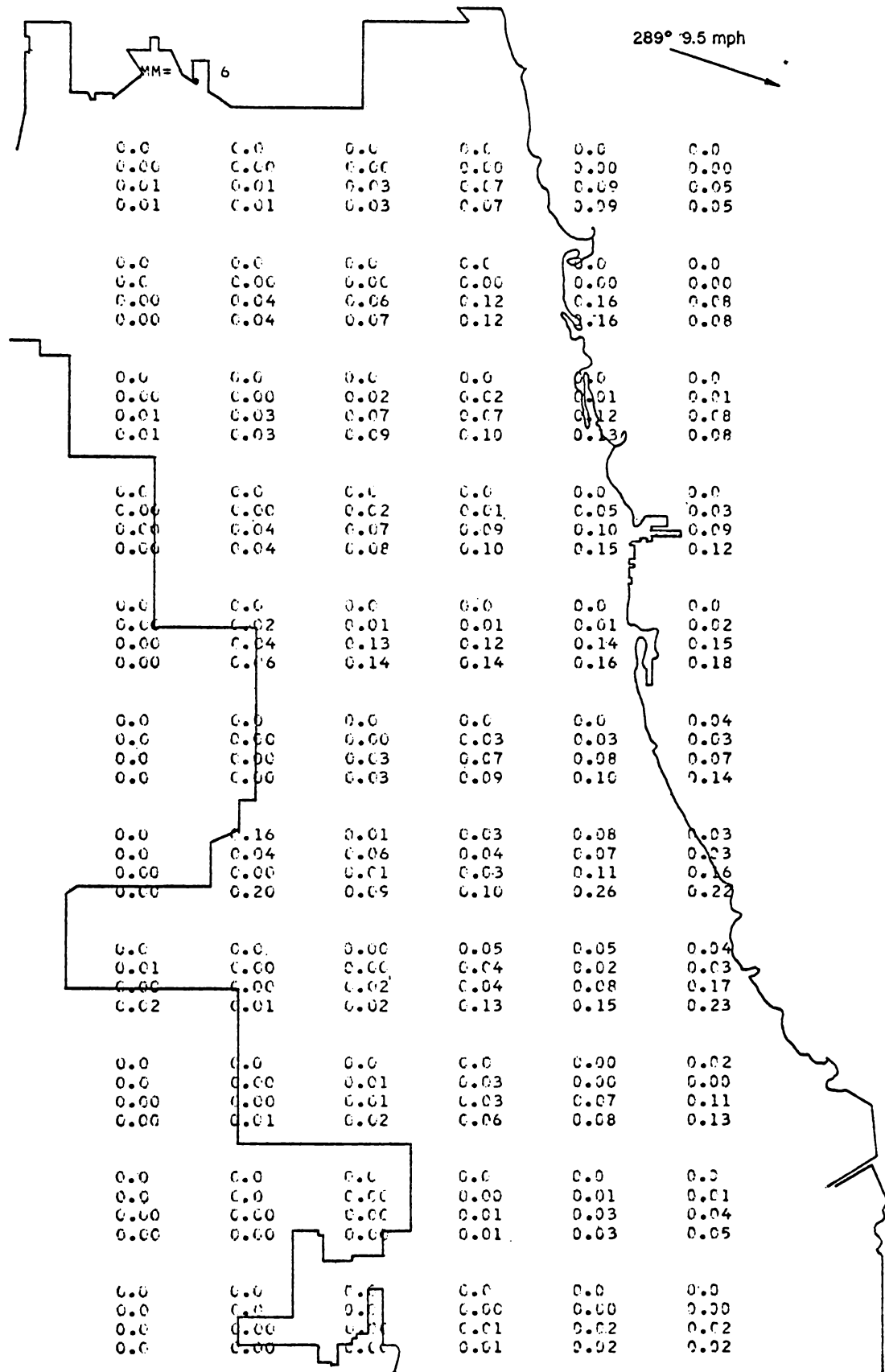


Fig. B.6 (Contd.)

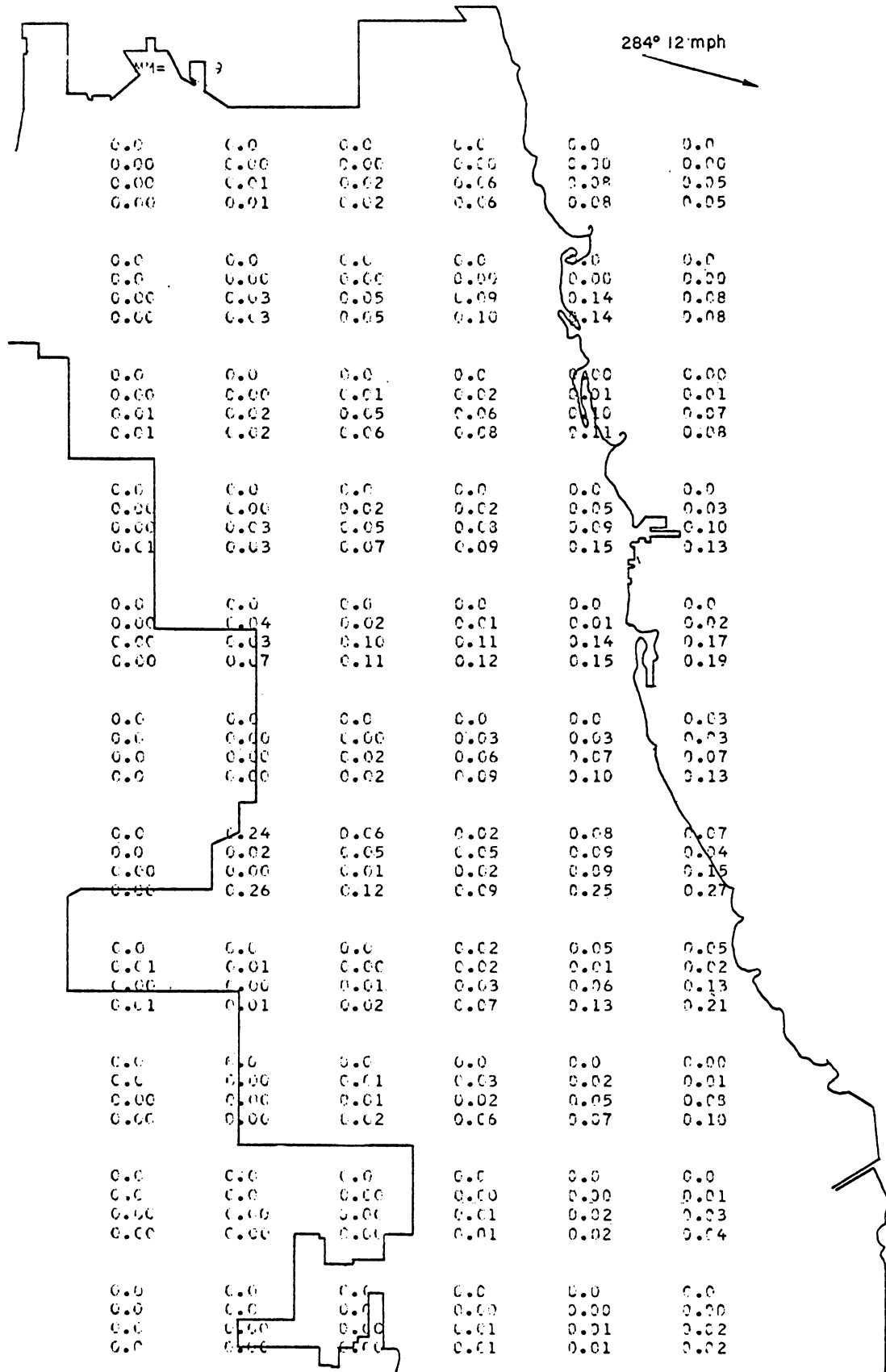


Fig. B.6 (Contd.)

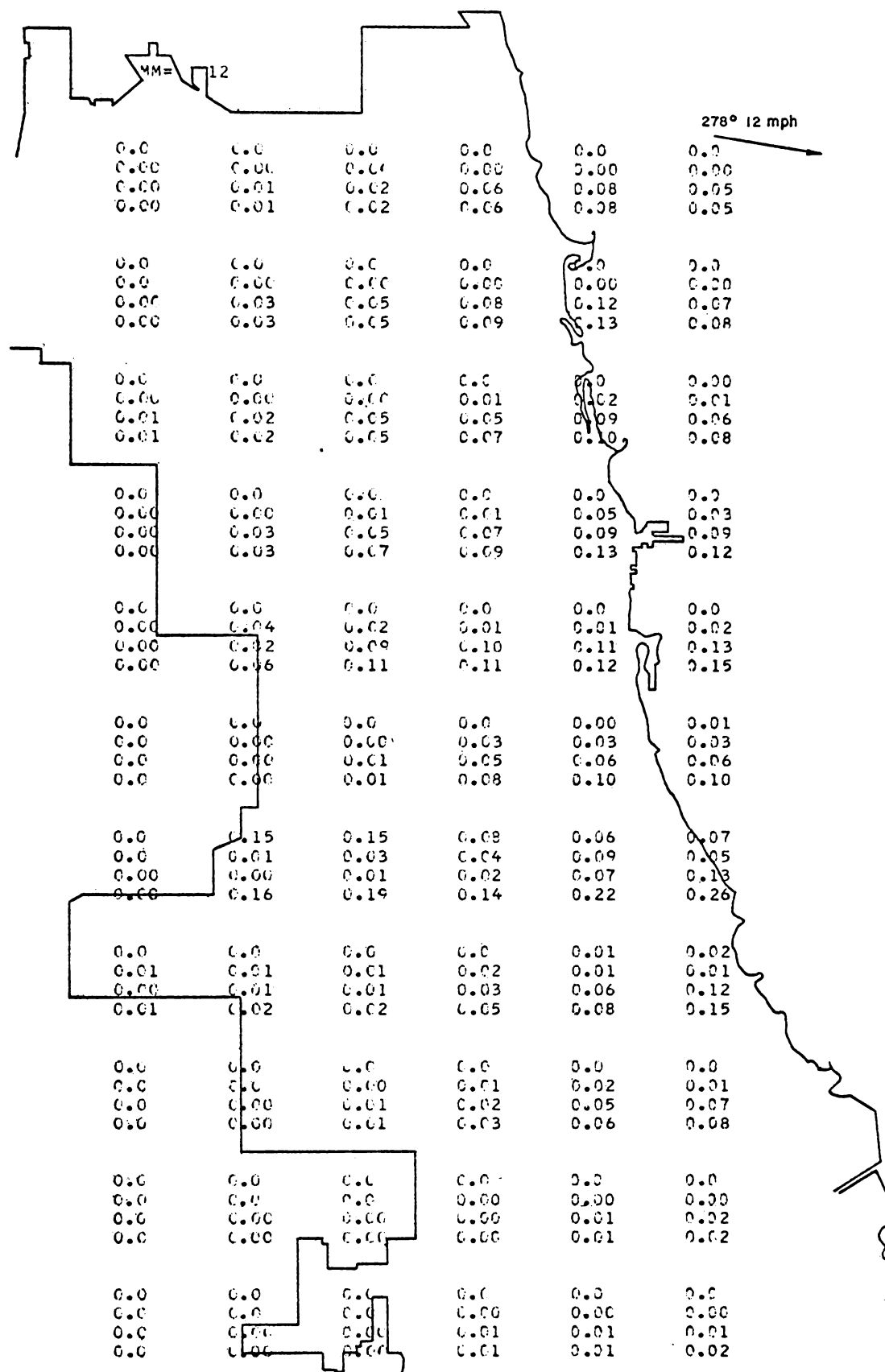


Fig. B.6 (Contd.)

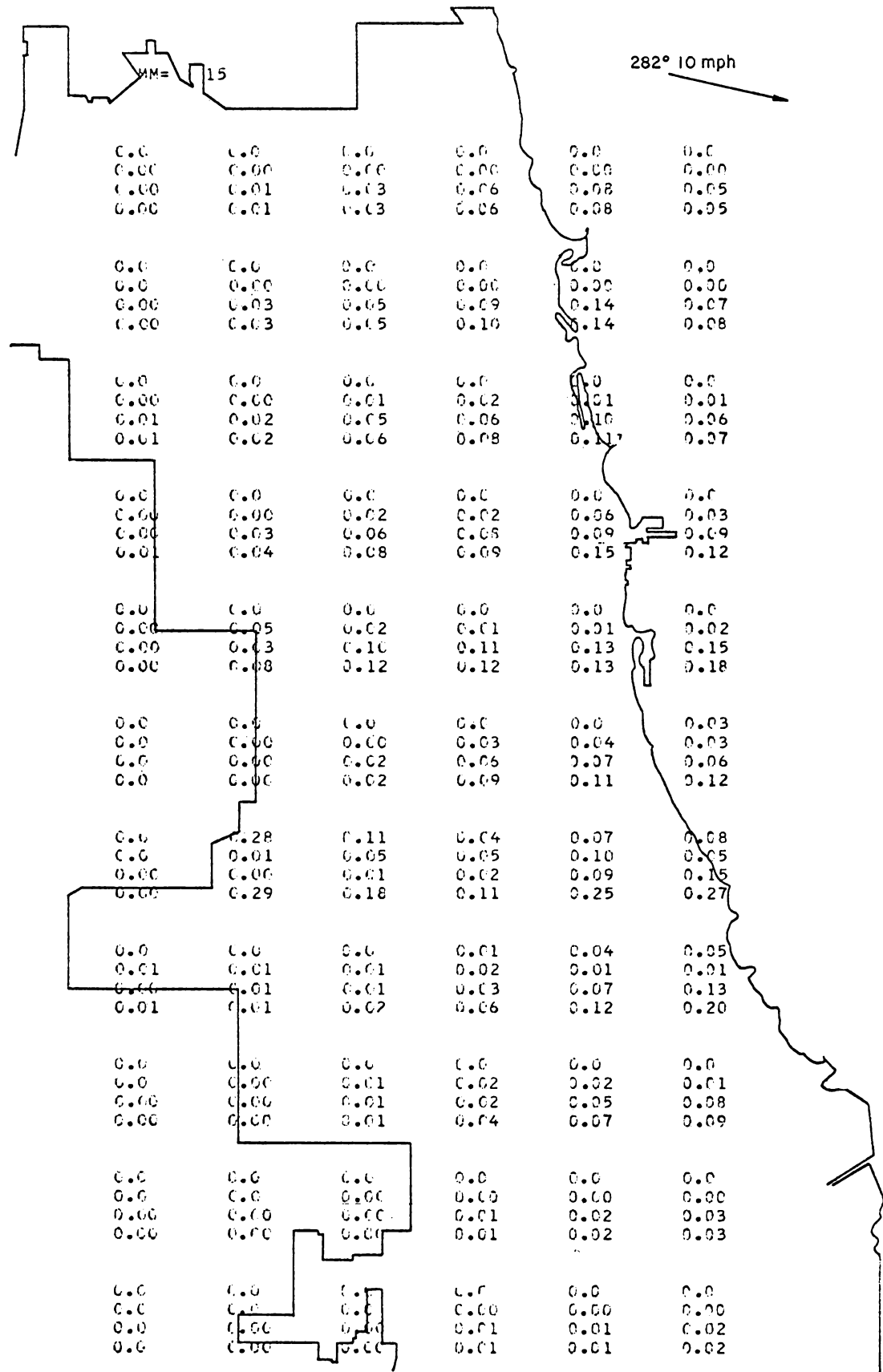


Fig. B.6 (Contd.)



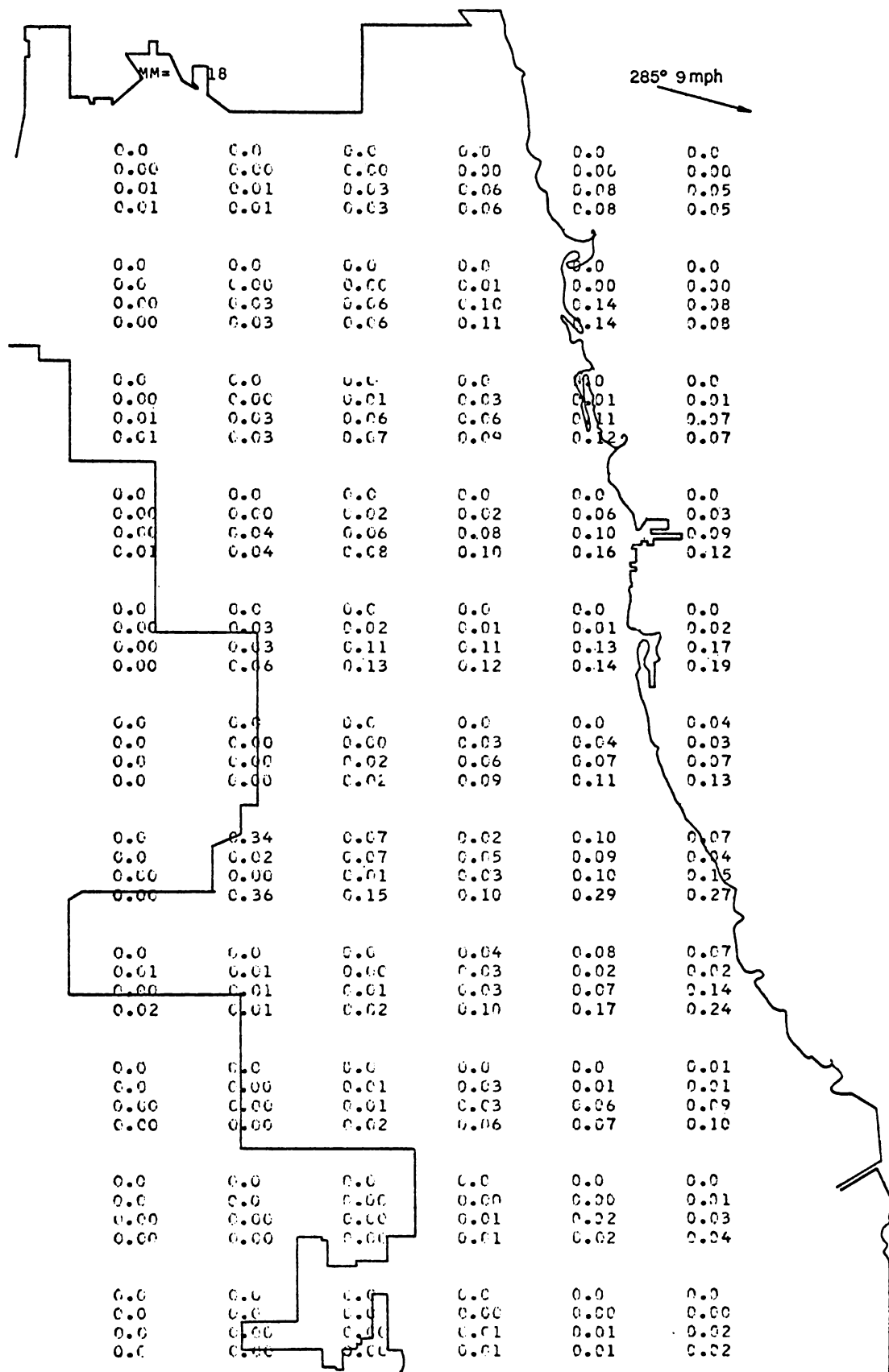


Fig. B.6 (Contd.)

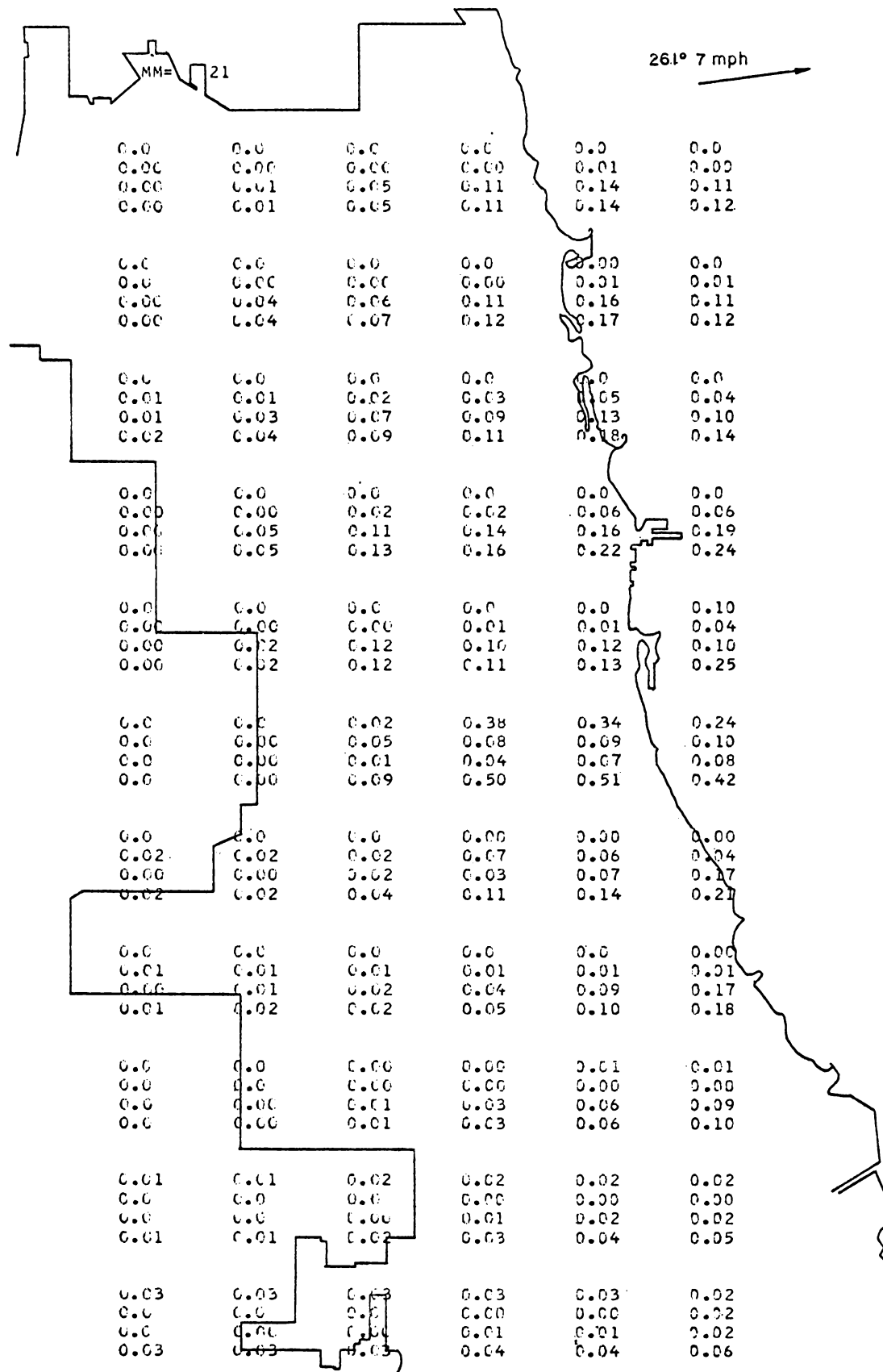


Fig. B.6 (Contd.)

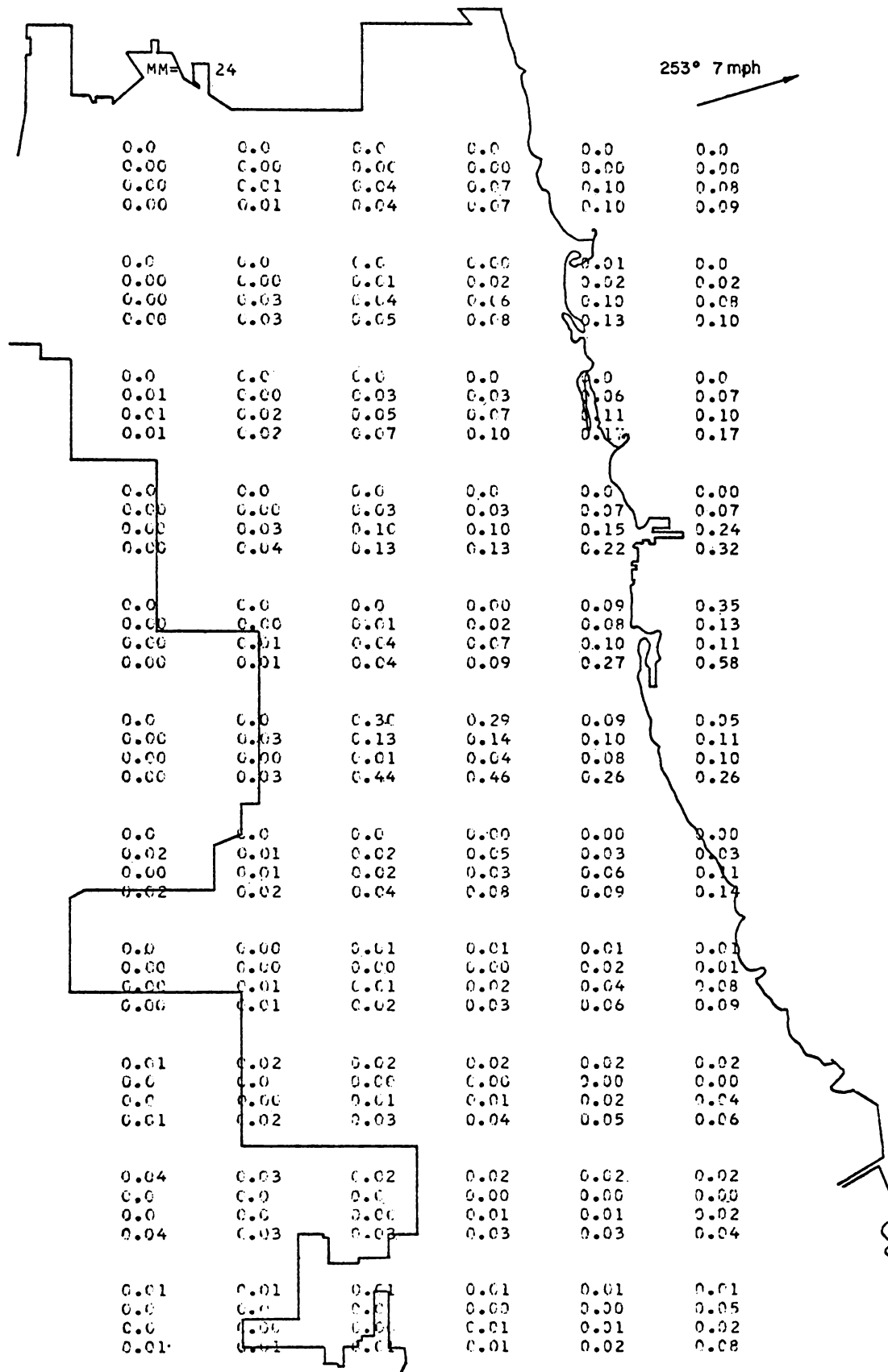


Fig. B.6 (Contd.)

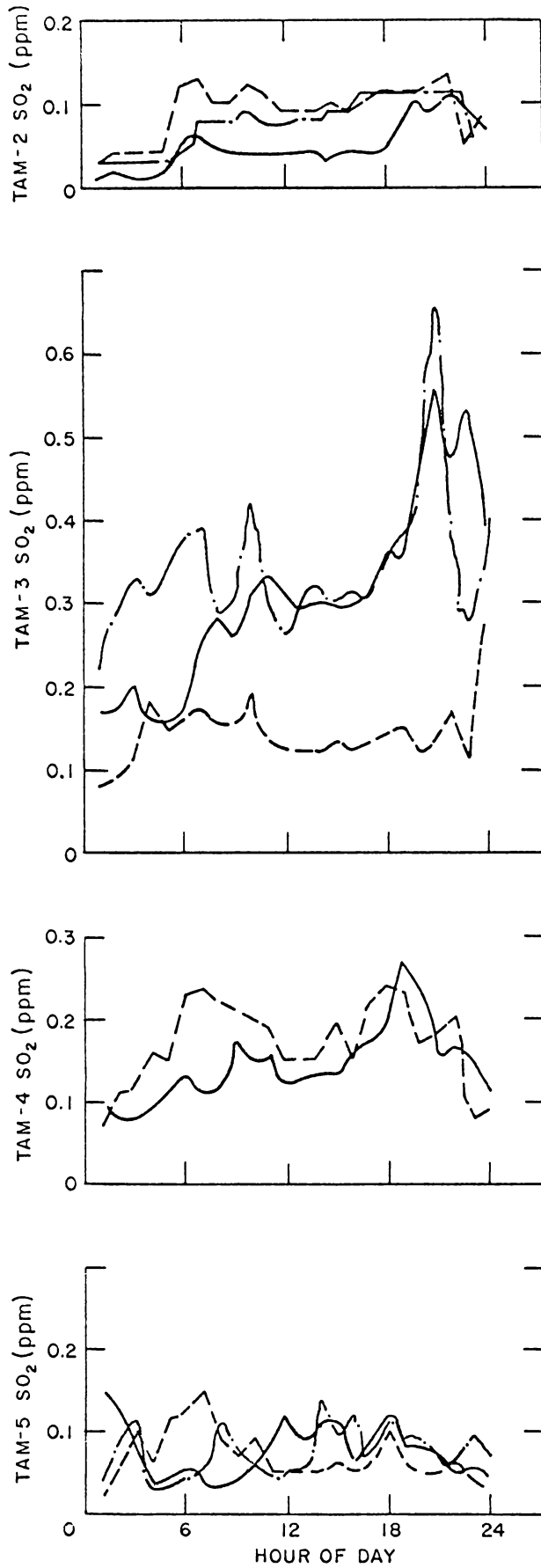


Fig. B.7  
 Time Series of SO<sub>2</sub> on 1/15/67.  
 — Observed TAM SO<sub>2</sub> values  
 - - - Estimated SO<sub>2</sub> values from nearest grid point based on TAM 4 winds with receptor at 75 ft (sample problem)  
 - · - Estimated SO<sub>2</sub> values from separate calculations based on actual receptor location and measured wind at each TAM station. (See Fig. B.1.)

## REFERENCES

- Bowden, K. F., (1965), *J. Fluid Mech.* 21, Part 2, pp. 83-95.
- Carpenter, S. G., *et al.*, (1967), "Report on Full-Scale Study of Plume Rise at Large Electric Generating Stations," Paper No. 67-82, Air Pollution Control Association Annual Meeting, Cleveland, Ohio, June 11-17, 1967.
- Carson, J. E., and Moses, H., (1967), "The Validity of Currently Popular Plume Rise Formulas," AECL-2787, *Proc. USAEC Meteorological Information Meeting*, Chalk River, Ontario, September 1967, pp. 1-20.
- Chamot, C., *et al.*, (1970), "APICS User Manual, A Computerized Air Pollution Data Management System," Chicago Air Pollution Systems Analysis Program--Argonne National Laboratory Report, ANL/ES-CC-006 (Feb 1970).
- Clarke, J. F., (1964), "A Simple Diffusion Model for Calculating Point Concentrations from Multiple Sources," *APCA Journal* 9 (Sept 1964).
- Cramer, H. E., and Dumbauld, R. K., (1968), *Experimental Designs for Dosage Predictions in CB Field Tests*, GCA Report No. 68-17-G, GCA Corporation, Bedford, Mass.
- Cramer, H. E., *et al.*, (1964), *Meteorological Prediction Techniques and Data System*, Geophysics Corporation of America, GCA Tech. Report No. 64-3-G, March 10, 1964, p. 34.
- Croke, E. J., *et al.*, (1968a), *Chicago Air Pollution System Model, First Quarterly Progress Report*, Argonne National Laboratory Report, ANL/ES-CC-001, February 1968.
- Croke, E. J., *et al.*, (1968b), *Chicago Air Pollution System Model, Second Quarterly Progress Report*, ANL/ES-CC-002 (May 1968).
- Croke, E. J., *et al.*, (1968c), *Chicago Air Pollution System Model, Third Quarterly Progress Report*, ANL/ES-CC-003 (Oct 1968).
- Croke, E. J., *et al.*, (1969), *Chicago Air Pollution System Model, Fourth Quarterly Progress Report*, ANL/ES-CC-004 (March 1969).
- Croke, E. J., and Booras, S., (1969), "Design of an Air Pollution Incident Control Plan," Paper No. 69-99, APCA Conf., New York City, N. Y.
- Croke, K., and Kennedy, A., "An Air Quality Control Program for Large Industrial Sources in the City of Chicago," APCA Paper 69-71, New York City, N. Y. (June 1969).
- DeMarrais, G. A., (1959), *Wind-Speed Profile at Brookhaven National Laboratory*, *Journal of Meteorology* 16, April 1959, pp. 181-190.
- Fortak, H. G., (1969), "Numerical Simulation of the Temporal and Spatial Distribution of Urban Air Pollution Concentrations," *Proc. Symp. Multiple Source Urban Diffusion Models*, Chapel Hill, N. C., October 27-30, 1969 (in press).
- Hilst, G. R., (1969), "The Sensitivities of Air Quality Predictions to Input Errors and Uncertainties," *Proc. Symp. Multiple Source Urban Diffusion Models*, Chapel Hill, N. C., October 27-30, 1969 (in press).

- Johnson, W. B., *et al.*, (1969), "Development of a Practical, Multipurpose Urban Diffusion Model for Carbon Monoxide," *Proc. Symp. Multiple Source Urban Diffusion Models*, Chapel Hill, N. C., October 27-30, 1969 (in press).
- Kennedy, A., and Anderson, J., "A Computerized Information and Computation System for Environmental Studies (1969)," APCA Paper No. 69-204, June 1969, APCA Conf., New York City, N. Y.
- Koogler, J. B., *et al.*, (1967), *A Multivariable Model for Atmospheric Dispersion Problems*, J. Air Pollution Control Administration 17, pp. 211-214.
- Marsh, K. J., and Withers, V. R., (1969), *An Experimental Study of the Dispersion of the Emissions from Chimneys in Reading--III: The Investigation of Dispersion Calculations*, Atmos. Environ. 3, pp. 281-302.
- Martin, D. O., and Tikvart, J. A., (1969), *A General Atmospheric Diffusion Model for Estimating the Effects of One or More Sources on Air Quality*, U.S. Dept. of Health, Education, and Welfare, NAPCA (internal document).
- McElroy, J. L., and Pooler, F., Jr., (1968), *St. Louis Dispersion Study Vol. II--Analysis*, U.S. Dept. of Health, Education, and Welfare, NAPCA Pub. No. AP-53.
- Moses, H., (1969), *Mathematical Urban Air Pollution Models*, ANL/ES-RPY-001.
- Ozolins, G., and Smith, R., (1966), *A Rapid Survey Technique for Estimating Community Air Pollution Emissions*, U.S. Dept. of Health, Education, and Welfare, Public Health Service Publication No. 999-AP-29.
- Pasquill, F., (1962), *Atmospheric Diffusion*, D. Van Nostrand Co., Ltd., London, pp. 179-204.
- Pasquill, F., (1969), "The Prediction of Diffusion over an Urban Area--Current Practice and Future Prospects," *Proc. Symp. Multiple Source Urban Diffusion Models*, Chapel Hill, N. C., October 27-30, 1969 (in press).
- Roberts, J. J., and Croke, E. J., "Design of Regional Implementation Plans for Stationary Sources," Paper No. 70-140, APCA Conf., St. Louis, Mo., June 1970 (in press).
- Roberts, J. J., *et al.*, "An Urban Atmospheric Dispersion Model," *Proc. Symp. Multiple Source Urban Diffusion Models*, Chapel Hill, N. C., October 27-30, 1969 (in press).
- Shieh, L., (1969), *A Multiple-Source Model of Turbulent Diffusion and Dispersion in Urban Atmospheres*, Report No. NR-69-11, Geophysical Sciences Laboratory, New York University (Dec 1969).
- Slade, D., (1966), *Estimates of Dispersion from Pollutant Releases of a Few Seconds to 8 Hours in Duration*, Tech. Note 39-ARL-3, Air Resource Laboratory, Washington, D.C.
- Start, G. E., and Markee, E. H., Jr., (1967), *Relative Dose Factors from Long-Period Point Source Emissions of Atmospheric Pollutants*, AECL-2787, Chalk River Nuclear Laboratories, Chalk River, Ontario, Canada.
- Turner, D. B., (1964), *A Diffusion Model for an Urban Area*, J. Appl. Met. 3, pp. 83-91.
- Turner, D. B., (1967), *Workbook of Atmospheric Dispersion Estimates*, U.S. Dept. of Health, Education, and Welfare, Public Health Service Pub. No. 999-AP-26.
- Turner, D. B., (1968), private communication.



ANL  
G-007  
ANL/ES-CC

LIBRARY  
OF  
WASHINGTON  
UNIVERSITY  
ST. LOUIS - MO.